A STUDY OF THE END POINT PATH GEOMETRY IN METEOR BURST SYSTEMS

J. C. WORSNOP

PH. D. 1990

A STUDY OF THE END POINT PATH GEOMETRY IN METEOR BURST SYSTEMS USING A MICROCOMPUTER SIGNAL LOGGER

John C Worsnop CEng MIEE

Submitted to the CNAA in partial fulfillment of the requirements for the degree of Doctor of Philosophy.

The research was carried out between August 1984 and October 1989 at Anglia Higher Education College and the Mullard Radio Astronomy Observatory, University of Cambridge .

Submitted February 1990

(c) J C Worsnop 1989

ABSTRACT

A STUDY OF THE END POINT PATH PATH GEOMETRY IN METEOR BURST SYSTEMS USING A MICROCOMPUTER SIGNAL LOGGER

John C Worsnop CEng MIEE

Radio propagation experiments generally need large amounts of data to be gathered over extended periods. This thesis describes the design of a signal logger for unattended gathering of signal statistics from a meteor burst radio path, using two receiving antennas.

Using a VHF broadcast radio station as a signal source, the data logger was used to investigate the properties of signals received with one antenna directed at the path mid point and a second at the receiving station zenith (end point). Calculations of path loss at 70 and 50 MHz showed that the mid point path loss should be lower than the end point path loss by up to 3dB for ranges up to about 900km but higher above this range. Calculations for the 70MHz 1173km experimental path showed that the path loss for end point illumination should be in the order of 1dB less than that for mid point. Results suggested a larger percentage of large amplitude signals on the end point antenna, but the mean end point path loss in the order of 1dB greater than mid point. Burst durations were found to be lower on end point but not to the extent predicted by theory. The sampling rate of the data logger was initially thought to be the main contributory factor to this effect, but further experiments showed that this was not the case.

Duty cycle of the two path geometries was also compared, and a computer model written, predicting a 4:1 advantage for mid point. Results confirmed the model, showing the advantage varying from 1.14 to 6.36 with a mean value of 4.0. This ratio shows a small reduction during periods of high shower activity.

In conclusion, the data logger has been proven, its limitations discussed, and the limitations and advantages of end point illumination investigated.

Acknowledgements

My two supervisors:

Dr Stanley Evans of Cambridge University.
Dr Peter diMambro of Anglia HEC.

And also:

Chris Rycroft for the initial idea for the project.

Philip Howarth of Cambridge Consultants for proof reading and help with the antenna experiments.

Professor Baldwin, Tony Brown and the Radio Astronomy group at the Mullard Radio Observatory for the use of their radio site for the second series of measurements.

Neville Dean, Mike Machen and all the other lecturers, technicians and students at Anglia who helped and listened.

Dr Paul Cannon of RAE Farnborough, and John Milsom of Marconi Research for early encouragement.

Regency aerials of Histon near Cambridge for erecting the antennas at Anglia.

Paul Turner for the program displaying the shower predictions.

John Wilson of Philips Radio Communications Systems, and all my other friends in the amateur radio community whose open minds, and enthusiasm to attempt, and succeed at, "the impossible", never cease to amaze me.

List of symbols used in this thesis

β = the angle between the trail and the line joining the transmitter to receiver. (radians)

$\varnothing$ = half the angle between the lines joining transmitter and receiver to the reflection point. (radians)

R_t = distance from the transmitter to the reflection point.(km)

R_r = distance from the receiver to the reflection point. (km)

TX = transmitter

RX = receiver

G_t = TX antenna gain relative to an isotropic radiator

G_r = RX antenna gain relative to an isotropic radiator

q = electron line density of a meteor trail (electrons/m)

α = angle between the electric vector at the meteor trail and R_r. (radians)

h = average trail height (km).

f = frequency (MHz).

r_0 = initial radius of a meteor trail (km).

λ_t = transition wavelength (m).

f_t = transition frequency (MHz).

p = probability density of detection of a trail.
r = backscatter range from transmitter to trail.(km)

p' = probability density associated with an artificial standard echo.

dBm = dB relative to 1mW in 50 ohms.

G_o = maximum gain of an antenna relative to an isotropic radiator.

a,b = azimuth and elevation angles of antenna system (radians).

P_r = received power (W)

P_t = transmitted power (W)

P_L = receiver threshold (W)

A = effective echoing area of trail. (m^2)

D = the diffusion coefficient characterising the trail expansion with time. (m^2/s)

r_e = classical radius of the electron. (2.8178×10^{-15} m)

λ = system wavelength. (m)

L = half the length of the first Fresnel zone of a trail.

v = meteor velocity. (m/s)

δ = angle between the z axis and the plane which is perpendicular at z = 0 to the bisector of the forward scattering angle. (radians)

z = trail length co-ordinate, z = 0 is the trail mid point.

τ = zenith angle of meteor radiant. (radians)

P_s = amplitude of standard echo. (W)

t_s = duration of standard echo. (s)

C_0 = yearly average meteor intensity.

N = standard echo rate.

N_0 p= path average duty cycle.

CONTENTS

SECTION 1	Introduction	1
SECTION 2	Review of meteor burst propagation	4
2.1	Introduction	4
2.2	Characteristics of meteors	4
2.3	Historical perspective	6
2.4	The application of meteor burst for comunication	9
2.4.1	Types of trail	9
2.4.2	Useable frequency range	10
2.4.3	Path geometry for reflection	11
2.4.4	System techniques	13
SECTION 3	Outline of experimental work	14
3.1	Objectives	14
3.2	Choice of signal source	14
3.3	Initial experiments	16
3.4	Main experiment	17
3.5	Second experiment	18
SECTION 4	Radio receiving equipment	19
4.1	Radio receiver	19
4.1.1	Receiver measurements	20
4.2	Antenna system	23
4.2.1	Antenna requirements	23
4.2.2	Factors affecting the performance of the practical antenna system	26
4.2.3	First experiment to confirm antenna isolation	27
4.2.4	Second experiment to measure the elevation discrimination between the antennas	29
SECTION 5	Computer interface	31
5.1	Introduction	31
5.2	Analog to digital conversion	32
5.2.1	Circuit description	32
5.3	Real time clock	33
5.3.1	Circuit description	34
5.4	Antenna changeover	35
5.4.1	Switching circuit	35
5.5	Modifications for second experiment	35
5.5.1	Objectives of modification	35
5.5.2	Details of modification	35
5.6	Data logger software	36
5.6.1	Introduction	36
5.6.2	Sampling software development	37
5.6.3	Disc filing routine	39
5.7	Modifications for second experiment	40
5.7.1	Objectives of modification	40
5.7.2	Details of modification	40

SECTION 6	System calculations	43
6.1	Path loss	43
6.1.1	Simple model	43
6.1.2	Effect of trail height and initial radius	45
6.1.3	Effect of transition wavelength	48
6.2	Trail duration	52
6.2.1	Experiment path durations	52
6.3	Probability of trail detection and duty cycle	55
6.3.1	Standard echo units	58
6.3.2	Calculated duty cycle	58
SECTION 7	Experimental results	59
7.1	Introduction	59
7.2	Measurement thresholds	59
7.3	Presentation of results	60
7.3.1	Daily plots of burst frequency and duty cycle	61
7.3.2	Monthly averages of amplitude burst frequency and duration	66
7.3.2.1	Amplitudes	66
7.3.2.2	Durations	69
7.3.2.3	Bursts per minute	72
7.3.3	Monthly distributions of amplitude and duration	74
7.3.4	Monthly percentage duty cycles	84
7.4	Effect of transition wavelength	90
SECTION 8	Discussion of results	91
8.1	Conclusions about end point geometry	91
SECTION 9	Recommendations for further work	93
REFERENCES		97
APPENDICES	A1 Interface circuit diagram	A1
	A2 Modified interface	A2
	(b) Antenna models	A4
	(c) Program listings and descriptions	A9
	(i) RUNPROG	A9
	(ii) METOR12	A13
	(iii) NUMBERS	A21
	DURATON	A24
	AMPLTDE	A26
	(iv) GRANAM5	A29
	GRANKS8	A33
	(v) LOSITES	A36
	LOSJCW	A39
	MSLOS	A41
	(vi) MSDUR	A43
	DURJCW	A45
	(vii) FTRANS1	A47
	(d) Derivation of path equations	A49
	(e) Duty cycle calculation	A56
	(f) Data logger memory map	A65

Section 1

Introduction

The work described by this thesis has two main objectives:

I. To describe the design and use of a low cost microcomputer data logger for the study of the characteristics of the propagation of VHF radio signals by meteor burst mode.

II. To use the data logger to study the effects on signal characteristics of antenna geometry. In particular, to study the effect of using a receiving antenna pointing overhead (end point illumination) as an alternative to the usual practice of pointing it at the path mid point.

Objective (I)

The first objective aims to encourage an interest in propagation studies in academic institutions, where financial constraints often preclude such work.

Most meteor burst studies have been carried out using dedicated high power transmitters on remote sites. These require licencing and the approval of the local radio regulatory bodies. This generally takes time and can be expensive to achieve. Many projects undertaken by undergraduate and post graduate students have limited time and resources, and this tends to be a barrier to the study of meteor burst.

Television and radio broadcasting stations have been used as beacons for many years by amateur radio operators to monitor propagation conditions. They act as a freely available resource for a number of possible propagation studies, both at HF and VHF. In the past, broadcast monitoring has been at the forefront of the initial discovery of many new radio propagation modes. Particularly in the discovery of the effects of meteors upon radio propagation (2).

This experiment uses a high power FM radio broadcast signal source on the fringe of a UK amateur frequency allocation. This removes the requirement for licencing, and running costs of a remote transmitter site. It shows how, with simple equipment, a long or short term propagation experiment may be carried out without investment in a dedicated point to point link, and still produce useful and interesting results.

The data logger itself is simple enough to be implemented in similar form on most inexpensive home microcomputers, with the addition of simple external hardware.

Objective (II)

Most meteor burst systems use antennas which are oriented to illuminate an area of the ionosphere over the approximate mid point of the path. This mid point illumination is generally assumed to optimise the use of the path by maximising its availability for communication. Of the three signal parameters, burst amplitude, duration and number of bursts per unit time, it is the combination of the last two which has the largest weighting when determining the capacity of a particular channel, when using fixed data rate systems. However, the signal amplitude increases in importance when adaptive data rate systems are used such as described in (3).

This research was prompted by a paper published in 1978 (6) stating that meteor burst path loss could be reduced by a factor of up to 3.8dB by the use of end point illumination.

The use of end point illumination holds out the possibility of more efficient use of short range paths, or paths where local obstructions reduce the Fresnel zone clearances available for low angles of antenna elevation. If this path loss reduction is realisable in practice, then this geometry shows promise for such applications as mobile terminals where directional antennas may be difficult to use and omnidirectional antennas may be difficult to design. Any saving on transmitter power in the mobile or transportable field

would be advantageous. Space and frequency diversity are already used in radio systems, and antenna elevation angle diversity utilising the end point path is a possible meteor burst application that may prove useful.

As no extensive practical measurements of the end point path geometry appear to have been carried out, the experimental work in this report includes a study of the use of this path geometry on a 1173 km East West path, and its effects on burst amplitude, duration and duty cycle.

This report also extends the theoretical study of the effects of end point illumination on burst characteristics. It uses a more extensive model than (6) for the calculation of burst duration and amplitude, predicts the effect on path availability, and studies the effect of operation at higher frequencies.

Section 2

Review of meteor burst propagation

2.1 Introduction

Beyond line of sight radio communication by scattering from the trails left by meteoric particles has generated much interest in recent years. Both military and commercial communicators are attracted to its reliability and security due to its low probability of intercept and jamming, and virtual independence from disturbance due to ionospheric changes. It also provides an inexpensive, easily installed alternative to HF or satellite circuits.

2.2 Characteristics of meteors

Every day, millions of particles or micrometeors are swept up by the Earth in its orbit round the sun. The majority of these particles burn up in the E region of the ionosphere at a mean height of about 100 km without reaching the ground, a few of the very large particles falling as meteorites.

The particles vary in mass from about 0.1 μg to 10kg and sizes from 200μm to 80mm in diameter. Masses are distributed such that there is approximately the same total mass of each size of particle .Therefore there will be 10 times the number of particles of mass 0.1μg as there are of mass 1μg etc. Their velocities on entry into the atmosphere vary from 11.3 to 72km/sec (20). As they collide with air molecules they leave behind a trail of ionised particles, mainly metal ions, and free electrons the trail taking the form of a long thin paraboloid with the meteor at the head. This trail can form a short lived reflecting or scattering medium for HF and VHF radio signals. The electron line density, a measure of ionisation, depends on the mass of the meteor. These trails can be utilised for the intermittent transmission of digital signals using a burst mode, or, if

the system is designed such that consecutive bursts overlap to give a continuous signal, analogue transmission techniques may be employed.

Meteors may be classified into two groups :

(a) Shower meteors

(b) Sporadic or random meteors

Shower meteors are thought to be the remnants of comet tails going round the sun with well known and predictable orbits which intersect with the earth's orbit at the same time each year. They radiate from a fixed point in the sky and have names which relate to the constellation associated with that point. (ie the "Geminids" appear to radiate from the constellation of Gemini). Due to their relatively infrequent appearance they only provide short term enhancements to the communications capability of a meteor burst path.

Of far greater importance are the sporadic or random meteors, as they are far more numerous and occur all the year round.

Sporadic meteors travel round the sun with no particular predictable orbit, and have no specific radiant point. Early work (23) established that the majority of useful sporadic meteors orbit the sun close to the plane of the ecliptic in the same direction as the earth. This gives rise to a diurnal variation in meteor activity giving a peak at around 0600 (local time at the path mid point) and a minimum at around 1800. This can be explained by the fact that the morning side of the earth is travelling with the orbital velocity into the main flux of meteors, and hence the relative velocities of earth and meteor are greater. Similarly the evening side of the earth is rotating away from the meteor flux and only meteors with sufficient velocity are swept up by the earth's atmosphere. There are also seasonal variations in average meteor activity with a peak

around mid July and a minimum in February due to the fact that the sporadic meteor orbits are not uniformly distributed along the earth's orbit.

2.3 Historical perspective

The effects of meteor trails on radio reception were first noted in 1929 (1) but it was only seen as a possible source of disruption to propagation. In 1931 (2) observations from the early 1920s were reported, and a first suggestion of correlation between major meteor showers and enhanced signals on broadcast reception was made. Only after World War 2 and the development of radar was this correlation confirmed. The University of Manchester's Jodrell Bank team produced much useful information about the phenomenon. Particularly, figures for the intensity of signals were calculated and compared with observed values (3).

It should be noted that the majority of work performed to this date was based on back scatter, radar – like observations, and little exploitation of the medium for communications was attempted.

The work accelerated in the mid 1950s with the experimental work of Eshelman and Manning at Stanford University (4). They described the properties of a forward scatter system with the transmitter and receiver at different geographical locations, as would be the case for a point to point communications link. A path loss formula was derived and compared with forward scatter measurements. This related the path loss and the angle of incidence of the transmitted ray to the trail. As will be seen this is one of the fundamental concepts used in this report.

Much of this early work was aimed at utilising the continuous radio background signal produced by time-overlapping bursts at low frequencies. This would have enabled the continuous use of the meteor burst path for analogue signals such as speech. High power and relatively low frequencies (in the order of 20MHz) were required, and such

systems could suffer interference, interception and jamming by normal ionospheric layer reflections.

Digital communication by radio was of course in its infancy and the technology to utilise the transient path available with lower power at higher frequencies was complicated, bulky and expensive. Notwithstanding, Eshleman (15) described the effects of wavelength on information capacity for such a system, and suggested the use of shorter wavelengths to overcome the aforementioned interference problems.

The issue of Proc. IRE containing reference 15 contained a whole series of papers on meteor burst communication including the description of two complete communication systems, one built by the team at Stanford (17), and the Canadian JANET system (5). Both of these systems utilised the intermittent signal for digital communications by transmitting a pilot signal and only sending data when the received signal was above a pre-determined threshold. They obtained long term data rates equivalent to the 50 baud telex systems available over HF radio at that time, but without the problems of security and interference to which such systems were prone.

In 1960 (18) the Hughes Aircraft company developed an experimental air to ground system using Automatic Repeat reQuest (ARQ) techniques for error correction. This allowed a minimisation of message start up delays and enabled information transmission to be continued until nearer to the end of the burst, hence allowing a greater throughput of information for a given path. This technique was also used with the COMET system (19) developed by SHAPE in the Netherlands but they added diversity techniques and used a fixed point to point link.

The classic 1964 review paper (20) from the Central Radio Propagation Laboratory of the US National Bureau of Standards described the characteristics of meteors and the reflecting properties of individual trails, and outlined the statistical characteristics of

signals reflected by such trails. It represented a full survey of meteor burst communications systems and techniques to that date.

Test results from traffic capacity measurements made on the COMET system were presented in 1978 in the AGARD conference publications (21). The transition between the long and short wavelength path loss formulae described by Sugar (20) was studied with measurements over the same path at 40 and 100MHz. This enabled a relationship between duty cycle, wavelength and transmitted power to be determined. (Duty cycle is a measure of path useability, simply the percentage of time that the path was available).

In the same proceedings (6) novel system techniques were discussed including a proposal to change the normal use of the midpoint of the path for scattering to overhead or end point scattering. This would have the advantages of enabling the use of simple zenith pointing antennas at remote stations, and (it was claimed) a reduction in transmitted power.

The rapid advances in computer and signal processing technology in the past two decades has seen the adoption of meteor burst propagation in non-military commercial systems where relatively small amounts of data are needed infrequently. Two examples are the US department of agriculture snow level monitoring system SNOTEL, and the Alaskan meteor burst communication system AMBCS collecting weather information from unmanned buoys. These rapid advances have also seen a resurgence in interest in meteor burst systems in general, with papers such as those by Oetting (9) and Nes (22) which concentrate on the practical systems engineering applications of meteor burst communications. They provide a source of practical design information for systems engineers.

Further work into modelling and path prediction has been carried out in recent years by Weitzen (38) and Brown (33) who have produced improved programs to predict the

annual, diurnal and geographical variations in the performance of meteor burst paths. These are based on better models of the meteor radiant distributions such as those derived by Rudie (37) from the measurements of Davies (36). These models use the physical parameters of the path rather than the more traditional methods of Nes (22), and this thesis, which use simple meteor radiant distributions and empirical rules of thumb to predict the variations. These advanced models are far more demanding in the use of computing power than the more traditional methods.

2.4 The application of meteor burst for communication

2.4.1 Trails may be classified into two types :

underdense

where the electron density is low enough to allow most of the incident energy to pass through it unaltered, scattering a small amount in other directions;

and overdense

where the electron density is high enough for the trail to act as a highly reflecting surface.

Figs 2.1 and 2.2 show the characteristic shapes of the two signal reflections. They plot reflected signal amplitude (y) against time (x) showing typical relative values.
See appendix (d) for derivations of the reflecting properties of underdense trails.

Fig 2.1 Underdense trail

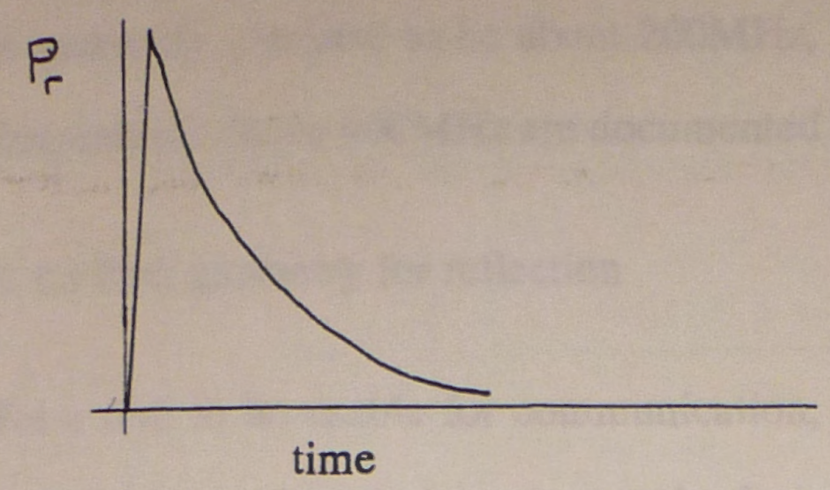

Fig 2.2 Overdense trail

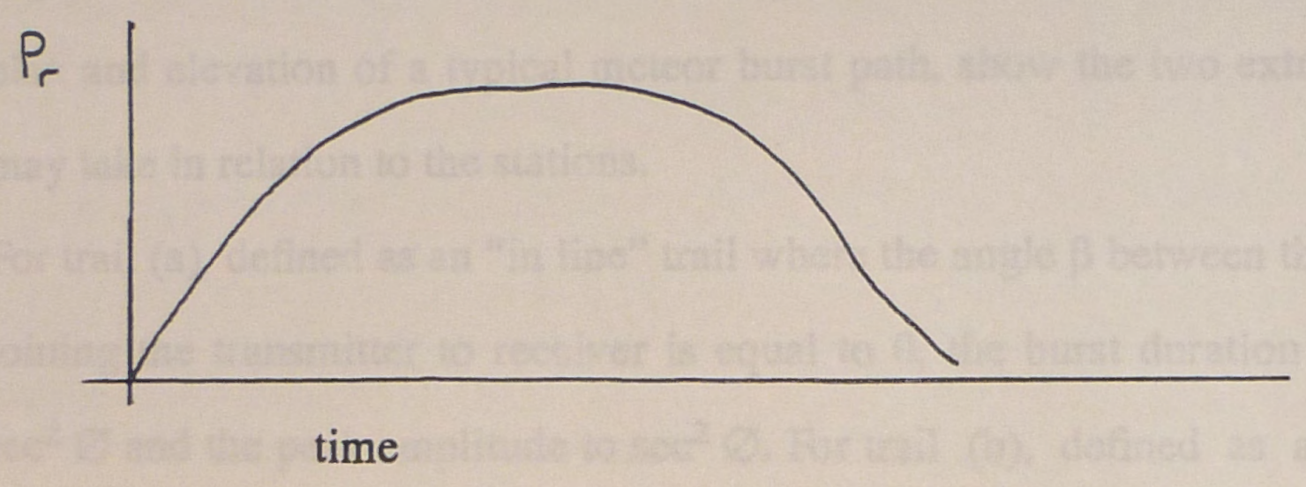

As the electron density depends on the mass of the meteoric particle and the large mass particles are less frequent, most systems rely on underdense bursts. Reference 22 gives a useful "rule of thumb" to determine whether a particular path relies on underdense or overdense bursts. The system described in this report relies mainly on underdense bursts, so the theory presented will relate to such bursts.

2.4.2 Usable frequency range

Systems operate above the normal ionospheric maximum usable frequency usually above 30MHz to avoid undue interference from ionospheric layer reflections, but the path losses increase in approximate proportion to the cube of the frequency (21). The upper radio frequency operating limit is therefore set by transmitter power and antenna gain limitations, and the lower limit by normal ionospheric reflections. Other factors affecting the choice of operating frequency are polarisation rotation around 40 MHz

(40), noise, and D- layer absorption at the lower frequencies. The practical upper limit is generally accepted to be about 200MHz, but reports of meteor burst experiments at frequencies above 400MHz are documented (24).

2.4.3 Path geometry for reflection

For a trail to be usable for communication, it must lie tangential to a prolate spheroid with the transmitter and receiver at the foci, reflection from the trail then being specular (2). The region in which most reflections take place is often assumed to be a plane at a nominal 100km height referred to as the meteor plane or h plane. Figs 2.3 and 2.4, the plan and elevation of a typical meteor burst path, show the two extremes that the trail may take in relation to the stations.

For trail (a), defined as an "in line" trail where the angle β between the trail and the line joining the transmitter to receiver is equal to 0, the burst duration is proportional to $\sec^2 \varnothing$ and the peak amplitude to $\sec^2 \varnothing$. For trail (b), defined as a "transverse" trail, where $\beta = 90°$ the burst amplitude is independent of $\varnothing$ and the duration proportional to $\sec^2 \varnothing$. (See appendix (d) for derivation of these assumptions.)

Of the two parameters, amplitude and duration, the duration has the largest importance as far as maximising the information throughput for a given number of detectable bursts.

Fig 2.3 Plan view of a meteor burst path

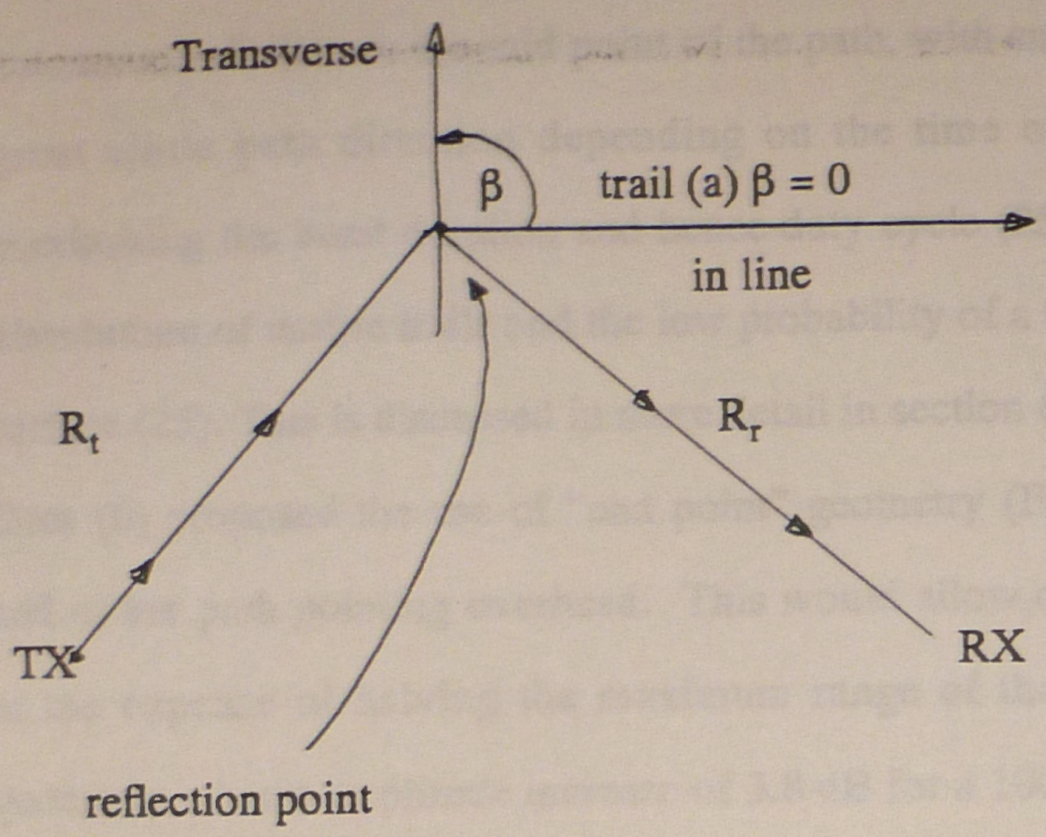

Fig 2.4 side elevation

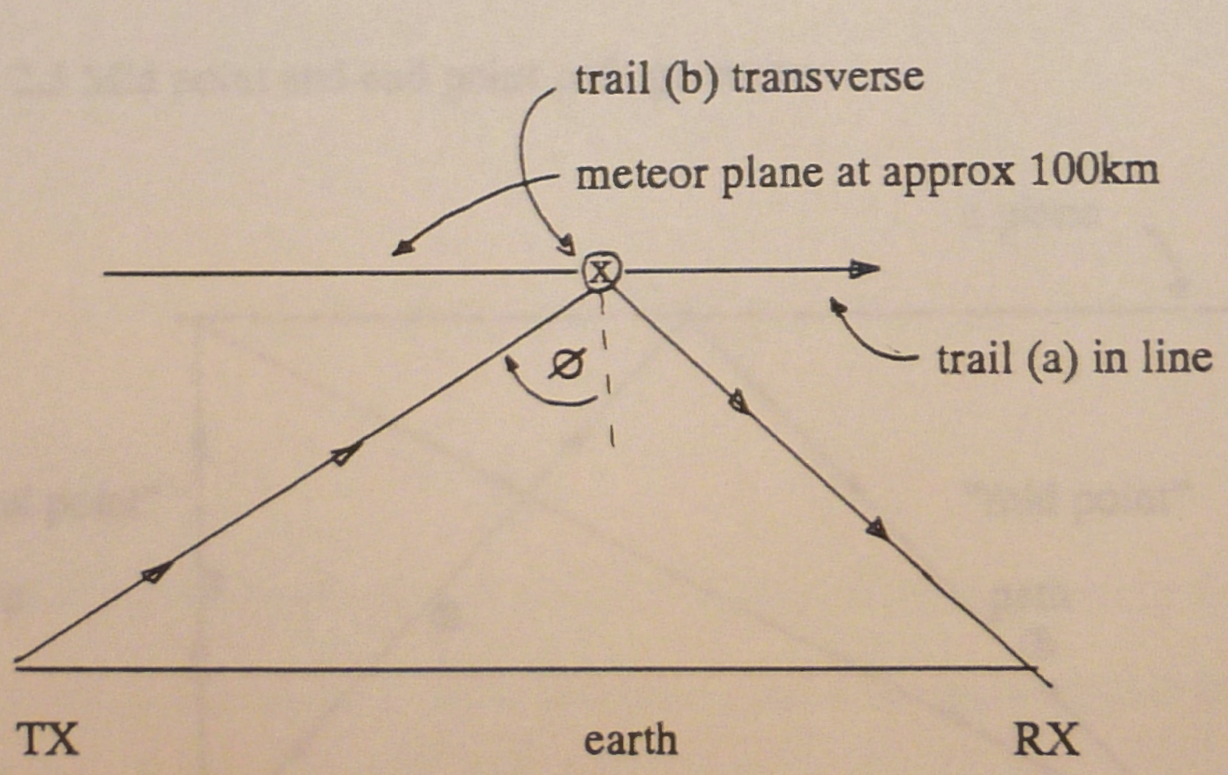

We can therefore deduce that as the angle Ø reduces with path length, the overall information rate for a system will also reduce with path length.

2.4.4 System Techniques

The standard method for the utilisation of meteor burst paths has been to orient the antennas to illuminate the mid point of the path, with small offsets to either side of the great circle path direction depending on the time of day. This has the effect of maximising the burst duration and hence duty cycle (25), (6). The offsets relate to the distribution of usable trails and the low probability of a trail lying parallel to the earth's surface (25). This is discussed in more detail in section 6 of this report.

Sites (6) proposed the use of "end point" geometry (Fig 2.5) with the antenna at one end of the path pointing overhead. This would allow omnidirectional radiation, albeit at the expense of halving the maximum range of the system. Sites claims for this geometry a burst amplitude increase of 3.8 dB for a 1000km path. Section 6 shows this calculation, describes the assumptions made, and shows that there is a consequent reduction in burst duration.

Fig 2.5 Mid point and end point path geometry

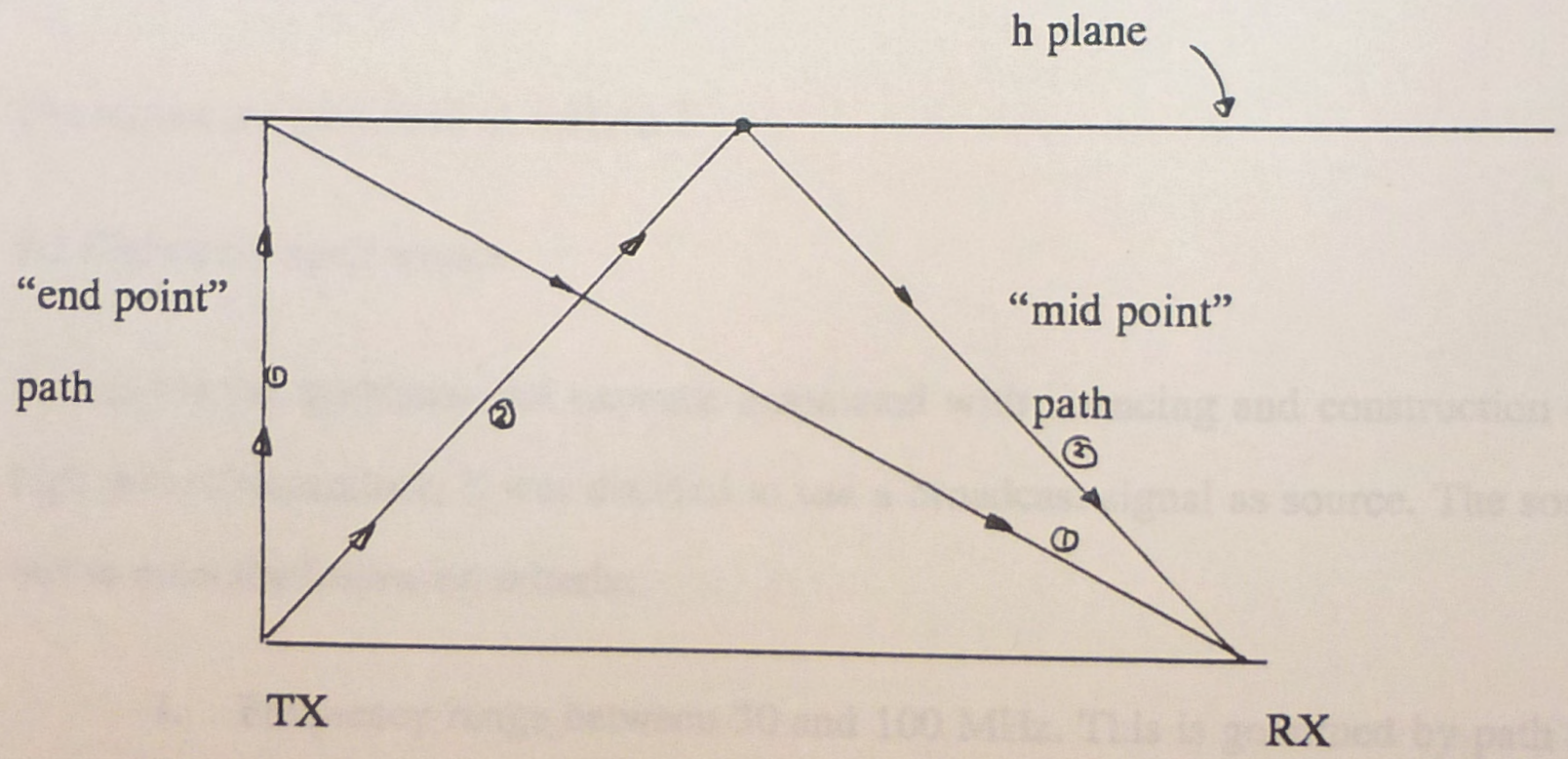

Better transmission protocols and modulation methods such as multi-level Phase Shift Keying will allow the higher data rates required to overcome the problem of shorter duration bursts.

Section 3

Experimental work

3.1 Objectives

The objective of the experimental work performed was to test the data logging system by monitoring a signal via meteor burst propagation using two antenna systems, and to gather data to allow a study of the end point effect. One antenna was oriented to favour signals from trails near the mid point and the other oriented to favour signals from trails near the end point of the path (See fig 2.5). Data was gathered over an extended period to note any seasonal and shower effects and a comparison made of the following signal parameters:

I. burst amplitude

II. burst duration

III. burst rate

The results are presented in section 7

3.2 Choice of signal source

To remove the problems and expense associated with licencing and construction of a high power transmitter, it was decided to use a broadcast signal as source. The source had to meet the following criteria:

I. Frequency range between 30 and 100 MHz. This is governed by path loss at high frequencies and normal ionospheric effects at low frequencies.

II. Operational for a large part of the 24 hour day

III. Great circle distance, transmitter to receiver between 1000 and 1200 km (see section 6)

IV. High power to overcome path losses

V. Transmitting antenna should have a low radiation angle pattern.

European television transmitters in Band 1 were considered, but thought to be unsuitable due to the large amount of frequency re-use and consequent uncertainty on signal source. The same argument applies to FM broadcasts in Band 2 with the added problem of the higher frequencies, and therefore path losses involved. It was decided to use one of the eastern bloc FM broadcast transmitters in the Band 65 – 74 MHz as used by Rycroft (7) in an earlier unpublished work. Radio Wroclaw service 4 (pronounced "vrotswaf") in Poland meets the requirements and is the only high power station on its frequency within meteor burst range.

Details of Radio Wroclaw service 4:

Frequency 70.67 MHz

Operating hours 0457-2400

Range 1173km

EIRP 120kW

Antenna omnidirectional low angle (ref 8)

A further advantage of using Radio Wroclaw was that it lies just outside the 70MHz band allocated to the UK radio amateur service. This allowed the use of inexpensive antennas designed for the amateur market.

3.3 Initial experiments

An initial experiment to get the feel of signal strengths and noise levels began in November 1984 using a calibrated receiver tuned to Radio Wroclaw and a temporary 5 element horizontally polarised Yagi. The receiver output was displayed on a chart recorder.

This experiment ran from 1500 on 19.11.84. to 1100 on 20.11.84 to coincide with the Leonids meteor shower. A rough estimate of the number of bursts above 0.8μV (-109dBm in 50 ohms) was made for each hour and the results presented in the histogram fig 3.1.The sinusoidal variation in activity is clearly visible.

Fig 3.1 No. of bursts > 0.8uV per hour

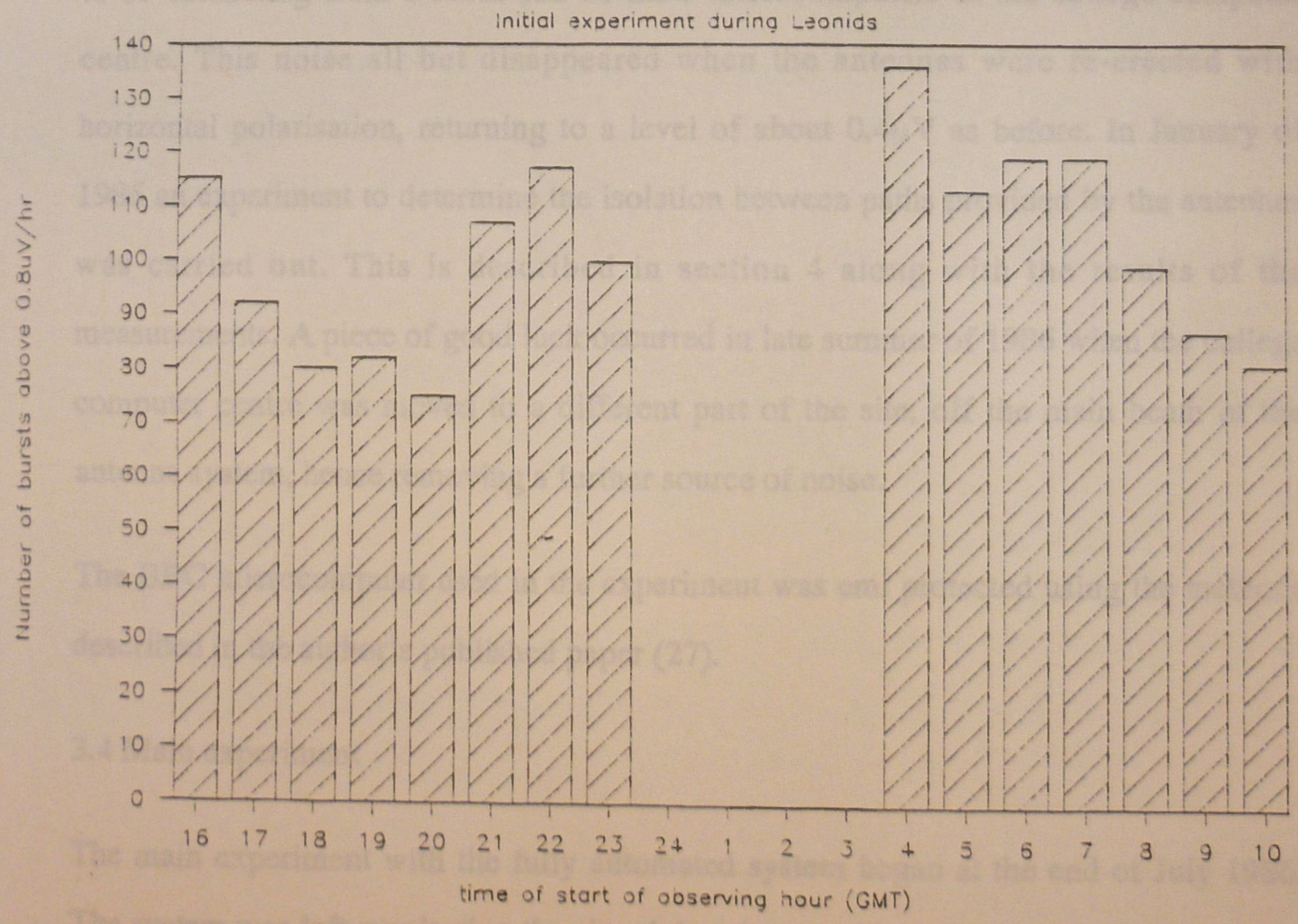

These initial results inspired confidence that the experiment would be practical, but the noise level was disturbingly high, averaging about –115dBm in 12.5KHz with peaks as

high as –107dBm. This corresponds to some 20 dB above cosmic noise at the operating frequency.

Work then continued with the building and testing of the radio receivers. The main antenna system was re-erected in June of 1985, after experiments with vertical polarisation to improve the isolation between the antennae were abandoned. It was realised after further research that the polarisation of the received signal was not random as had been wrongly believed, but mainly horizontal.

In the time between March, when the antennas were initially erected, and June, much time was spent trying to trace the very high level of noise. Much of the noise appeared to be emanating from a room full of BBC microcomputers in the college computer centre. This noise all but disappeared when the antennas were re-erected with horizontal polarisation, returning to a level of about 0.4μV as before. In January of 1986 an experiment to determine the isolation between paths provided by the antennas was carried out. This is described in section 4 along with the results of the measurements. A piece of good luck occurred in late summer of 1986 when the college computer centre was moved to a different part of the site, off the main beam of the antenna system, hence removing a further source of noise.

The BBC microcomputer used in the experiment was emi protected using the methods described in the author's published paper (27).

3.4 Main experiment

The main experiment with the fully automated system began at the end of July 1986. The system was left monitoring the signal, logging amplitude burst length and duration until early 1988. During this time various thresholds of duration and amplitude were tried, and the results noted in section 7.

The aim was to gather data over at least a complete year to account for the effects of showers and other seasonal variations in meteor activity. The results during the summer months were of particular interest due to the prevalence of Sporadic E (Es) propagation at 70 MHz during this period, and the possible effects on the results.

3.5 Second Experiment

During Winter 1988 and Spring 1989, the data logger was modified to respond to shorter bursts. This was a direct result of analysis of the data from the main experiment. In June of 1989 the equipment was moved to the Mullard Radio Astronomy observatory at Barton near Cambridge to take measurements on a quiet radio site. The details of the modifications and the results of this experiment are discussed later in the report. (Sections 5 and 7)

Section 4

Radio receiving equipment

4.1 Receiver

The receiver used in the experiment had to meet the following criteria:

I. Sufficient sensitivity to produce an acceptable signal to noise ratio at the output.

As man made noise tends to dominate in the 70MHz region in a semi urban environment, it was considered unnecessary to attempt to improve the receiver noise figure with a preamplifier as this could have a detrimental effect on the front end linearity.

II. Fast transient response to input signals.

Rise time to be in the order of 1ms due to the nature of the signals being received. Ideally the fall time should be of the same order but this was considered to be less important as the fast transient of the received signal is on the rising edge.

III. Calibrated output voltage to feed analogue to digital converter (ADC).

More accuracy could be obtained if some kind of logarithmic calibration law was used, as the received signals should fall mainly within a narrow range of values.

The initial measurements, using the manual chart recorder system, were made using a high frequency communications receiver from Icom type ICR70 with a crystal controlled frequency converter with dual gate MOSFET front end. The signal strength meter was calibrated in microvolts. This was replaced in December 1984 with a dedicated receiver based on a modified Pye R4000 series AM radio-telephone base

station receiver with a 12.5kHz channel spacing IF filter. An AM receiver was chosen, as the automatic gain control (AGC) line would provide a suitable measure of signal amplitude. The noise blanker was removed and the AGC response speeded up by the removal of a capacitor from the control line.

4.1.1 Receiver measurements

Fig 4.1 Shows the test set up to measure the transient response of the receiver. The results show the rise and fall times compared to those of the the input rf signal pulse. The oscilloscope photographs show that the rise time (10 to 90% of full output) was 0.5ms and the fall time 3.5ms.

Fig 4.1 Pulse testing of receiver

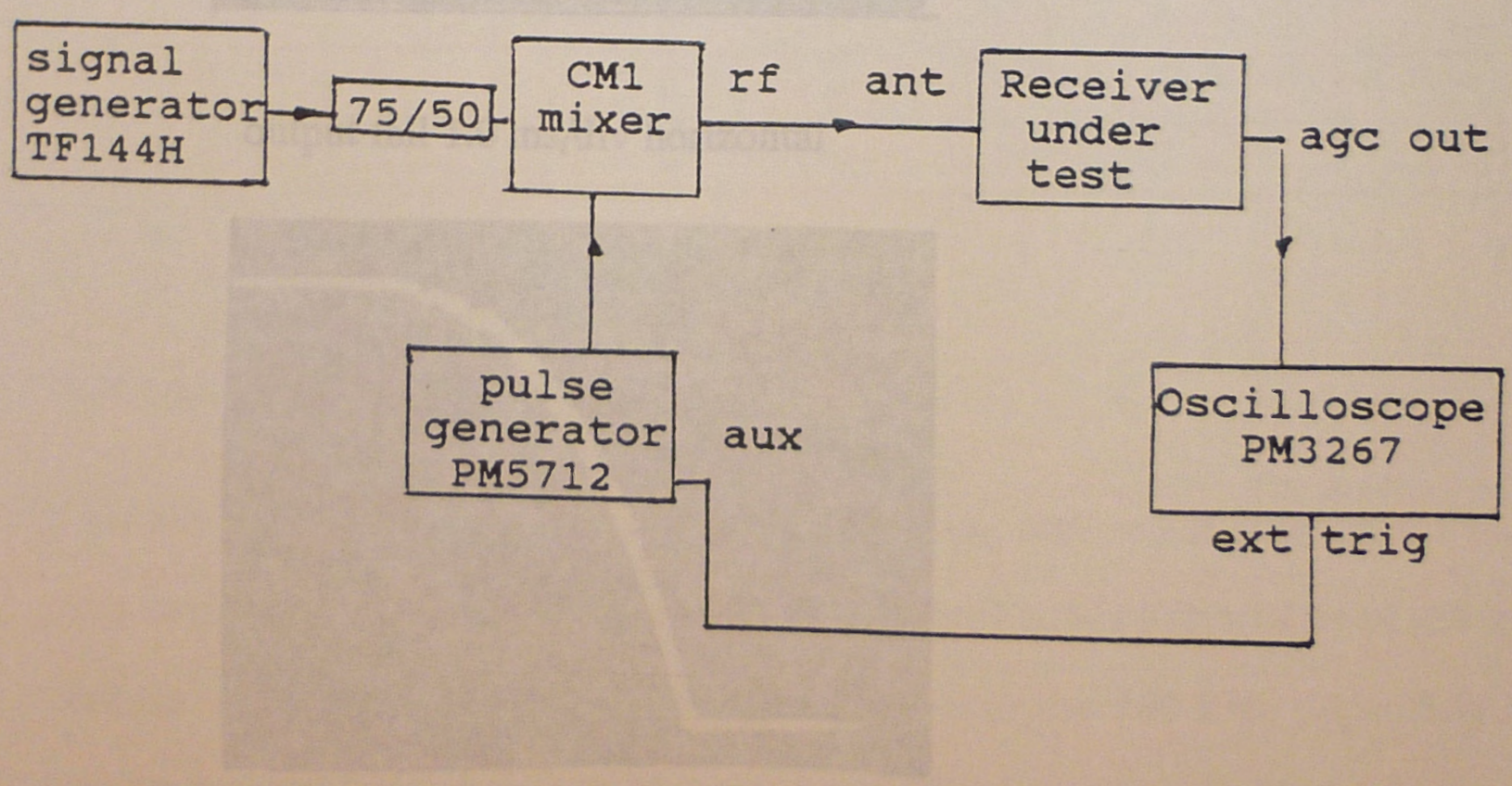

input signal to receiver rise and fall times < 1us

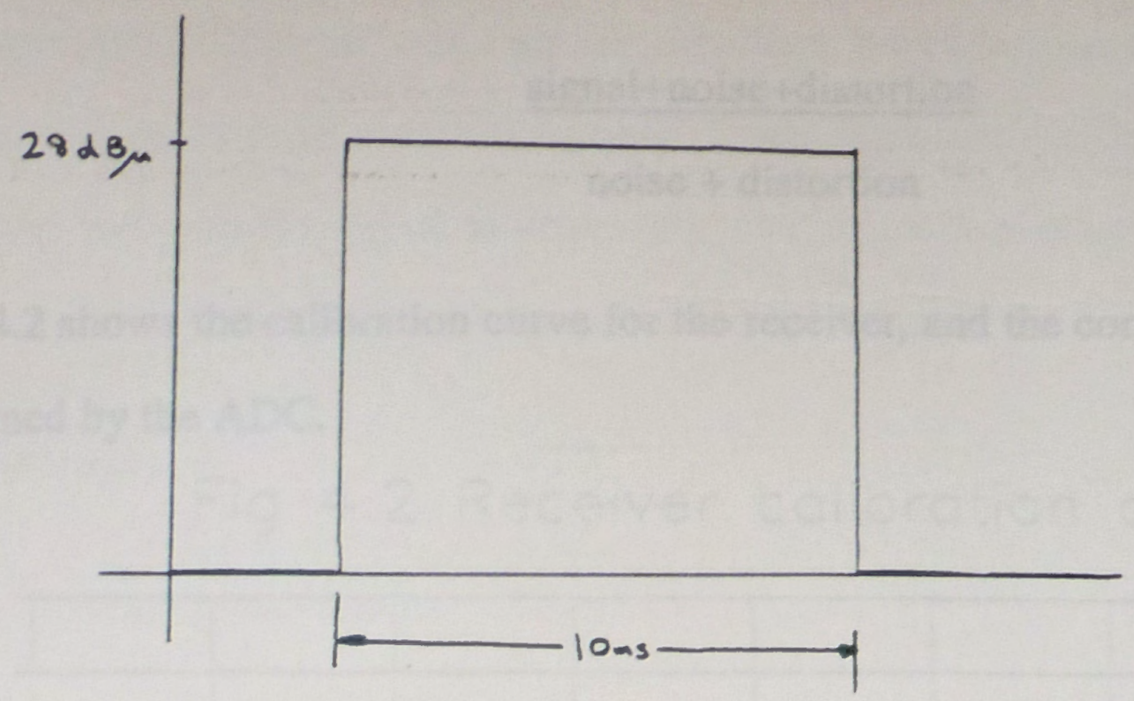

output rise 0.1 ms/div horizontal

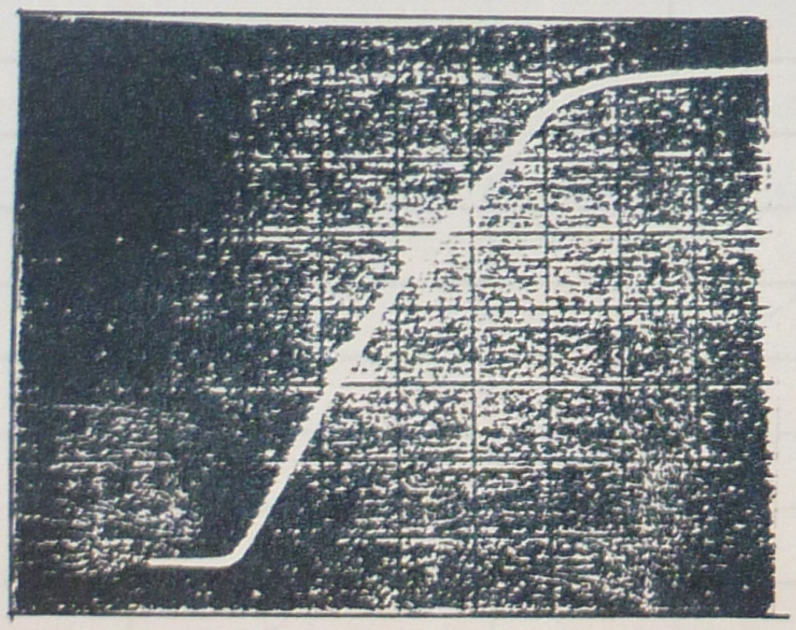

output fall 1.0 ms/div horizontal



The sensitivity of the receiver was measured as 0.3 microvolts for 12 dB SINAD at 70.67MHz. (All signal voltages rms in a 50 ohm line)

SINAD is defined as the ratio of

$$\frac{\text{signal+noise+distortion}}{\text{noise + distortion}}$$

Fig 4.2 shows the calibration curve for the receiver, and the corresponding HEX values returned by the ADC.

Fig 4.2 Receiver calibration chart

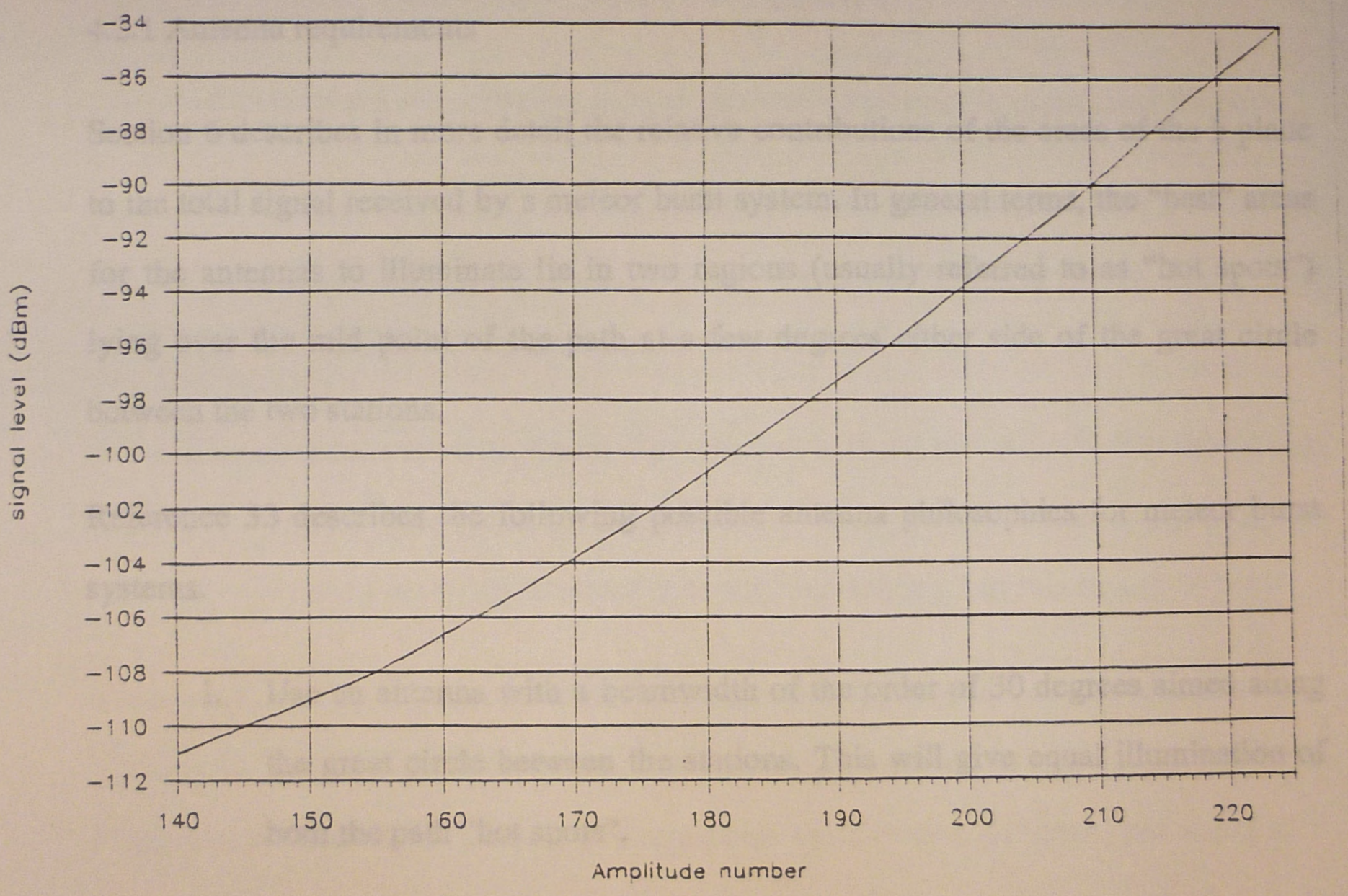

Note on the choice of receiver.

It should be noted at this point that the signal being received is wide band FM with a peak deviation of 75kHz. This means that the signal bandwidth will be of the order of 180kHz. The power will be distributed throughout the 180 kHz depending on the baseband signal being transmitted at the time of the burst. The receiver is designed for 12.5kHz channel spaced mobile radio and hence the IF filter will remove much of the sideband power. This means that there could be large inaccuracies in the measured

absolute signal levels. This experiment is only concerned with a relative measurement of signal level from the same source therefore the change in absolute amplitude will affect both paths in an identical manner. It was therefore decided to use a narrow band receiver and gain the signal to noise ratio and adjacent channel rejection improvement at the expense of loss of absolute amplitude accuracy.

4.2 Antennas

4.2.1 Antenna requirements

Section 6 describes in more detail the relative contributions of the areas of the h plane to the total signal received by a meteor burst system. In general terms, the "best" areas for the antennas to illuminate lie in two regions (usually referred to as "hot spots") lying over the mid point of the path at a few degrees either side of the great circle between the two stations.

Reference 33 describes the following possible antenna philosophies for meteor burst systems.

I. Use an antenna with a beamwidth of the order of 30 degrees aimed along the great circle between the stations. This will give equal illumination of both the path "hot spots".

II. Use an antenna with a beamwidth of about 10 degrees, and steer it gradually to follow the diurnal variations of the path "hot spots"

III. Use a dynamically steerable antenna with a beamwidth of< 0.5 degrees to pick out the single active trail.

It is clearly impossible without physically large antennas to achieve (II) or (III), at 70 MHz. Small antennas such as single yagis with relatively wide azimuth and elevation beamwidths will therefore only "favour" each of the two path geometries described in

this report. Each will illuminate a large area of the plane where the majority of the scattering sources will occur. (See appendix (b) for antenna patterns used in the experiment). Some overlap of patterns is inevitable, with the end point antenna receiving mid point signals and vice versa. The experiment follows the philosophy of investigating the possible effects of the two path geometries with the sizes of antennas that would be utilised with small transportable systems.

The antenna system must, though, meet three main criteria:

I. It must have sufficient gain to produce a measurable signal over the path.

II. There must be sufficient isolation between the elevation polar patterns for each to favour the path geometry being observed. (In future this will be referred to this as the antenna discrimination.)

III. It must not be so physically large that it is not representative of the type of antenna that could be used in a simple inexpensive remote monitoring site as used in the applications mentioned in section 2 of this report.

Clearly (I) and (II) are directly related, and increasing the gain will also sharpen the H plane polar diagram. It is this polar diagram that is important in this application when horizontal polarisation is used, as this represents the elevation pattern of the antenna.

With reference to (III) A five element Yagi has a boom length of 0.8 wavelengths (29), this corresponds to about 3.2 metres at 70 MHz. It was considered that this size was typical of the antennas used in remote sites and it was decided to investigate the performance of a system based on such an antenna. In an effort to keep the project costs to a minimum, it was decided to use antennas designed for the amateur radio market. The performance of such antennas is generally as good as, if not better than, equivalent professional systems, as they are designed for a market requiring maximum performance related to size and cost. The cost reduction is inevitably at the expense of

poorer mechanical construction. This is possible as most amateur radio antennas are not generally used in the high wind or ice loaded environments experienced on hill top professional communications sites.

Five element Yagi-Uda arrays to US National Bureau of Standards specification (29) supplied by MET antennas Ltd and fed via identical lengths of Uniradio UR67 coaxial cable were used. Details of their theoretical free space polar patterns are given in appendix (b). In the main experiment performed in Cambridge one antenna, hereafter referred to as the end point antenna, was mounted with the boom vertical, pointing to the zenith. The other antenna, hereafter referred to as the mid point antenna, was mounted at a height of 19 metres above ground on a brick chimney. This placed it 4.5 wavelengths above the ground and in theory the system should have a pattern null to the zenith.

For the second experiment with the fast data logger performed at the Mullard Radio Astronomy Observatory, the mid point antenna was mounted at a the correct height above ground to give a take off angle of 8 degrees to illuminate the mid point, and the end point antenna was mounted one quarter wavelength above ground to maximise its upward radiation.

Appendix (b) shows the predicted vertical polar pattern of the system, and its "footprint" on the meteor plane.

The following practical point in favour of end point operation should be noted here. In most systems, the elevation pattern of the end point antenna is likely to be well known, whereas the mid point antenna pattern is likely to be highly uncertain at low elevations. This is due to the effect of obstructions and ground reflections.

4.2.2 Factors affecting the performance of the practical antenna system.

The environment surrounding an antenna is the main factor affecting its performance in a radio system. Surrounding objects can affect its performance in two ways:

I. Modification of polar pattern due to reflections from the ground and surrounding objects.

II. Degradation of match due to proximity of conducting objects such as the antenna support structure, the ground and surrounding buildings.

The effects of (II) may be measured easily using swept reflection techniques, and steps taken to reduce problems by careful siting and use of non metallic supports. Match degradation usually only occurs if the object is closer than a few wavelengths. A few basic rules such as using support structures at right angles to the plane of polarisation of the antenna or, if the diameter of the mast is of the same order as the wavelength, use of mountings behind the reflector of the array (end mounting).

In the low VHF region with horizontally polarised antennas as used in this experiment, the mast may pass through the centre of gravity of the boom without noticeable match degradation, allowing secure, balanced, mechanical mounting. Reference (30) describes measurements to confirm these assumptions.

It can also be stated that if the antennas meet criteria (I), no match degradation should be apparent.

To tackle the problem of measuring the effects of (I) on the discrimination of the Cambridge antenna, two approaches were used:

I. Measure the discrimination directly by remote signal strength measurements and plotting the polar patterns in situ.

II. Monitor the signals from the meteor burst source and identify bursts received by one antenna and not the other.

Two further approaches based on measurements on a scale model or a theoretical model of the antennas and environment were considered but rejected as beyond the scope of this project.

4.2.3 First experiment to confirm antenna isolation

It should be noted that these experiments were carried out on the antennae used in the main experiment only. The site at Barton used for the second experiment was a flat field with few obstructions, and it was considered that the antennae should perform even nearer to their free space performance in such a situation, and a repeat of the experiments was considered unnecessary.

In the first experiment two carefully matched receivers were used, one connected to each of the antennas, and their output agc voltages compared in a differential amplifier. This enabled a plot of the difference between the signal amplitudes from each antenna to be made by recording the difference voltage on a chart recorder. If the discrimination between the antennas was poor there would be only slight variation in the difference amplifier output on reception of a burst. On the other hand, if the discrimination was good, definite “end point only” or “mid point only” transitions should be seen on the difference output.

The experiment was run from 2000 to 0000 GMT on 4/11/85 and a section of the resulting plot is shown in fig 4.3.The continuous offset of the output from zero is due to the higher noise level on the horizon pointing (mid point) antenna. As can be seen there are a number of transitions above and below the mean line which seem to indicate independent bursts on each antenna system.

Fig 4.3 Section of plot from experiment to determine antenna discrimination by recording difference between signal levels from mid and end point antennas.

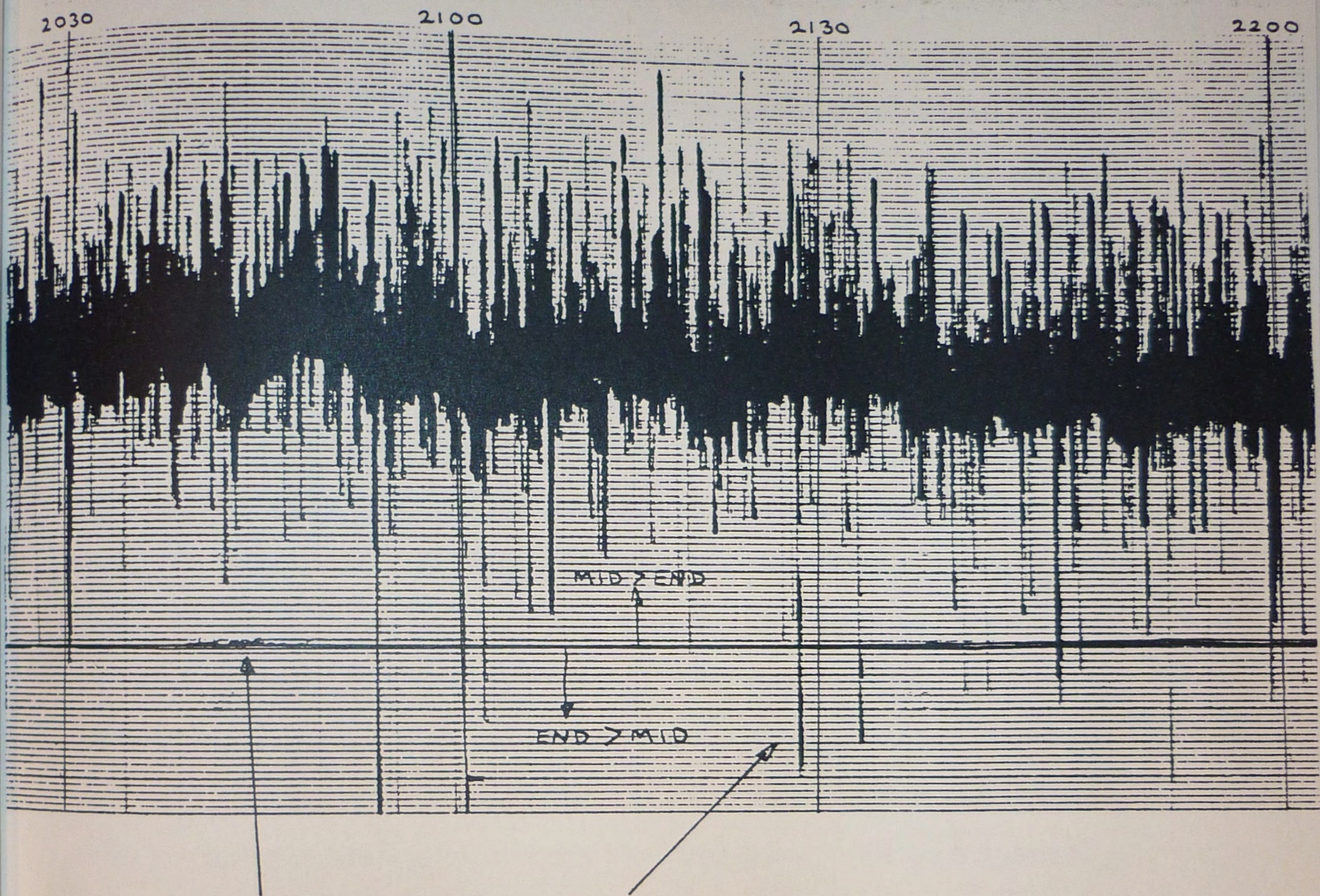

4.2.4 Second experiment to measure elevation discrimination between endpoint and midpoint antenna.

The antenna system was pointed on a bearing of 85 degrees that is about 5 degrees north of the great circle between Cambridge and Wroclaw to maximise the morning received signal (31). Reference to Ordnance Survey 1:50 000 series sheet 154 shows that the region in an arc from bearing 45 degrees to 135 degrees from the experiment site (TL461584) is a relatively flat featureless plain for a radial distance of approximately 20 km at 45 degrees with a rising ridge at this distance as one travels in a southerly arc. The only major obstruction is the Wandlebury ridge at Limepit hill (TL507552) on a bearing of about 120 degrees.

By following the A142 south from Soham to Newmarket and then the B1061 to Balsham it is possible to drive along this ridge and be in line of sight of the antenna system and on its approximate horizon by choosing hill top sites. A mobile transmitter and antenna system was taken along this route and a series of comparative signal strength measurements were taken from each antenna at the experiment site in Cambridge. Each transmission was made using a horizontal half wave dipole oriented for maximum received signal. To act as a comparison, transmissions were made from the same site using a vertical quarter wave monopole in the centre of the car roof. This was being used for communicating by voice to the main antenna site. The frequency used was 70.3MHz, as near as practicable to the experiment frequency but within the UK amateur radio allocation. The difference between the received signals on the mid point antenna pointing approximately at the horizon and the end point antenna pointing overhead, and its variation with azimuthal angle gives a measure of the elevation discrimination of the antenna system. The results are presented graphically in fig 4.4. The points marked with a circle were based on measurements on paths over the ridge mentioned earlier. This probably explains the fact that they seem to stray away from the general shape of the plot.

The graph shows the discrimination increasing as we move into the main lobe of the antenna system reaching a maximum of about 25 dB at a bearing of 80 degrees (10 degrees north of east) coinciding well with the physical azimuthal orientation of the antenna system.

Reference to appendix (b) shows that the H plane pattern at 90 degrees from the main lobe is 15 dB down on the main lobe in free space.

This second experiment therefore seems to confirm that the elevation discrimination between the two antennas will enable each to favour its particular path geometry.

Fig 4·4 Antenna Discrimination

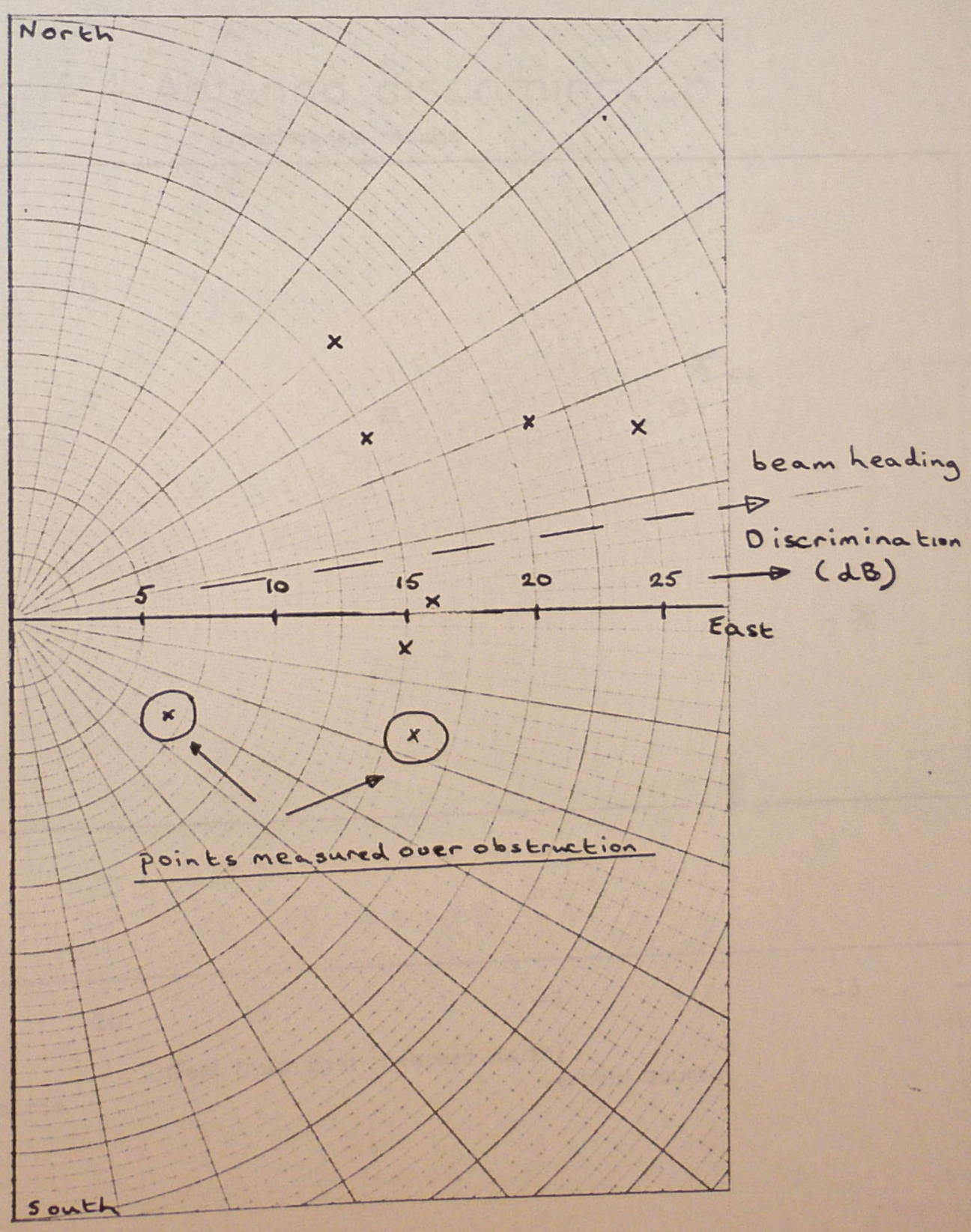

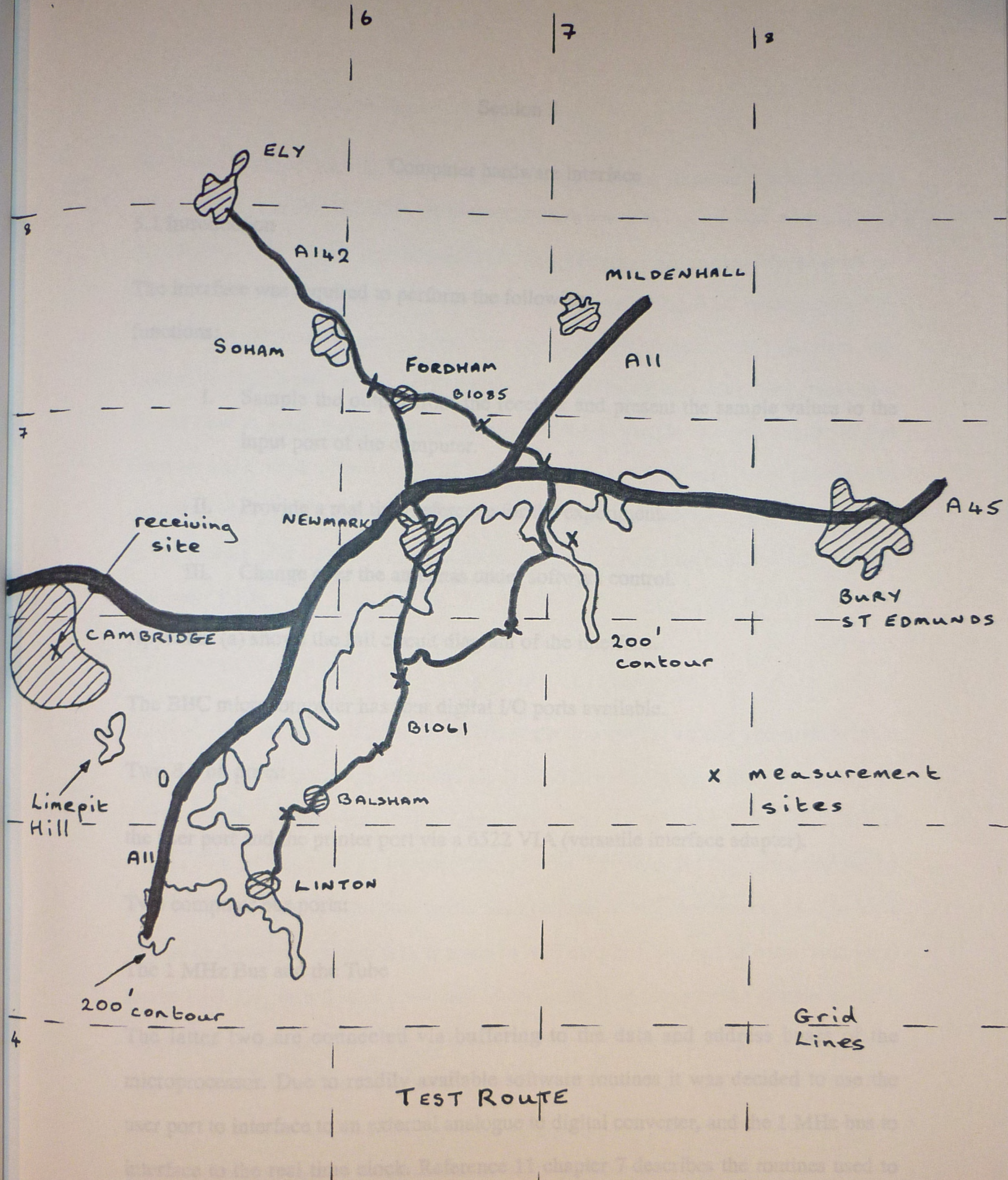
6
7
8
ELY
8
A142
MILDENHALL
SOHAM
FORDHAM
B1085
A11
7
receiving site
NEWMARKET
A45
BURY ST EDMUNDS
CAMBRIDGE
200' contour
B1061
X measurement sites
Limepit Hill
A11
BALSHAM
LINTON
200' contour
Grid Lines
4
TEST ROUTE

Section 5

Computer hardware interface

5.1 Introduction

The interface was required to perform the following functions:

I. Sample the output from the receiver and present the sample values to the input port of the computer.

II. Provide a real time reference for the experiment.

III. Change over the antennas under software control.

Appendix (a) shows the full circuit diagram of the interface.

The BBC microcomputer has four digital I/O ports available.

Two 8 – bit ports:

the user port and the printer port via a 6522 VIA (versatile interface adapter).

Two computer bus ports:

The 1 MHz Bus and the Tube

The latter two are connected via buffering to the data and address buses of the microprocessor. Due to readily available software routines it was decided to use the user port to interface to an external analogue to digital converter, and the 1 MHz bus to interface to the real time clock. Reference 11 chapter 7 describes the routines used to read the 1MHz bus, and reference 12 appendix 7 describes the basis of the user port routines.

5.2 Analog to digital conversion

The output voltage from the receiver representing the signal amplitude varies from 0 to 5 volts and a readily available 8 bit converter will allow a change of 5/28 or 19.5mV to be detected. This is more than adequate for the application, and to simplify the software this one byte per sample representation was adopted. The ADC was required to perform its conversion every 5 ms and signal to the processor that the data was available. The sample rate of 5ms was chosen after discussions with other researchers in this field at RAE Farnborough, confirmed that this sample rate was similar to that used on their work. The results of testing the system with associated software as described in section 5.6.2 confirmed that this sample rate was adequate. Any increase in the sample rate would have reduced the amount of data that could be stored in the computer RAM.

5.2.1 Circuit description

U3 is an 8 bit analog to digital converter, controlled by U6, a clock and divide circuit with a 3.2768 MHz crystal reference x2. A 200Hz square wave (reference divided by 214) provides the start conversion signal every 5ms for U3. The main ADC clock at U3 pin 3 is provided via an inverter from U6 pin 7 a 409.6kHz (reference divided by 2). This sets the conversion time (nine clock periods) to to 22 microseconds. The ADC signals to the computer that data is ready to read via pin 1, the end of conversion (eoc) to the CB1 line (pin 2 user port), and at the same time presents the sample to the 8 input lines of the user port. Timing delays from CB1 to reading the port are enough to ensure the data is settled on the ADC output before it is read. Reference to lines 600 and 610 of routine METOR12 (appendix c(ii)) show two instructions amounting to 6 processor clock cycles or 3 microseconds before the port is read.

5.3 Real time clock

The experiment required date and time information to be stored with the data, to allow the production of plots of meteor activity over the proposed 12 month period. Three solutions to the problem were considered.

I. The "TIME" function in the BBC micro

II. The 60kHz MSF time standard at Rugby

III. A battery backed real time clock integrated circuit.

The first solution was rejected initially as the long term accuracy of the TIME function depends on the accuracy of the computer clock crystal oscillator. Reference 11 advises against its use for long term timing. A second problem is providing backup in the event of power failure.

The second solution looked promising, as the time standard is very accurate and self setting in event of power failure at the clock. The hardware to decode the signals into a form that may be read by computer, or to decode the signals in software is possible but necessarily complex. The problem of decoding the signals using the BBC microcomputer was in fact set as a project for a second year HND student, and based on his early work, the idea was abandoned in favour of the third solution.

5.3.1 Circuit description

The real time clock circuit, U4, uses a 32.768kHz crystal X1 as reference and contains date and time information down to tenths of seconds in fourteen registers. Each may be read by presenting the correct address to four address lines on pins 9 to 12. These address lines connect to the corresponding address lines of the 1MHz bus. The contents of each register are presented at the data output lines, pins 4 to 7 of U4, and to the corresponding data input lines of the 1MHz bus. The clock requires chip select (cs) read (rd) and write (wr) signals which are active low. These are available from the 1MHz bus pin 10 (cs) and pin 2 (r/w). Inverter U2b provides separate rd and wr from the r/w line. U1 is used to clean up the cs signal from the BBC micro as timing problems may occur under certain conditions and the reasons for this are described in detail in reference 4. The circuit was not tried without this clean up circuit but it was thought to be good practice to include the few extra components to avoid possible problems.

A problem arose with the battery back up circuit for the real time clock. When the power was removed, the control lines pulled low and caused false reads and writes, corrupting the time data in the registers. To overcome this problem the three lines cs, rd and wr were buffered by U5, a CMOS quad analog switch, and pull up resistors r11, r12, r14 were fitted on the lines. The enable pins (U5 pins 6, 12, 13) for all three switches are fed at half the unprotected supply voltage via r9 and r10 , this allowed the switches to open before the supply dropped to zero, effectively isolating U4 control lines from the 1MHz bus in the event of a power failure.

5.4 Antenna change-over relay

It was initially decided to use two separate receivers for the experiment but this idea was rejected due to difficulties matching the performance of each. It was decided to switch the antennas with a coaxial relay. This removes some uncertainty of calibration

and means that any drift in performance in the receiver will be reflected in the results from both antenna systems. As this experiment is concerned with a relative measurement of signal characteristics this becomes insignificant. The only possible causes of error are changes in performance of the antenna systems or change-over relay.

5.4.1 Switching circuit

Q1 is fed from the CB2 line of the microcomputer to enable the antenna change-over relay to be activated by the computer. The relay is situated on the radio receiver chassis. The antenna change-over relay is a 951 type 50 ohm coaxial relay as used in many low loss antenna change-over applications in mobile radio equipment. It was modified by fitting 3 BNC connectors to replace the coaxial cable entry terminations, as these have proved unreliable in past experience. Measurements on the modified relay at 70MHz showed a loss of less than 0.2 dB, an isolation between ports of 44 dB and an input return loss of greater than 25 dB at each port.

5.5 Modifications for second experiment.

5.5.1 Objectives of modification

To achieve a tenfold increase the in sample rate of the ADC.

5.5.2 Details of modification

The modified interface is shown in appendix (a2). The modification consists of taking the 204800 Hz output from U6 and passing it through cascaded 4018 divide by ten counters U7, U8, to produce a 2048 Hz clock for the ADC. This produces a sample time of 488.28 μs.

5.6 Data logger software

5.6.1 Introduction

A BBC model B microcomputer with 32K of RAM was chosen for the project, solely because it was available in the department. It represented at the time the "top end" of the home computer market. As will be seen, this choice placed severe restrictions on the work that could be done, due to speed and memory capacity, but the results obtained proved that the restrictions were not insurmountable. The information required from the received signal is as follows:

I. The average number of bursts per unit time

II. The peak amplitude of the bursts

III. The duration of the bursts

As described in section 5.1, it was required to take one 8 bit measurement of the incoming signal every 5ms. This meant that the internal analog to digital converter in the BBC could not be used, as it requires approximately 10ms to perform a single conversion, not allowing any time to store the sample. Simple timing experiments showed that with an external ADC the BASIC programming language available on the BBC was too slow to perform the sampling and storage procedure. It was therefore decided to use 6502 assembly language and the BBC assembler. Reference 11 describes the facilities available.

A few simple calculations showed that to store all the samples from the receiver would be totally impractical and unnecessary. To estimate the data storage capacity required, an average burst duration of 0.58s and approximately 10s between bursts was assumed, (9) giving approximately 60480 bursts per week, if the waveform was stored only when a burst occurred. This meant 35078 seconds of signal and at 200 samples per second,

each sample represented by one byte of data, giving in excess of 68K bytes per week. To store this amount of data, a Winchester hard disc or an almost weekly change of floppy disc would be required. Both were discounted as impractical on cost and convenience grounds. There was the second problem that, even with a Winchester hard disc as mass storage, it would not be possible in 200ms, to store each sample individually to disc in real time. It was decided therefore, to try to reduce the data stored to a minimum, without losing its statistical significance. Allowing about 2K of RAM for the Basic Program and variable storage leaves 24k available as RAM for temporary data storage.(refer to Appendix (f) and ref 13 for memory map of the BBC micro). This corresponds to only 2 minutes of real time sampling of signal. It was therefore decided to sample and store the signal from each antenna for two out of five minutes, and to use the 24K of available RAM as a "scratch pad" to store the two minutes of samples in real time (2x60x200 bytes = 24kbytes). This would then allow the remaining three minutes for the computer to switch antennas, sort the samples, detect bursts, measure their peak amplitude, duration, and number of bursts in the period. These three items then could be stored in a different RAM location and the 24K re-used for the next two minutes of data. The next problem was to decide where to store the assembler code for the sampling routine. As the cassette tape filing system is not required for this application, it was decided to use its working area of memory to store the code. (See Appendix (f)). Appendices (c)(i) and (ii) describe in detail the final form of the software for sampling and storage.

5.6.2 Sampling software development

BBC BASIC was used for all high level software, as it was resident in the machine available for the project. Note that a structured approach has been used for the BASIC programs. BASIC has a bad reputation for being an unstructured language, but the dialect used in the BBC enables the writer to use procedures in a similar way to structured languages such as PASCAL. Wherever possible a structured approach to the

assembler language programming has been used, by breaking the problem into blocks and testing each block individually before tying the whole together.

As the first stage of the design it was decided to attempt to read the user port and print on the screen if the number presented to the port was greater than 100. A routine was written to store the numbers in a table in memory, under control of the CB1 line. The numbers input via switches were replaced with an external ADC controlling the CB1 line and analog values read in.

The next stage was to add routines to measure the analogue voltage and decide how long it stayed above a preset threshold. Initially, signal thresholds less than 50ms were ignored as non valid. This would help the software to discriminate against false triggers caused by impulse noise.

To test the routine under real conditions the output from the radio receiver was connected to the ADC and its input fed with a switched RF signal at a level sufficient to produce a voltage at the ADC input varying from 1 to 4.2 Volts. Initially, a 100ms square wave was used for two minutes (a total of 600 pulses of RF), and the routine returned a value of 600 for counted “bursts”. Pulses of 40ms width at 100ms intervals were then used to check that the software ignored any pulses less than 50ms. As expected the routine returned a zero value. Finally, 56ms pulses at 100ms intervals were used and the routine again returned 600 “bursts”.

Next, the facility to measure burst amplitude and duration from the stored data needed to be added. The amplitude was measured by finding the maximum value in the stored burst, and the duration by counting the number of samples that were above a preset amplitude threshold. It was decided to keep a cumulative store of burst lengths and amplitudes and divide the total time (or amplitude) by the number of bursts in the period to produce an average. This required storing the total durations and amplitudes

as two bytes. The routine returned a representation of the number of bursts, and their cumulative amplitude and duration. It could save the data from one hour in this form.

The next stage was to store this information to floppy disc. Floppy disc was chosen as the main storage medium on grounds of cost and easy access, the sorted data being dumped to a file every hour under the control of the real time clock.

5.6.3 Disc filing routine.

The BBC filing system uses 5 bytes to store an integer and 6 bytes to store a real number. It was decided to arrange the file thus:

Filename "DDMM" ie 13 January would be 1301

File contents:

Hour header.....integer number from 00 to 23

midpoint average length.....real

midpoint average amplitude.....real

midpoint number of bursts.....real

endpoint average length.....real

endpoint average amplitude.....real

endpoint number of bursts.....real

: repeated 5 more times per hour

: Next hour header

etc

ie 246 bytes per hour.

The complete file then contains data that represents an average value of each quantity based on the data from the first two minutes of each ten minute period. The mid point data taken from minutes 1 and 2 and the end point data from minutes 6 and 7. This

format would enable a future data analysis program to read the data using a pointer to count position in the file and use the hour headers if required. The averaging of each period's data was done in BASIC for ease of programming as time was available in the three minutes between sampling periods. The data reduction is necessary to make efficient use of the storage medium and reduce the cost of the system by enabling use of inexpensive floppy discs.

5.7 Modifications for second experiment

5.7.1 Objectives of modification

To allow for a reduction in the minimum length of burst that can be detected to the order of 10ms by a tenfold increase in the sample rate.

To improve the system's ability to overcome the problems of noise caused by this increase.

5.7.2 Details of modification

The modified control program and code for the data logger are listed in appendices c(i) and c(ii).

To allow for the increase in data rate, and the limitation in size of computer RAM, the modified system monitored the receiver output for 12 seconds from 30 and wrote to disc every 10 minutes.

The control program produces the following new file layout:

tenhour/tenminute header.....integer number from 0 to 235 *

midpoint average length.....real

midpoint average amplitude.....real

midpoint number of bursts.....real

endpoint average length.....real

endpoint average amplitude.....real

endpoint number of bursts.....real

: repeated 9 more times per ten minutes

: Next header

etc

ie 410 bytes per ten minutes

* eg a header of '0' would represent data from the 10 minute period from 2350 to 0000, '1' the period from 0000 to 0010, and '225' the period from 2240 to 2250 etc.

The assembler code was modified to test a threshold transition to not only see if it met a criteria for minimum time above a threshold (10ms) but also that it ended by staying low for a given length of time (40ms). This was done to discriminate against impulse type signal transitions being logged as large numbers of short bursts. It would also allow single bursts with short fades to be logged as such instead of as a number of short bursts.

This modification is justified by the fact that the waiting time between real meteor bursts is much longer that their durations.

The software was extensively tested by applying known signal bursts to the system in a similar fashion to the tests described in section 5.6.2.

The actual values of 10 and 40 ms were found to be optimum by making measurements on real signals with the amplitude threshold set close to the noise level and examining the effect of varying the two times.

Section 6

System Calculations

The experimental work in this project provided data on the burst amplitude, frequency and duration differences between the mid point and end point meteor burst paths between Cambridge and Wroclaw. These values will then be compared with values calculated from present theory.

The section will first consider the properties of a single trail, and assume that it lies in the plane parallel to the earth on the great circle line joining the two ends of the path. Two extreme cases will be considered, one with the trail at the zenith for one end of the path, and a second with the trail over the path mid point. It will then go on to consider the properties of the whole signal, taking into account the probability of detection of a suitable trail, enabling a comparison of path usability to be made for each system geometry.

6.1 Path loss

6.1.1 Simple model

The paper by Sites (6) predicts a path loss reduction for an end point path of 1000Km of 3.8dB. To enable this statement to be checked we need to apply equation (viii) appendix (d) using the calculated values of R_t ,R_r and $\varnothing$ for each path geometry. As a comparison between losses and not an absolute value is needed a "Normalised path loss" is defined based on the following assumptions:

I. Unity gain transmit and receive antennas $G_t = G_r = 1$

II. Electron density of trail $q = 10^{14}$ electrons per metre

(a typical value for an underdense trail)

As this calculation would be likely to be repeated frequently, a BASIC program "LOSITES" was written to handle the calculation. It required the input of system frequency, great circle path length, and trail orientation. This is described in appendix (c)(v), and as can be seen, calculates the values of R_r ,and R_t from the input data.

During the development of this program it was realised that Sites had made the following assumptions to arrive at the 3.8dB figure for end point improvement.

I. A fixed trail height of 100 km

II. Zero initial trail radius

III. Both path geometries are such that the system operates above the transition wavelength mentioned in appendix (d)

IV. All trails are transverse ($\beta = 90°$)

The difference between transverse and in line trails is defined in section 2.4.1. Assumption IV is based on Eshleman's reasoning (25) which suggests that with an assumed isotropic distribution of meteor radiants ,that the majority of trails will be transverse. He argues that setting the term $\cos^2\beta \sin^2\phi = 0$ ((appendix (d) equation (vii) will produce an error only comparable with the other uncertainties in the model.

The results of two runs of the program are shown in Tables 6.1 and 6.2.

Table 6.1 is for the 1000km path at 50MHz used by Sites.

Comparing the results shows the 3.8dB loss reduction on the end point path as predicted in (6), but for trails in line with the path ($\beta = 0$) we see the reverse effect, the mid point path having a reduced loss of some 6.5 dB compared to end point. If we now apply the calculations to the path used in the experiment at 70.67 MHz and a range of 1173 Km, we get the results in Table 6.2. Note the 4.5 dB reduction in loss for the end

point path using transverse trails and the 6.6dB increase for the end point for in line trails.

Table 6.1 Normalised path losses for 1000km path at 50MHz

Assuming simple loss model, both paths below transition frequency

mid point loss (dB)		end point loss (dB)	
β= 0	β= 90	β= 0	β= 90
171.3	184.0	177.8	180.2

for β= 0 end > mid by 6.5dB

for β= 90 end < mid by 3.8dB

Table 6.2 Normalised path losses for 1173km path at 70.67MHz

Assuming simple loss model, both paths below transition frequency

mid point loss (dB)		end point loss (dB)	
β= 0	β= 90	β= 0	β= 90
177.0	190.5	183.7	186.0

for β= 0 end > mid by 6.7dB

for β= 90 end < mid by 4.5dB

6.1.2 Effect of trail height and initial trail radius

The effects of assumptions (I) and (II) were then examined. To this end a second program was written, "LOSJCW" (appendix (c)(v)) this included a calculated value for the aforementioned parameters.

Trail height

Trail formation begins when the meteor enters the region of relatively dense air at a height of approximately 120 km, and most particles are totally burned out by the time they reach 85 km.

The average trail height (h) in Km is related to the system frequency (f MHz) as below (21):

$$h = -17\log f + 124$$

This is an empirical formula based on measurements by Greenhow and Hall (32). They found an approximate Gaussian distribution of the number of echoes versus height. It replaces the fixed value of 100 km in the program.

Initial trail radius

As the frequency of the incident wave increases, the initial radius of the trail becomes significant when compared to the wavelength, and may not be assumed to be zero (appendix (d)). The rate of diffusion increases with height due to the decreasing atmospheric density, therefore the initial trail radius r_0 is related to trail height.

Ref 21 gives this relationship as:

$$\log r_0 = 0.035h - 3.45$$

Once again this is an empirical formula based on measurements from ref 32. This was included in the path loss calculation and the results for the same conditions are shown in Tables 6.3 and 6.4

Note that in Table 6.3 the end point advantage has reduced to 1.1 dB for transverse trails and the mid point advantage for in line trails has increased to 9.6 dB.

Table 6.4 shows the results of the calculation on the path of 1173 km at 70.67MHz used in the experiment. The end point advantage for transverse trails is now only 0.9 dB, and the mid point advantage for in line trails is now 10.7 dB. These results begin to cast doubts about the practical significance of the end point advantage as proposed in (6) if the figures are verified in practice.

Table 6.3 Normalised path losses for 1000km path at 50MHz

Assuming actual trail height and initial trail radius both paths below transition frequency

mid point loss (dB)		end point loss (dB)	
β= 0	β= 90	β= 0	β= 90
171.2	184.2	180.8	183.1

for β= 0 end > mid by 9.6dB

for β= 90 end < mid by 1.1dB

Table 6.4 Normalised path losses for 1173km path at 70.67MHz

Assuming simple loss model, both paths below transition frequency

mid point loss (dB)		end point loss (dB)	
β= 0	β= 90	β= 0	β= 90
176.8	190.7	187.5	189.8

for β= 0 end > mid by 10.7dB

for β= 90 end < mid by 0.9dB

6.1.3 Effect of transition wavelength

Below a specified wavelength, the effects of the time for formation of the trail must be taken into account in the path calculations. This is defined more fully in appendix (d).

We must now examine the effects of operation of a system at or below this transition wavelength. We must also look at the effects of path geometry on transition wavelength (λ_t), (or transition frequency f_t).

A BASIC program was written (FTRANS2 appendix (c)(vii)) to plot transition frequency against path length for end point or mid point paths both for the case of transverse and in line trails. The results are shown in Figs 6.1 to 6.4. (The frequencies quoted on the x axis refer to the values used to calculate the effective trail height and hence diffusion constant.)

Fig 6.1 Midpoint transition frequency

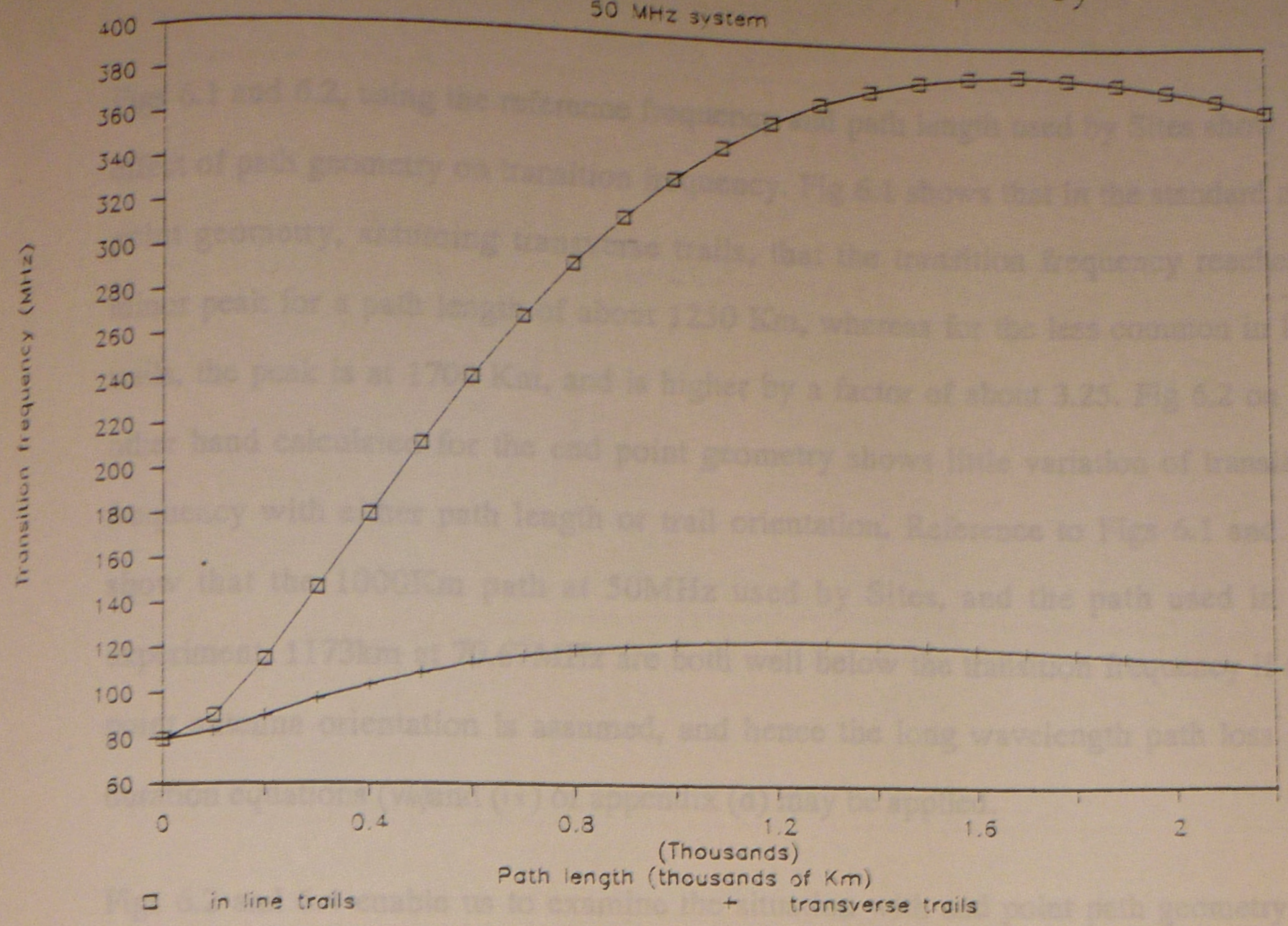

Fig 6.2 Endpoint transition frequency

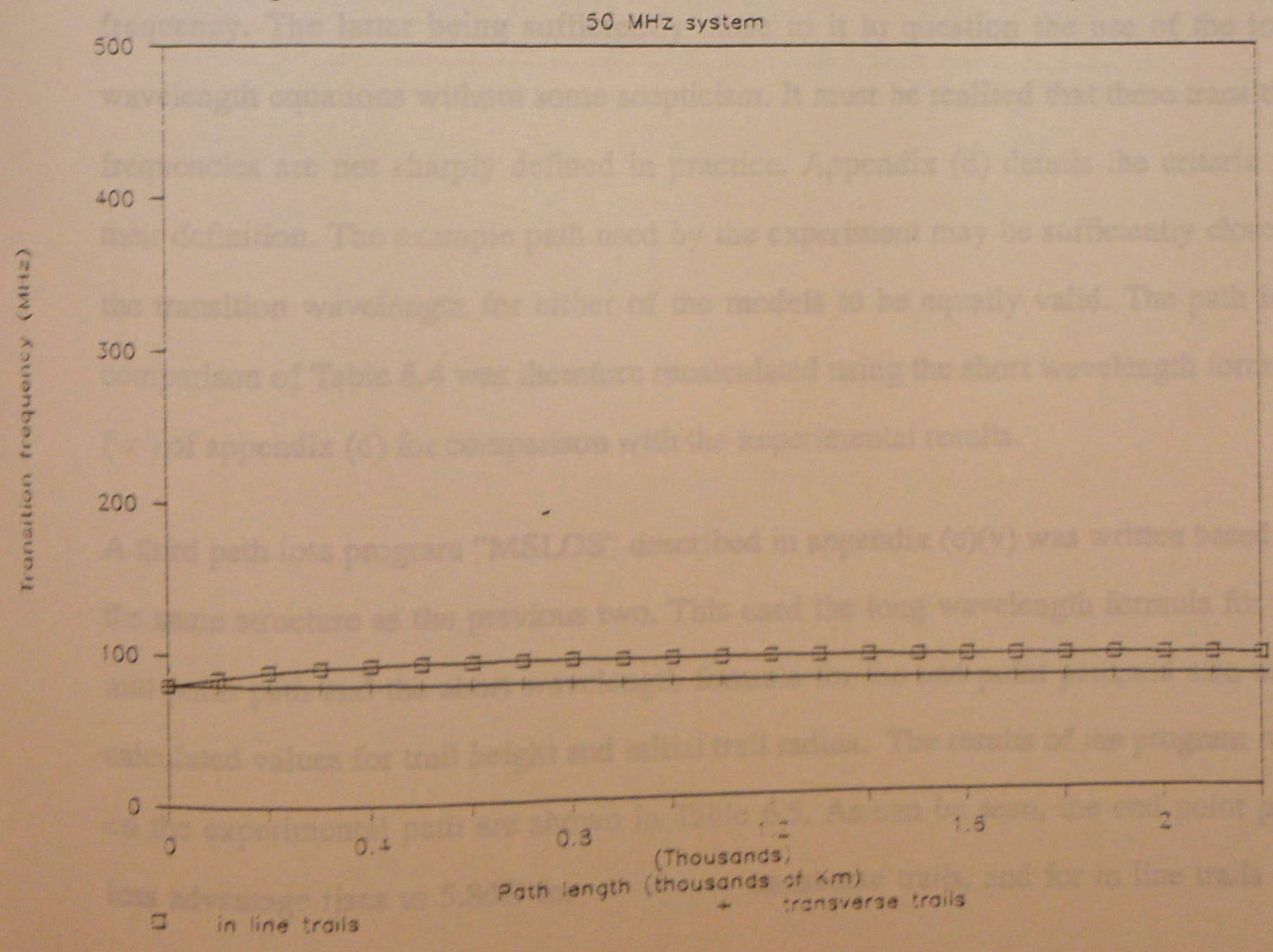

Figs 6.1 and 6.2, using the reference frequency and path length used by Sites show the effect of path geometry on transition frequency. Fig 6.1 shows that in the standard mid point geometry, assuming transverse trails, that the transition frequency reaches a minor peak for a path length of about 1250 Km, whereas for the less common in line trails, the peak is at 1700 Km, and is higher by a factor of about 3.25. Fig 6.2 on the other hand calculated for the end point geometry shows little variation of transition frequency with either path length or trail orientation. Reference to Figs 6.1 and 6.3 show that the 1000Km path at 50MHz used by Sites, and the path used in the experiment, 1173km at 70.67MHz are both well below the transition frequency if mid point antenna orientation is assumed, and hence the long wavelength path loss and duration equations (viii)and (ix) of appendix (d) may be applied.

Figs 6.2 and 6.4 enable us to examine the situation with end point path geometry for the two examples. Fig 6.2 shows that both the reference 1000Km 50MHz path and the 1173 km, 70.67 MHz path from Cambridge to Wroclaw also lie below the transition frequency. The latter being sufficiently close to it to question the use of the long wavelength equations without some scepticism. It must be realised that these transition frequencies are not sharply defined in practice. Appendix (d) details the criteria for their definition. The example path used by the experiment may be sufficiently close to the transition wavelength for either of the models to be equally valid. The path loss comparison of Table 6.4 was therefore recalculated using the short wavelength formula (x) of appendix (d) for comparison with the experimental results.

A third path loss program "MSLOS" described in appendix (c)(v) was written based on the same structure as the previous two. This used the long wavelength formula for the mid point path and the short wavelength formula for the end point path,and also used calculated values for trail height and initial trail radius. The results of the program runs on the experimental path are shown in Table 6.5. As can be seen, the end point path loss advantage rises to 5.8dB for transverse trails, and for in line trails the

Fig 6.3 Midpoint transition frequency

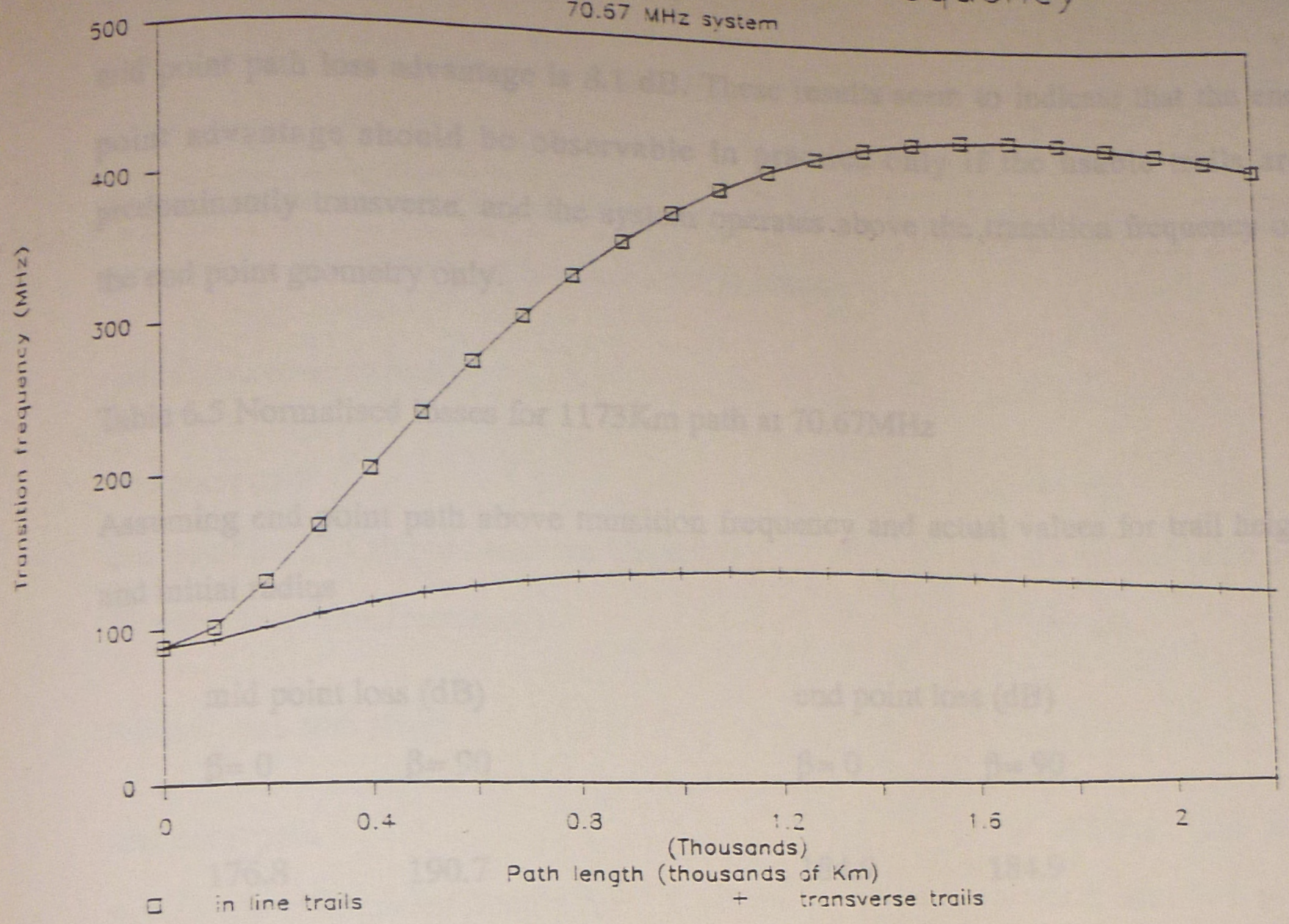

Fig 6.4 Endpoint transition frequency

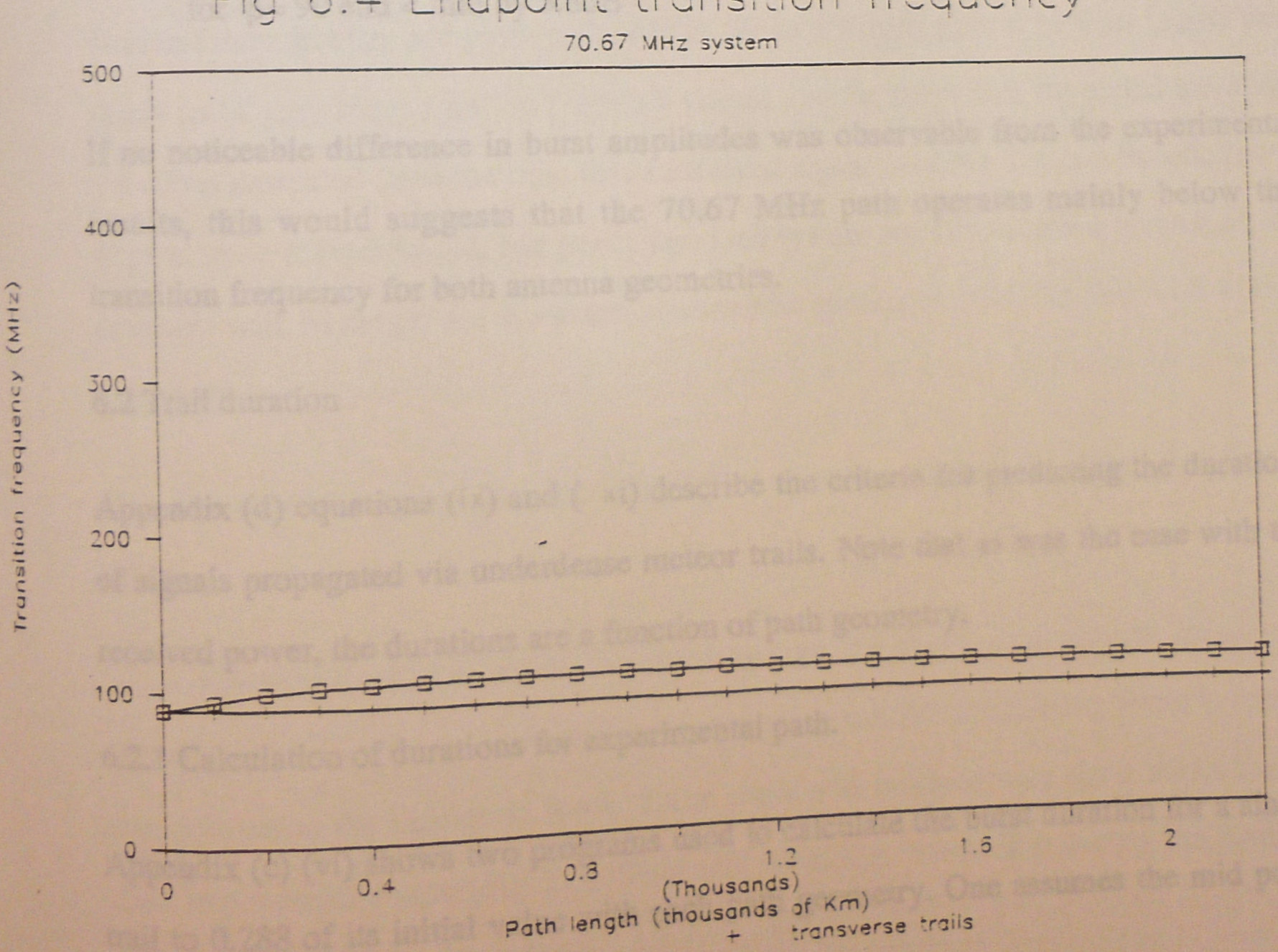

mid point path loss advantage is 8.1 dB. These results seem to indicate that the end point advantage should be observable in practice only if the usable trails are predominantly transverse, and the system operates above the transition frequency on the end point geometry only.

Table 6.5 Normalised losses for 1173Km path at 70.67MHz

Assuming end point path above transition frequency and actual values for trail height and initial radius

mid point loss (dB)		end point loss (dB)	
β= 0	β= 90	β= 0	β= 90
176.8	190.7	184.9	184.9

for β= 0 end > mid by 8.1dB

for β= 90 end < mid by 5.8dB

If no noticeable difference in burst amplitudes was observable from the experimental results, this would suggests that the 70.67 MHz path operates mainly below the transition frequency for both antenna geometries.

6.2 Trail duration

Appendix (d) equations (ix) and (xi) describe the criteria for predicting the durations of signals propagated via underdense meteor trails. Note that as was the case with the received power, the durations are a function of path geometry.

6.2.1 Calculation of durations for experimental path.

Appendix (c) (vi) shows two programs used to calculate the burst duration for a single trail to 0.288 of its initial value with each path geometry. One assumes the mid point

path is above the transition wavelength, the other assumes both paths are below. The 0.288 criteria is chosen for both conditions, by using appendix (d) equation (ix) , for the below transition wavelength case and a scaled equation (xi) for the above transition wavelength case. The values produced are as follows:

(trails transverse to path)

Mid point path = 446 ms

End point path (if above transition frequency) = 8.5 ms End point path

(if below transition frequency) = 30.5 ms

(trails in line with path)

Mid point path = 446 ms End point

path (if above transition frequency) = 13.3 ms End point

path (if below transition frequency) = 30.5 ms

It seems then that the end point path used in the experiment should have its usable time made up of very short duration bursts. It should also be noted that the actual measured durations extracted from the time that a received signal is above a preset threshold will depend upon that threshold, and hence upon the system sensitivity. For a given trail, the duration will be larger for a system with a low threshold than for one with a high threshold.

This fact should produce an interesting effect upon the measured average duration of trails:

If the power budget of a link is increased by, say, an increase in antenna gain, more meteor trails will appear above the measurement threshold, the number being inversely proportional to the change in level. These trails will produce very short bursts due to their exponential shape (Fig 2.1). This will have the effect of reducing the average

burst duration. The trails that were already above the threshold will lengthen by an amount proportional to the logarithm of the change in level. The duration decrease will therefore predominate, causing the average duration to fall with increasing antenna gain or transmitter power/receiver sensitivity.

The ratio between the mean trail durations for the two path geometries is therefore of more interest in this experiment than the absolute values.

6.3 Probability of detection of trails and path duty cycle.

So far in this section, only the properties of a single reflection from a trail have been considered. The communications systems designer must be concerned with the properties of the total signal over a period of time.

To this end, a third factor must be considered when analysing the performance of a meteor burst path. The number of usable trails per unit time. This can then be combined with the individual trail durations and amplitudes to give a measure of the duty cycle of a link.

Duty cycle is defined as the percentage of total time that the received signal is above a preset threshold.

Section 2.4.3 described the requirements for trails to be oriented tangential to a prolate spheroidal surface with transmitter and receiver at the foci for specular reflection to occur.

The number of usable trails will depend upon the following factors:

I. Average arrival rate of meteors

II. Position of the trail radiant in the sky

III. Path geometry with respect to the meteor radiants

IV. Antenna radiation pattern

I. This factor is readily available in Ref (31)

II. For sporadic meteors, there are two possible approaches. Eshleman and Manning (4) assumed isotropic distribution meteor radiants, whereas Meeks and James (23) analysed the effect of assuming meteor radiants concentrated in the plane of the ecliptic. Davies(36), made measurements of this radiant distribution, and Rudie (37) derived a model for Davies's results in the form of a set of closed form equations. The first approach has been tested by a number of authors, most recently by Nes (22), and found to give good results on path lengths in the region of 1000km. The second, more general approach has been used recently by Weitzen (38) and Brown (33). This has enabled them to produce much better models of short range meteor burst systems, and highlighted the duty cycle advantages of end point antenna systems on these paths.

The position of the single radiant that characterises shower meteors can be predicted accurately, and the effects of a particular shower accounted for.

III. The time of day and year, and the latitude and longitude of the path ends specify the orientation of the path with respect to the meteor radiant. The evaluation of the probability density of detection p, even for isotropic meteor radiants is purely geometric, and somewhat involved. Appendix (e) outlines the steps involved, for a model of the first kind assuming isotropic distribution of radiants, and evaluates p in terms of x and y co-ordinates in the h plane (a plane containing the midpoints of the trails). This enables contour maps to be plotted to show the relative contributions to meteoric rate of areas of the h plane. Such maps showing one of 4 symmetrical quadrants of the h plane have been plotted for a 1000km path (4). It should

be noted that there is an elliptical "hole" over the path mid point where the probability of detection is low. This is explained by the fact that trails with the correct orientation in this area would have to be travelling almost parallel to the surface of the earth. There is a ridge of high probability forming an ellipse enclosing the transmitter and receiver locations.

IV. The previous section points to the relevance of the antenna radiation patterns. The total number of usable trails can be found by summing the number of trails per second over the "footprint" of the antenna radiation pattern on the h plane. This number of trails will vary depending upon the area of the h plane illuminated. For example a narrow beamwidth antenna aimed at the mid point "hole" will detect fewer trails than one aimed at some part of the high probability ridge. As the burst amplitudes and durations are also geometric functions of the position of the reflection on the h plane (Appendix (d)), similar contour maps could be drawn for each of these quantities, and the characteristics of the propagated signal could be evaluated.

Fig 6.5 probability duration factor

for 1173km path Cambridge – Wroclaw

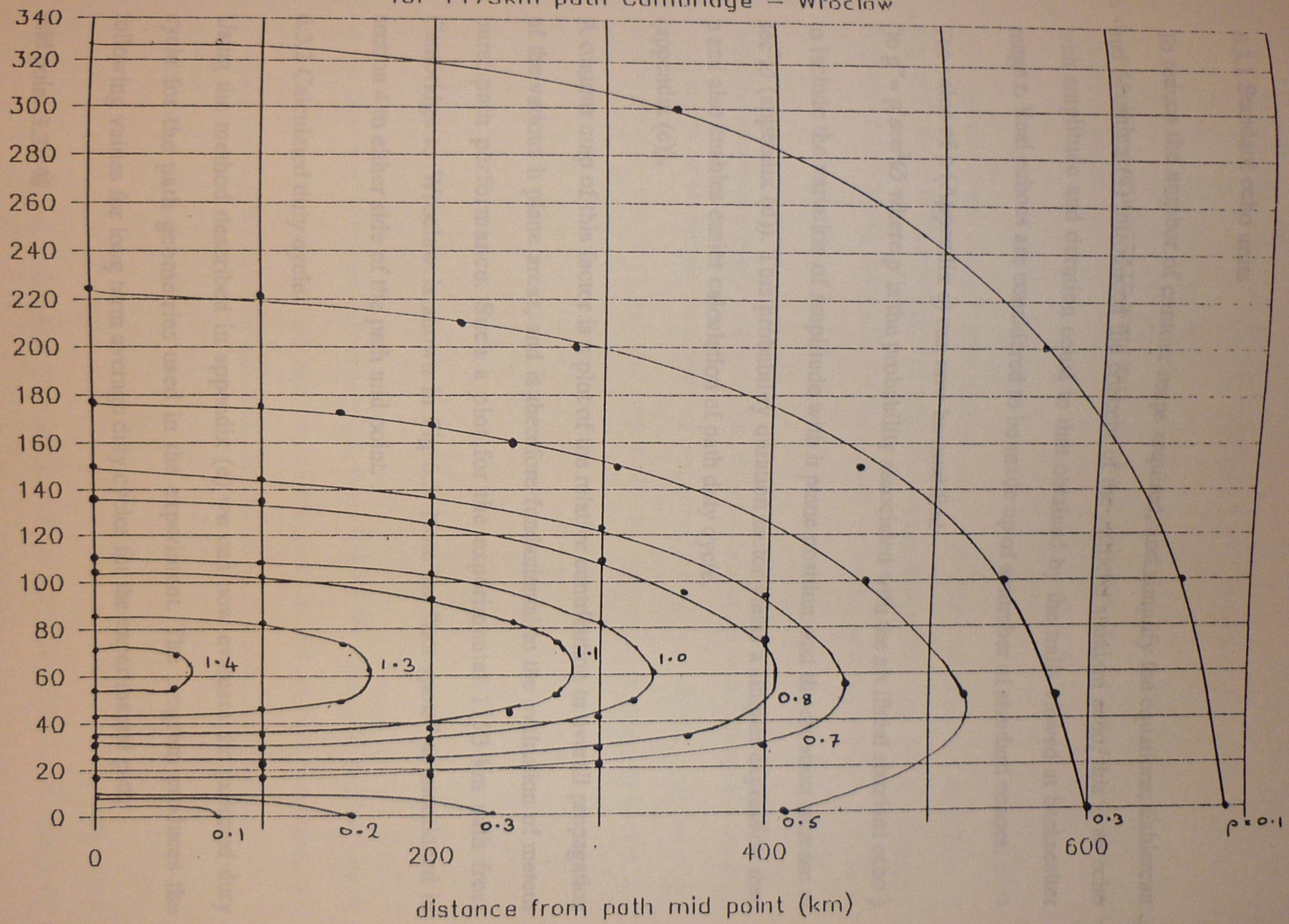

6.3.1 Standard echo units

To reduce the number of contour maps required, and simplify the equations, Eshleman and Manning (4) introduced the concept of the artificial standard echo, this is an echo with amplitude and duration equal to that obtained by the trails viewed at backscatter range r. Real echoes are considered to be made up of a number of standard echoes.

The value of p (Appendix e) can now be modified

(to $p'' = p' \sec^2 \varnothing$ where p' is the probability associated with the art ificial standard echo)

to include the variation of amplitude with h plane position, and the duration increase of $\sec^2 \varnothing$ (appendix (d)). This probability duration factor yields a simpler expression than p and also enables easier calculation of path duty cycle.
(appendix (e)).

A contour map of this factor is a plot of the relative contribution to overall propagation of the various h plane areas, and is therefore fundamental to the evaluation of meteor burst path performance. Such a plot for the experimental 1173 km path from Cambridge to Wroclaw is shown in Fig 6.5. Note the "hot spots" as mentioned in section 4 to either side of the path mid point.

6.3.2 Calculated duty cycle

Using the method described in appendix (e) we can now evaluate the expected duty cycle for the path geometries used in the experiment. The program produces the following values for long term average duty cycles for the experimental path:

mid point 3.34 %

end point 0.81 %

A 4 to 1 advantage in duty cycle for the mid point path geometry.

Section 7

Experimental results

7.1 Introduction

This section presents the results of the two main experiments, based on data gathered over a period from August 1986 to February 1988 from the original data logger at Anglia College, in Cambridge, and from July to October 1989 on the improved system at the Mullard Radio Astronomy Observatory at Barton near Cambridge. It aims to cover the main objectives described in section 3.1 of this report.

In the measurements made in Cambridge, the raw data as stored consisted of arithmetic mean values of amplitude, duration and number of bursts over a two minute out of ten minute period, from each antenna system. In the measurements made at Barton, the averages were taken over a 12 second period out of 30 seconds. This choice for storage was imposed by the limited random access memory of the BBC microcomputer. Section 5 describes the philosophy behind the data logger and shows how the fast calculation of the short term arithmetic mean was achieved.

As the data was averaged before storage, the shape of the statistical distributions of burst length and amplitude are not true distributions of the original quantities, the averaging tending to distort the distributions towards a Normal distribution.

7.2 Measurement thresholds

Various combinations of amplitude and duration threshold were tried throughout the experiment, as these determine the absolute values of burst duration so measured. Reference to Figs 2.1 and 2.2 (section 2) will clearly show that a duration measurement based on time above a threshold will depend on the level at which that threshold is set.

For the purposes of this experiment, where a ratio of amplitudes and durations is required, their absolute values are of less importance.

In the early part of the experiment to May 1987 the measurement thresholds were set such that signals above 0.5μV (-113dBm) for more than 50ms were counted as valid bursts. This was based on the measured local noise level and the predicted typical burst durations for the mid point signals. During the experimental run in May, calculations showed that the expected values of end point duration would be considerably less than 50ms, so the duration threshold was reduced to 15ms, and data gathered. This level was determined to be the lowest sensible value that could be achieved without major modifications to hardware and software to increase the system sample rate. This meant that a 15ms burst was only three samples, so these results must be treated with some caution. Some 15ms data was also gathered with a higher amplitude threshold of 1.05μV. This represents an increase of 6.5dB to –106.5dBm, and is summarised in Tables 7.7 to 7.9 for comparison.

The 1989 data gathered by the modified data logger had a duration threshold of 10 ms, corresponding to 20 samples, and an amplitude threshold of –110dBm. This was some 10 dB higher than the level of background noise at the Barton site.

7.3 Presentation of results

The raw data as described in section 7.1 was further examined statistically to obtain long term median values for mean duration and amplitude of the received signals over the measurement interval (2 minutes for the Cambridge measurements and 12 seconds for the Barton measurements).The mean value was also calculated as a representative average of the original data. As the data logger itself only stores a mean value over the measurement interval, the analysis is based on distributions of these mean values. It would be incorrect to quote this as a median of the original data, as the median of a selection of mean values is not a true median of the original data. A “mean of means”

is though a true mean. The original design of the data logger therefore precludes the calculation of true median values, even though they would have been a better measure of average, as they are less affected by extreme values. The distribution shapes plotted from the amplitude and duration data will differ from those expected for plots of raw burst data. Due to the averaging, the expected exponential distributions will tend towards a normal distribution.

The results are presented in a number of ways, as follows :

7.3.1 Daily plots of burst frequency and duty cycle.

The first data analysis programs written were designed to produce daily graphical plots of meteor activity, in the form of number of bursts per 2 minute period, and amplitude and duration against time for the two path geometries. This would enable the user to note the daily variations and also see short term events such as meteor showers or Sporadic E (Es) events. Appendix (c) (iv) describes the programs. Note the use of many common procedures.

Fig 7.1 shows an output from "NUMBERS" clearly showing the daily variation in meteor activity.The peak in the early morning at around 0600 and the minimum around 1800 can clearly be seen, as can the period of closedown of the Radio Wroclaw transmitter.

The day displayed was February 8 1987 during a period of the year at the minimum of the sporadic meteor activity, and outside any of the major showers. As a comparison, Fig 7.2 shows a plot taken under the same conditions, but on the 8th of August 1987, a time of year when the random meteor activity is high, but away from any major shower peak. It can be clearly seen that the general level of activity is higher, but the same diurnal variation is obvious.

The effect of a shower peak is shown in fig 7.3, a plot taken over the peak of the 1986 Geminids shower. The large morning peak is again present, but a second evening peak in activity shows clearly with a pronounced minimum at 1400. This can be compared with the E – W column of the computer predicted activity histogram fig 7.4, showing relative activity against time and azimuth and elevation of shower radiant. We see the same variation in activity, with the morning and evening peaks, and the minimum at 1400 when the shower radiant is below the horizon.

Fig 7.1 Typical plot of bursts per minute : 8th Feb 1987

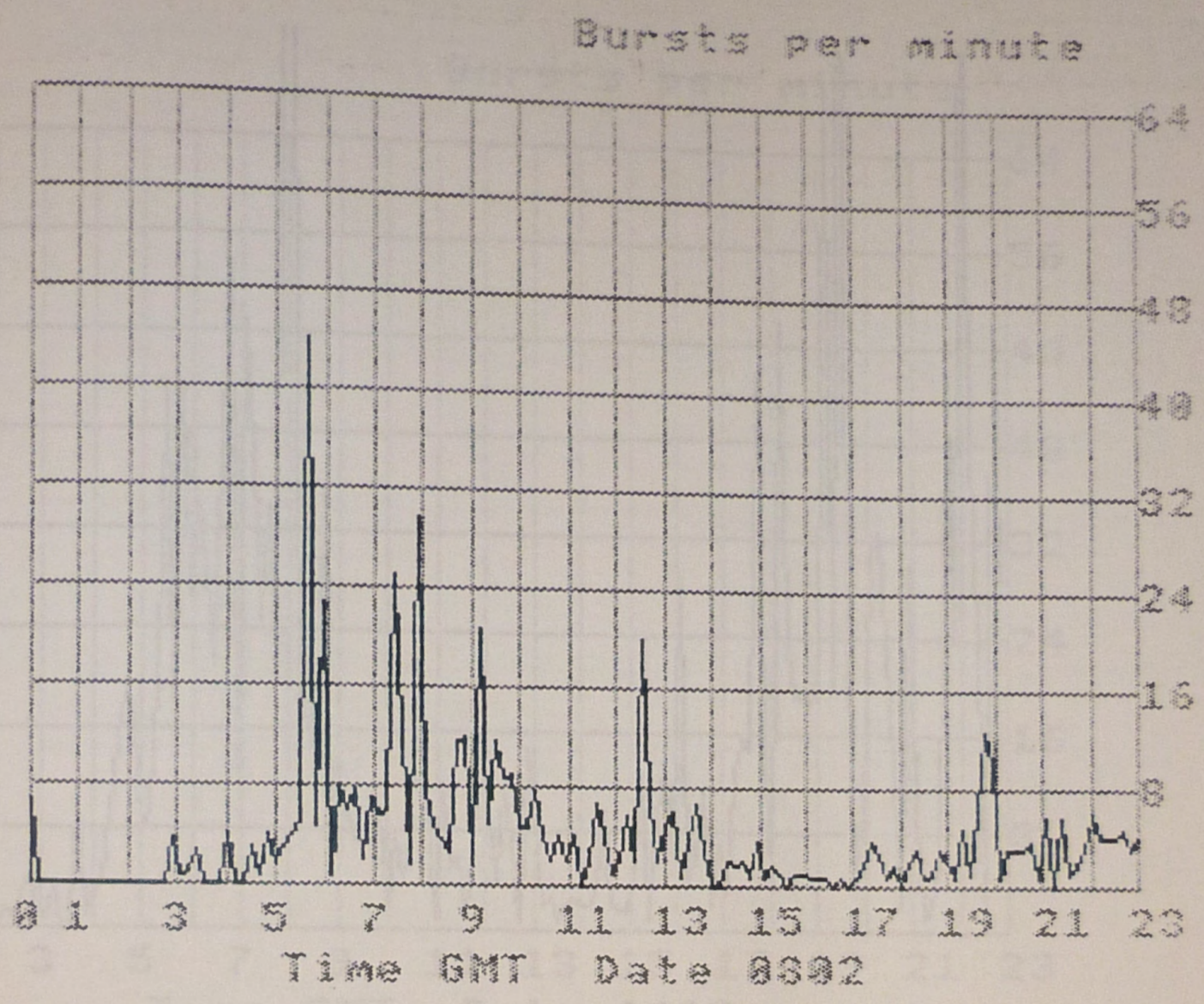

Fig 7.2 Typical plot of bursts per minute : 8th Aug 1987

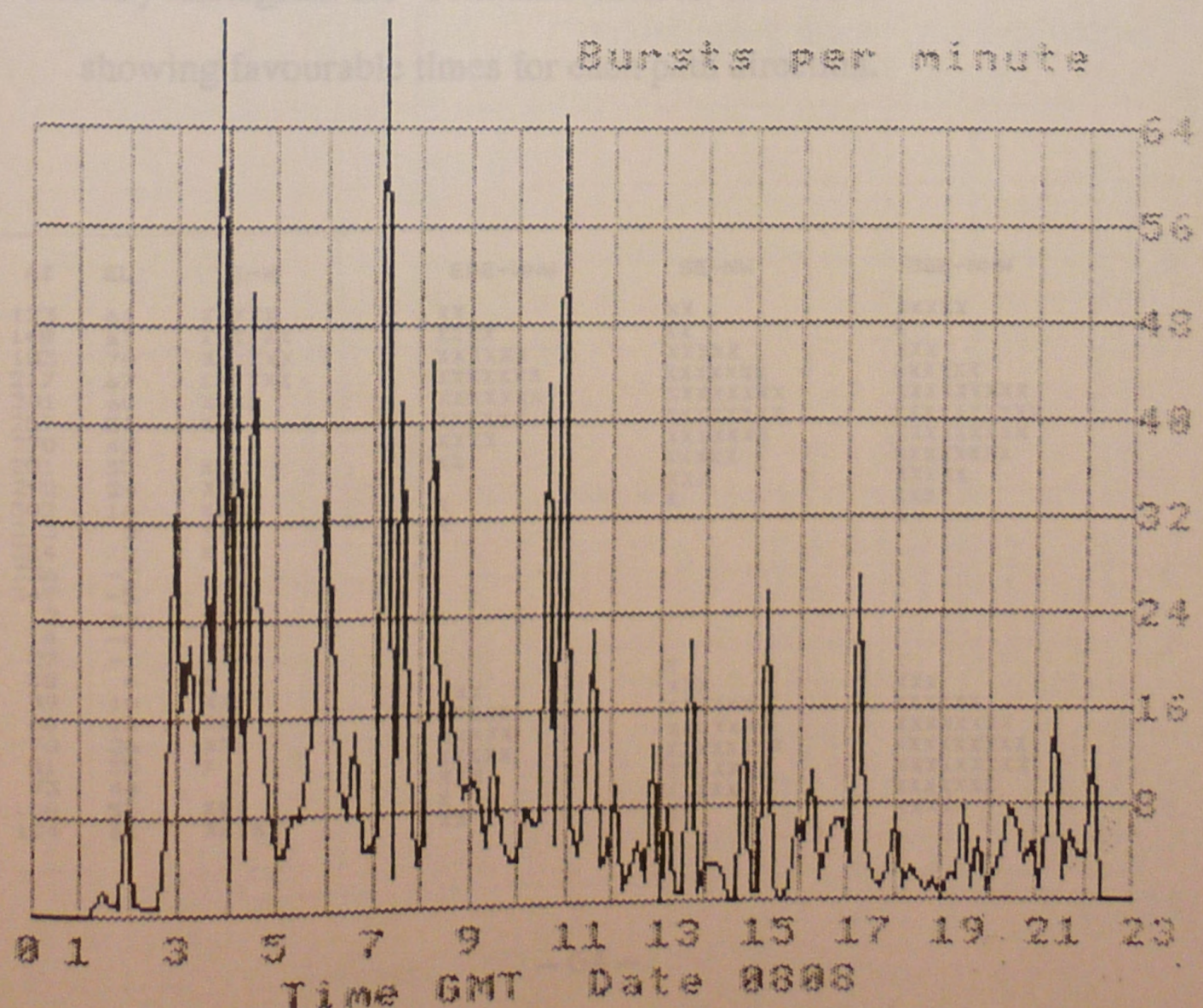

Fig 7.3 Typical plot of bursts per minute : 14th Dec 1986

Showing effect of peak of Geminids meteor shower.

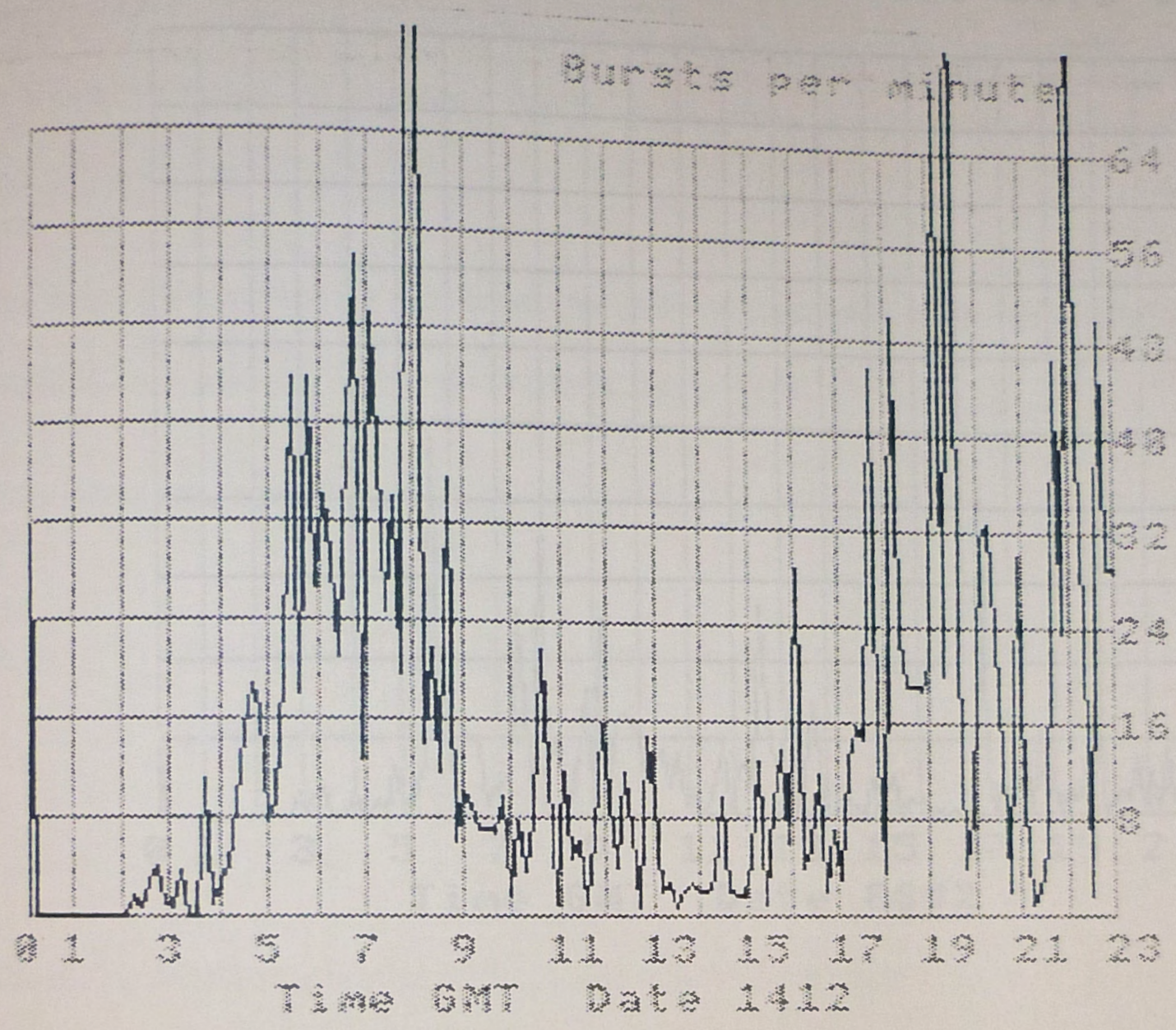

Fig 7.4 Activity Histogram for Geminids meteor shower

showing favourable times for each path direction.

HRS	AZ	EL	E-W	ESE-WNW	SE-NW	SSE-NNW
00	123	61	XXXXX	XX	XX	XXXXX
01	148	67	XXXXXX	XXXX	XX	X
02	183	70	XXXXXX	XXXXXX	XXXXX	XXX
03	217	67	XXXXXX	XXXXXXX	XXXXXXX	XXXXXX
04	241	60	XXXX	XXXXXXX	XXXXXXXX	XXXXXXXXX
05	257	51	XX	XXXXXX	XXXXXXXX	XXXXXXXXXX
06	270	42		XXXX	XXXXXXX	XXXXXXXXX
07	281	33	XX	XX	XXXXX	XXXXXXXX
08	292	24	XXX		XXX	XXXXX
09	302	16	XXX	X	X	XXX
10	313	8	XX	X		X
11	324	2	X			
12	336	-2				
13	349	-5				
14	2	-6				
15	14	-4				
16	27	-1		X	X	X
17	38	4	X	XXX	XXX	XXX
18	49	10	XX	XXXXX	XXXXXX	XXXXXX
19	60	18	XXX	XXXXX	XXXXXXX	XXXXXXXX
20	70	26	XXX	XXXXX	XXXXXXXX	XXXXXXXXX
21	81	35	X	XXX	XXXXXXX	XXXXXXXXX
22	93	44		X	XXXXX	XXXXXXX
23	106	53	XXX	XX	XX	XXXXX
24	124	61	XXXXX			

Fig 7.5 Typical plot of daily duty cycle : 8th Feb 1987

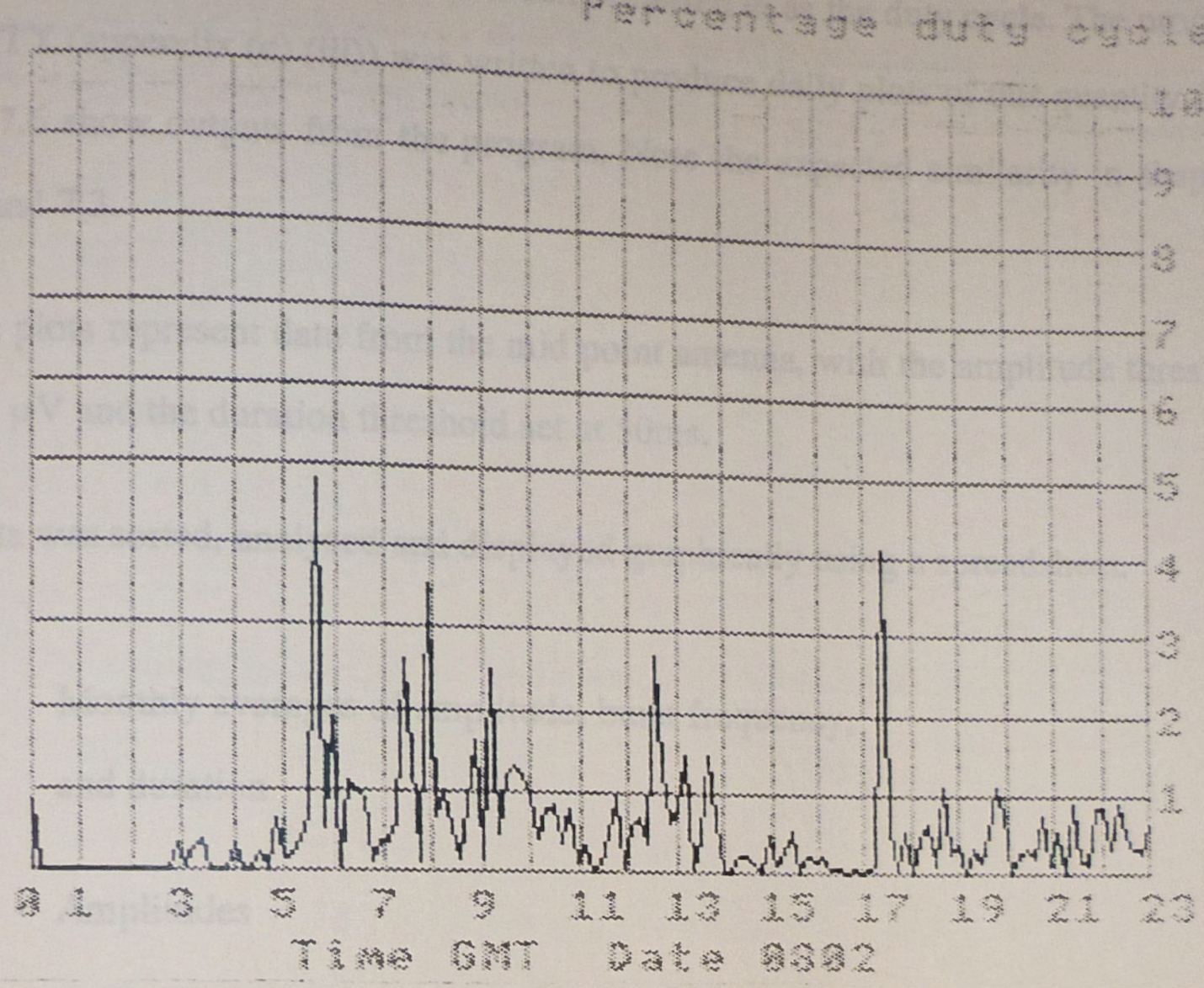

Fig 7.6 Typical plot of daily duty cycle : 14th Dec 1987

Showing effect of peak of Geminids meteor shower.

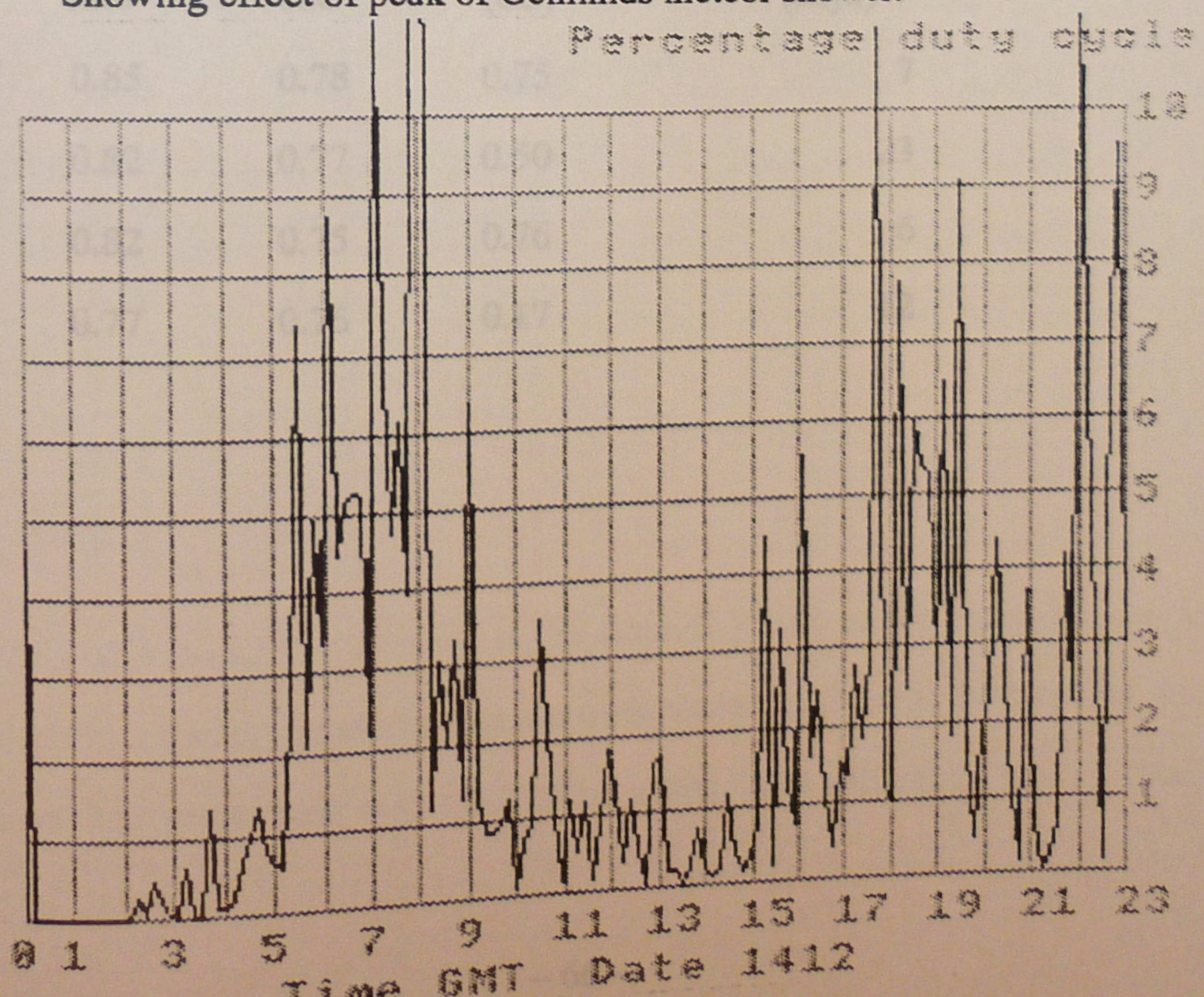

One measure of path usability used by many authors is the percentage of time that the signal is above a set threshold.This is usually referred to as the duty cycle. The program DAYDUTY (appendix (c) (iii)) was written to produce daily plots of this quantity. Figs 7.5 and 7.6 show outputs from the program. Note the expected similarity in shape to figs 7.1 and 7.3.

All these plots represent data from the mid point antenna, with the amplitude threshold set at 0.5 μV and the duration threshold set at 50ms.

Other data was sorted, analysed and displayed graphically using a spreadsheet.

7.3.2 Monthly averages of amplitude, burst frequency, and duration

7.3.2.1 Amplitudes

Table 7.1 Mean amplitudes : 15 ms and 0.5μV thresholds

Date	mean amplitude (μV)		mid/end	no of observations
	mid	end	(dB)	(days)
May 87	0.85	0.78	0.75	7
June 87	0.82	0.77	0.50	23
July 87	0.82	0.75	0.76	6
Feb 88	0.77	0.76	0.17	12

Table 7.2 Mean amplitudes : 50 ms and 0.5μV thresholds

Date	mean amplitude (μV)		mid/end	no of observations
	mid	end	(dB)	(days)
Jan 87	1.19	0.99	1.60	21
Feb 87	1.17	1.03	1.15	16
July 87	1.23	1.18	0.35	7
Aug 87	1.18	1.16	0.59	23

Table 7.3 Mean amplitudes : 15 ms and 1.05μV thresholds

Date	Mean amplitude (μV)		mid/end	no of observations
	mid	end	(dB)	(days)
July 87	1.69	1.55	0.7	8
Nov 87	1.69	1.58	0.6	27
Jan 88	1.69	1.60	0.47	13

Table 7.4 Mean Amplitudes : 10ms and 0.7μV threshold for second experiment

Date	Mean amplitude (μV)		mid/end	no of observations
	mid	end	(dB)	(days)
June 89	1.19	1.08	0.8	6
July 89	1.20	1.12	0.6	3
Aug 89	1.21	1.12	0.7	8
Sept 89	1.15	1.07	0.6	10
Oct 89	1.15	1.07	0.6	17

Tables 7.1, 7.2,7.3 and 7.4, show that the antenna aimed at the receiving site zenith, (the end point antenna) produces signals with mean amplitudes slightly less than the antenna pointed at the path mid point in all cases. This difference is very small, but

consistent, having a mean value of about 0.6dB. the measured values of its variation over the year is plotted in Fig 7.7.

Fig 7.7 Mid point amplitude advantage

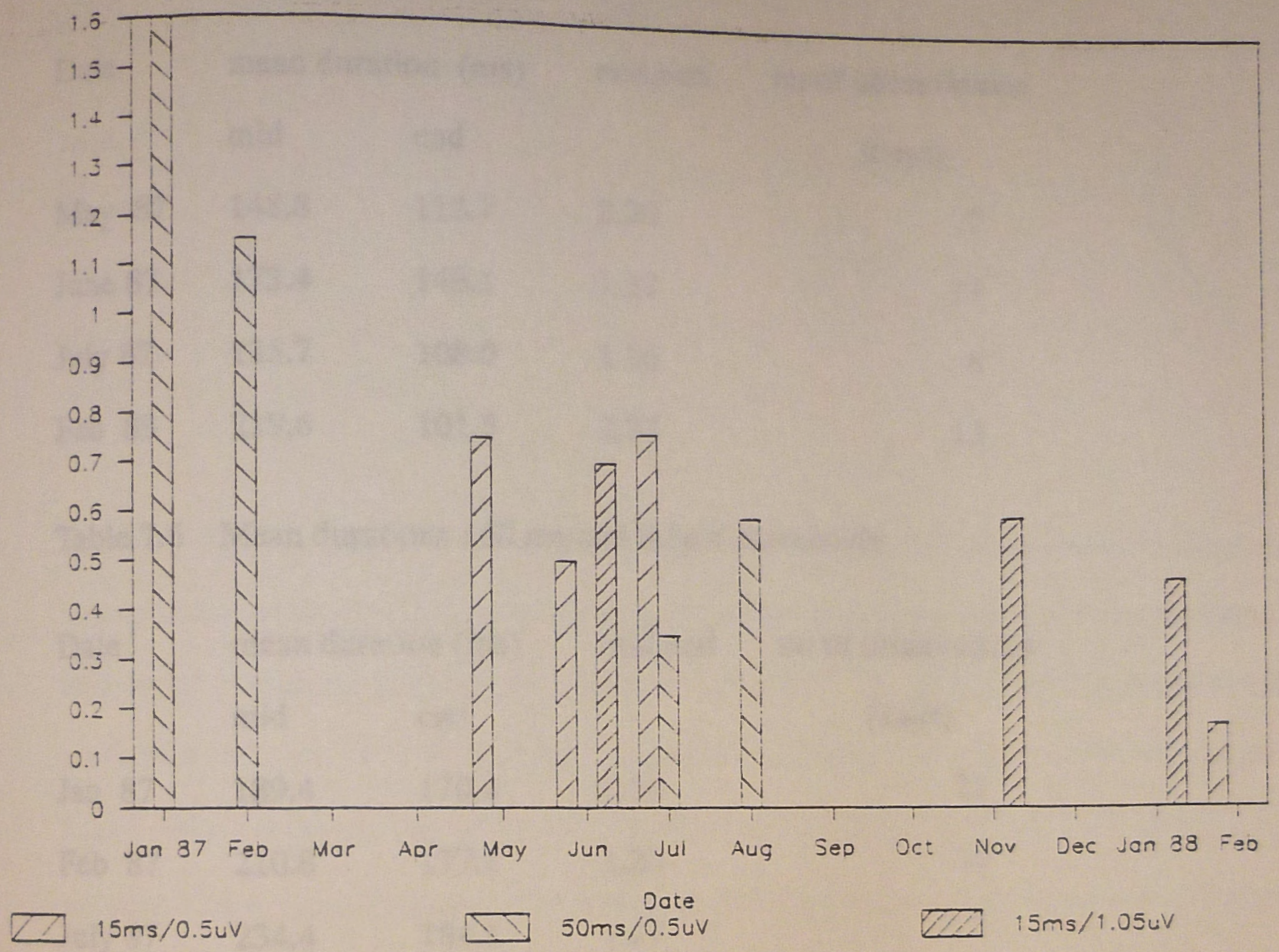

The end point improvement for transverse trails of 0.9 dB or the mid point improvement of 10.7dB predicted for in line trails are not apparent.

It can therefore be safely assumed that the hypothesis that transverse trails predominate, holds, and the slight reversal of the end point improvement effect could be put down to the minority effect of in line trails.

There is no large end point improvement (5.8dB, Table 6.5) predicted if the end point path was operating above the transition frequency.

7.3.2.2 Durations

Table 7.5 Mean durations : 15 ms and 0.5μV thresholds

Date	mean duration (ms)		mid/end	no of observations
	mid	end		(days)
May 87	148.8	112.7	2.20	7
June 87	173.4	148.1	1.32	17
July 87	125.7	108.0	1.16	6
Feb 88	219.6	101.5	2.27	13

Table 7.6 Mean durations : 50 ms and 0.5μV thresholds

Date	mean duration (ms)		mid/end	no of observations
	mid	end		(days)
Jan 87	189.4	170.4	1.10	21
Feb 87	210.8	177.1	1.20	16
July 87	234.4	184.1	1.27	7
Aug 87	222.9	166.5	1.34	23

Table 7.7 Mean durations : 15 ms and 1.05μV thresholds

Date	Mean duration (ms)		mid/end	no of observations
	mid	end		(days)
July 87	106.5	56.5	1.88	8
Nov 87	70.3	58.12	1.20	27
Jan 88	71.1	62.1	1.14	12

Table 7.8 Mean durations : 10ms and 0.7μV threshold for second experiment

Date	Mean duration (ms)		mid/end	no of observations (days)
	mid	end		
June 89	176	121	1.45	6
July 89	172	116	1.48	3
Aug 89	269	148	1.82	8
Sep 89	151	122	1.24	10
Oct 89	142	102	1.39	17

Tables 7.5, 7.6, and 7.7 show the monthly mean durations calculated from the experimental data. The first point of note is that the end point bursts are shorter than the mid point bursts by a factor of between 1.1 and 2.27. The theory in section 6.2.1 predicts a ratio of 14.6. It assumes a simple approach, (Appendix (d)) with duration based only on the values of ∅, R_t and R_r. It takes no account of the antenna polar patterns and the fact that many trails will be simultaneously receivable on both antenna systems due to pattern overlap.

A second factor could be the lack of sensitivity to very short bursts inherent in the data logger, due to its sample rate and duration threshold setting.

If we take the mean of the mid point durations of tables 7.5, 7.6, and 7.7 (161.2) and scale it down by the same factor of 14.6 we arrive at a value of about 11 ms for the mean expected end point duration for this path, based on the experimental results. This is less than the threshold duration for the measuring equipment used in the first two experiments, and just above it in the Barton experiment. Hence many end point signal bursts may not have been logged. If this was the case, we would expect the ratio of mid to end to increase with a reduction in duration threshold. Comparing the ratio of number of bursts logged per minute for July and August 1987 (Table 7.10 50ms

threshold) and 1989 (Table 7.12 10ms threshold), on each antenna shows a general increase, but no noticeable increase in the ratio of mid to end.

The general effect of shorter bursts on the end point antenna can be seen but the effect is not as marked as theory predicts. Comparing tables 7.5 and 7.7 we can see the effective duration of the bursts reducing as the receiver amplitude threshold is raised. The factor can be seen to be approximately proportional to the logarithm of the change in level.(33) Fig 7.8 plots the measured mid point duration increase over a year, and no large variations are apparent.

Fig 7.8 Mid point duration advantage

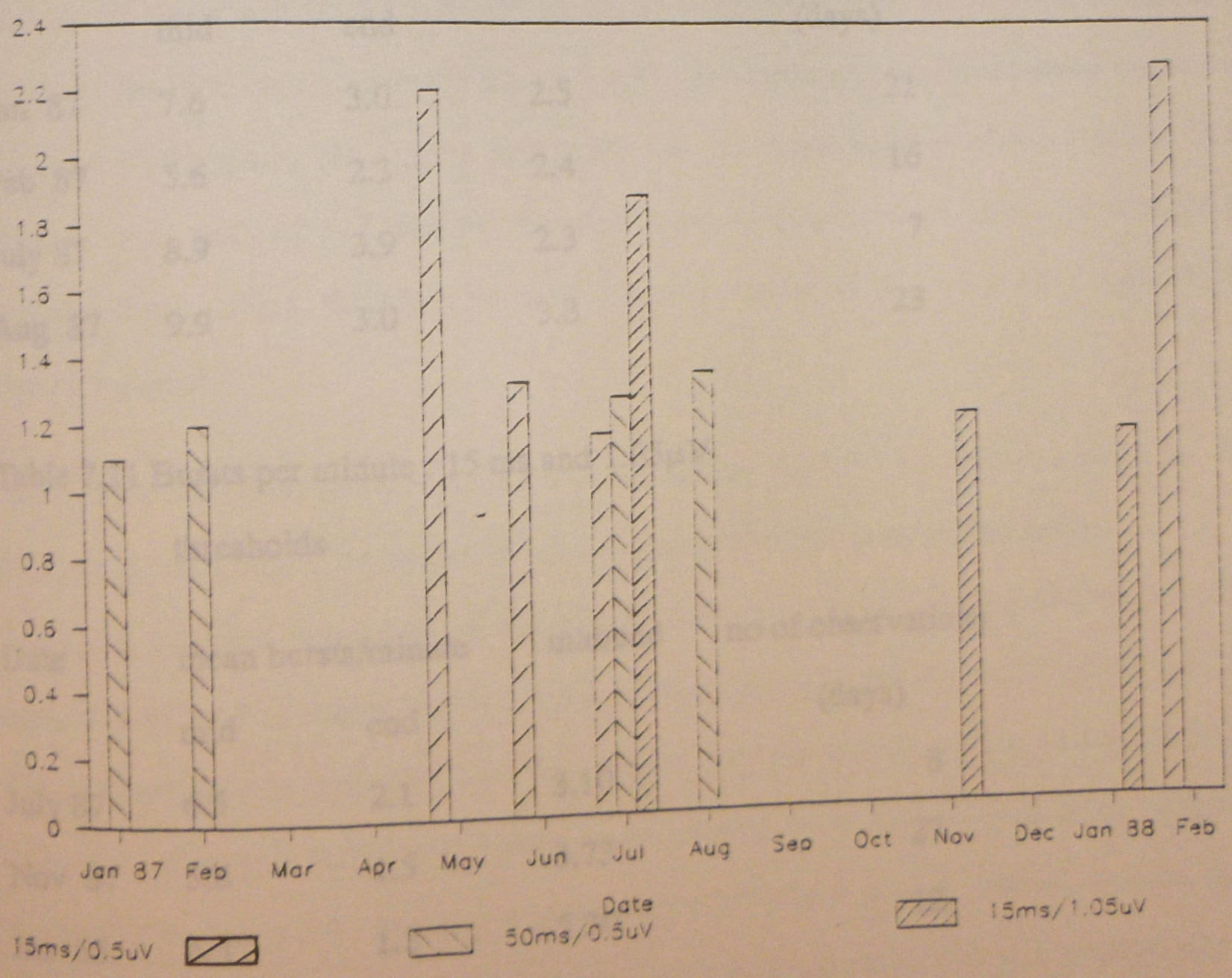

7.3.2.3 Bursts per minute

Table 7.9 Bursts per minute : 15 ms and 0.5μV thresholds

Date	mean bursts/ minute		mid/end	no of observations
	mid	end		(days)
May 87	19.0	12.0	1.60	7
June 87	26.0	14.6	1.80	23
July 87	22.0	9.0	2.40	6
Feb 88	32.5	22.0	2.90	13

Table 7.10 Bursts per minute : 50 ms and 0.5μV thresholds

Date	mean bursts/ minute		mid/end	no of observations
	mid	end		(days)
Jan 87	7.6	3.0	2.5	21
Feb 87	5.6	2.3	2.4	16
July 87	8.9	3.9	2.3	7
Aug 87	9.9	3.0	3.3	23

Table 7.11 Bursts per minute : 15 ms and 1.05μV thresholds

Date	mean bursts/minute		mid/end	no of observations
	mid	end		(days)
July 87	6.5	2.1	3.10	8
Nov 87	5.6	1.5	3.73	27
Jan 88	6.4	1.2	5.30	12

Table 7.12 Bursts per minute : 10ms and 0.7μV threshold for second experiment

Date	mean bursts/minute		mid/end	no of observations
	mid	end		(days)
June 89	14.7	3.83	3.84	6
July 89	12.2	2.97	4.1	3
Aug 89	17.4	5.4	3.22	8
Sep 89	11.15	3.34	3.34	10
Oct 89	11.5	3.77	3.05	17

Tables 7.9, 7.10, 7.11 and 7.12, show the long term mean number of bursts per minute calculated from the experimental data. All results show a larger number of bursts on the mid point antenna than on the end point antenna by a factor varying from 1.6 to 5.3. The model described by Brown (ref 33 fig 6) predicts a slight increase in detectable bursts at the receiving station zenith on a 1000 Km path, and a similar small decrease for a 1400 Km path. No figures are given for the magnitudes of these effects. The experimental path of 1174km in this report has a length which lies approximately between these values, therefore the experimental results seem to generally agree with Brown's model.

The yearly variation of meteor activity in tables 7.9 to 7.11 shows a peak in the summer months, and a minimum in winter, apart from one notable exception.
Table 7.9 shows a maximum of activity in February 1988. Looking further into the data, this seems to be mainly due to high activity on the 2nd 3rd and 4th of the month. These dates do not coincide with any major showers known to the author, and the apparent increased activity is likely to be caused by noise causing false triggers. Reference to table 7.9 shows a larger number of bursts on the 15ms threshold data gathered in Cambridge than that gathered with a 10ms threshold at the quiet site at

Barton. This tends to confirm that the noise was the limiting factor on the earlier experiment in Cambridge.

Fig 7.9 plots the measured ratio of mid point to end point burst frequency, and apart from the anomalous value for February 1988 there seems to be some evidence for a maximum of this mid point burst number advantage ratio in the summer months.

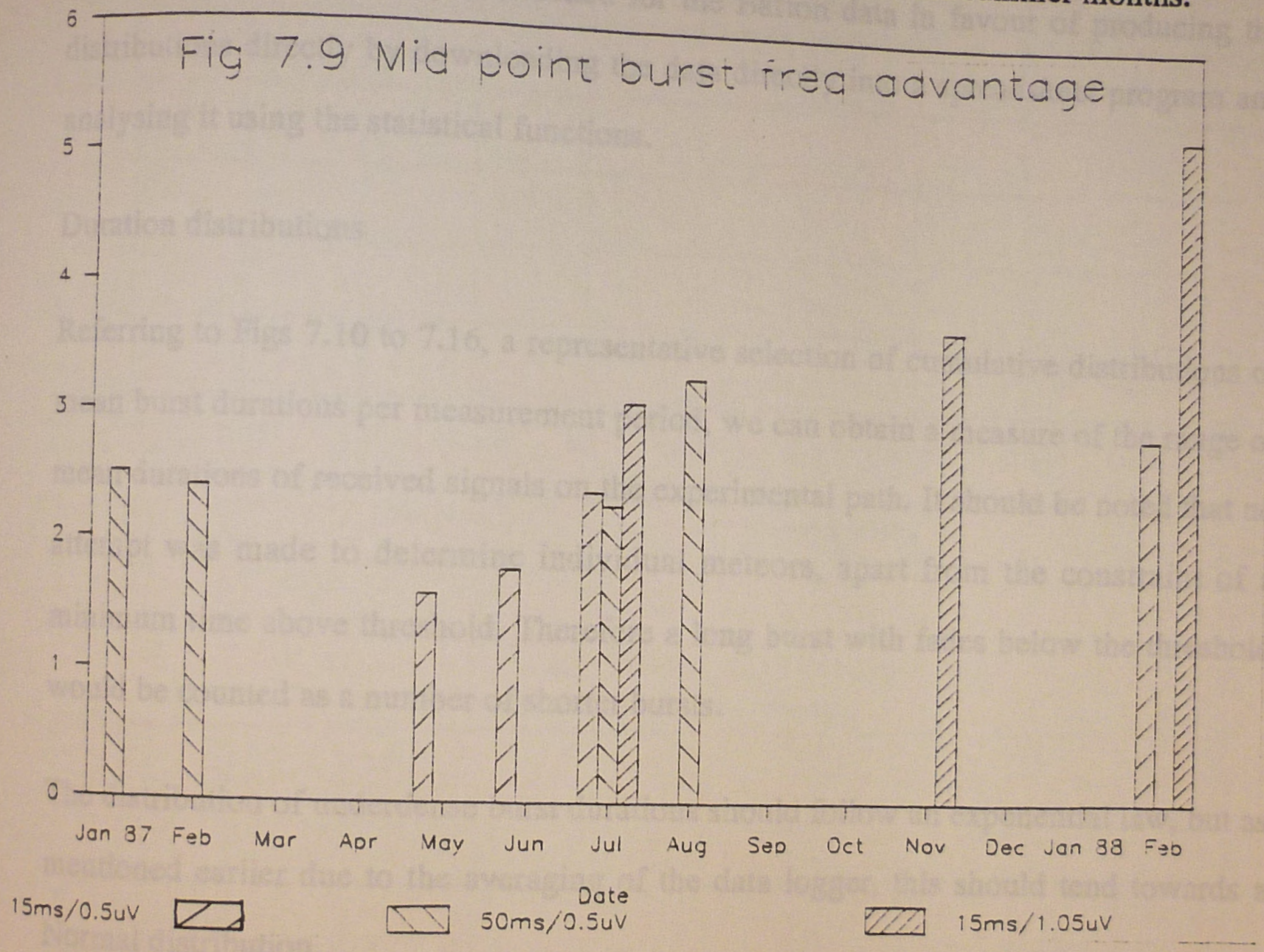

7.3.3 Monthly distributions of amplitude, and duration.

One of the aims of this investigation was to gather data to study statistically, the duration and amplitude of signals from two antenna systems. It was decided to produce a set of programs to sort the data into rank order and plot the cumulative distributions of amplitude, burst frequency and duration. This enabled a measure of the range of values to be obtained for the signal parameters and a further comparison to be made against the predicted values for the path that were calculated in section 6. The programs were originally written to produce tables of ranked values directly from the stored data

on disc. It was considered useful to produce the graphs by computer to allow a quick visual inspection of the data. The listings and program descriptions in appendices (c)(iv) are the graph plotting programs but the graphs presented in the thesis were prepared using a spreadsheet with data from the tabular programs, as the graphs produced by the BBC microcomputer were not of sufficient quality for publication.
The programs were finally abandoned for the Barton data in favour of producing the distributions directly by downloading the data directly into a spreadsheet program and analysing it using the statistical functions.

Duration distributions

Referring to Figs 7.10 to 7.16, a representative selection of cumulative distributions of mean burst durations per measurement period, we can obtain a measure of the range of mean durations of received signals on the experimental path. It should be noted that no attempt was made to determine individual meteors, apart from the constraint of a minimum time above threshold. Therefore a long burst with fades below the threshold would be counted as a number of shorter bursts.

The distribution of underdense burst durations should follow an exponential law, but as mentioned earlier due to the averaging of the data logger, this should tend towards a Normal distribution.

Fig 7.10 shows an example of a plot from the experimental data based on bursts greater than 50ms. The following points are of note. There are a larger number of longer bursts than could be expected from underdense bursts alone. This is explained by the presence of overdense bursts, beginning to predominate the data at large amplitudes. The plot of end point data crosses the mid point line at about 360ms. This seems to indicate that there are a larger percentage of overdense bursts with the end point path geometry.
If we now examine Fig 7.11 based on measurements with a 15ms duration threshold, and taken one year later over the same period, we see that the cross-over does not take

Fig 7.10 Duration distribution

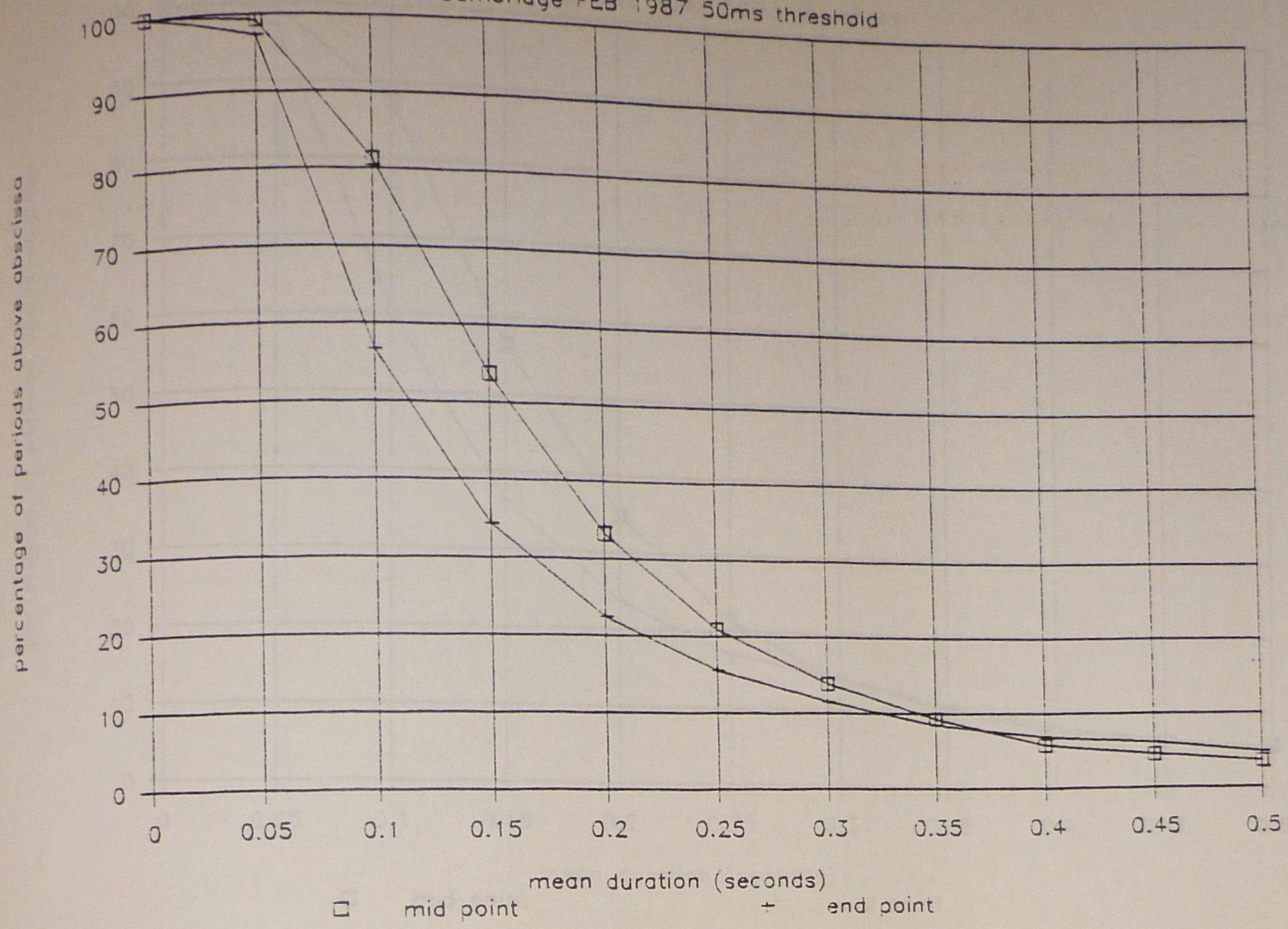

Fig 7.11 Duration distribution

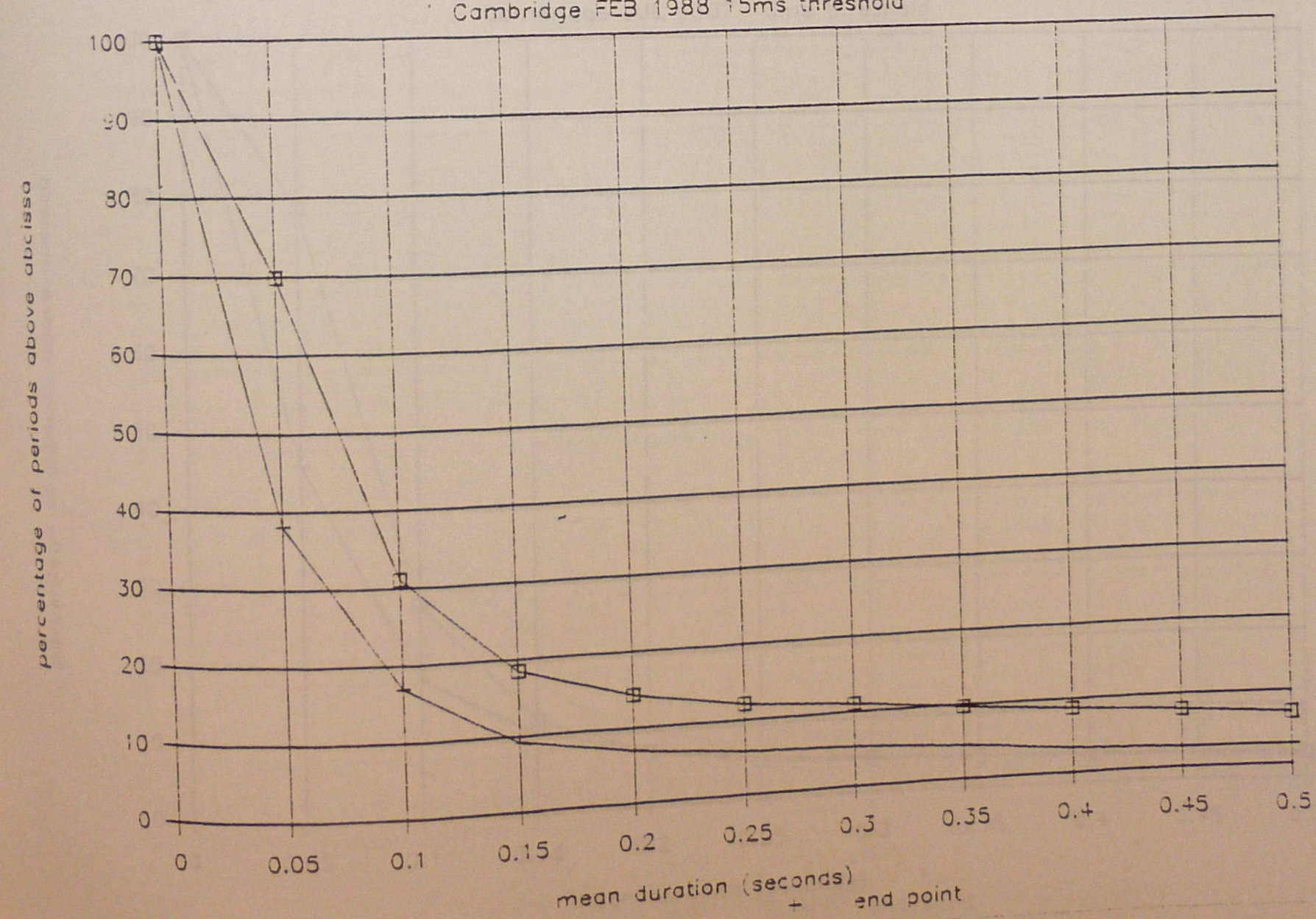

Fig 7.12 Duration distribution

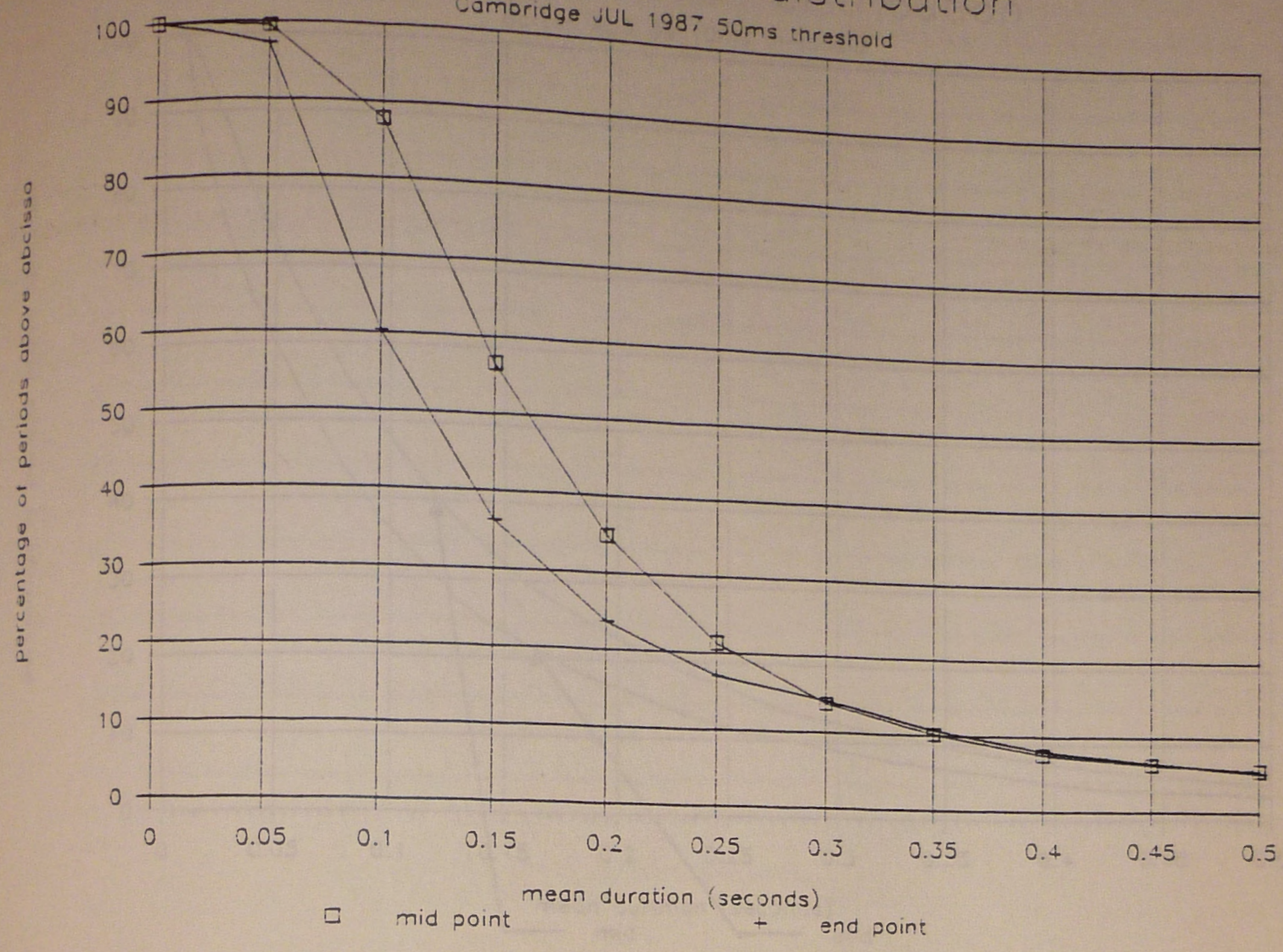

Fig 7.13 Duration distribution

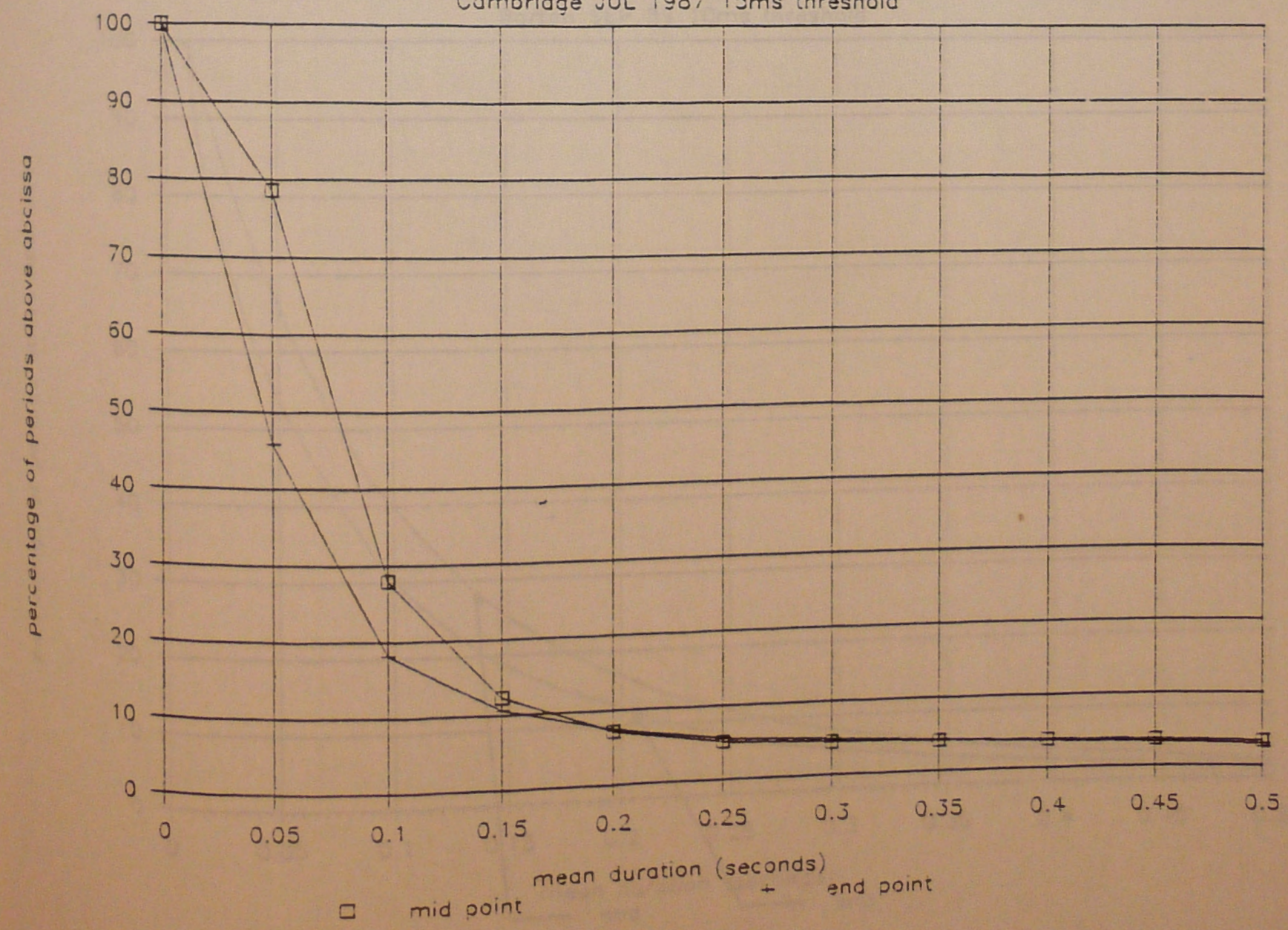

Fig 7.14 Duration distribution

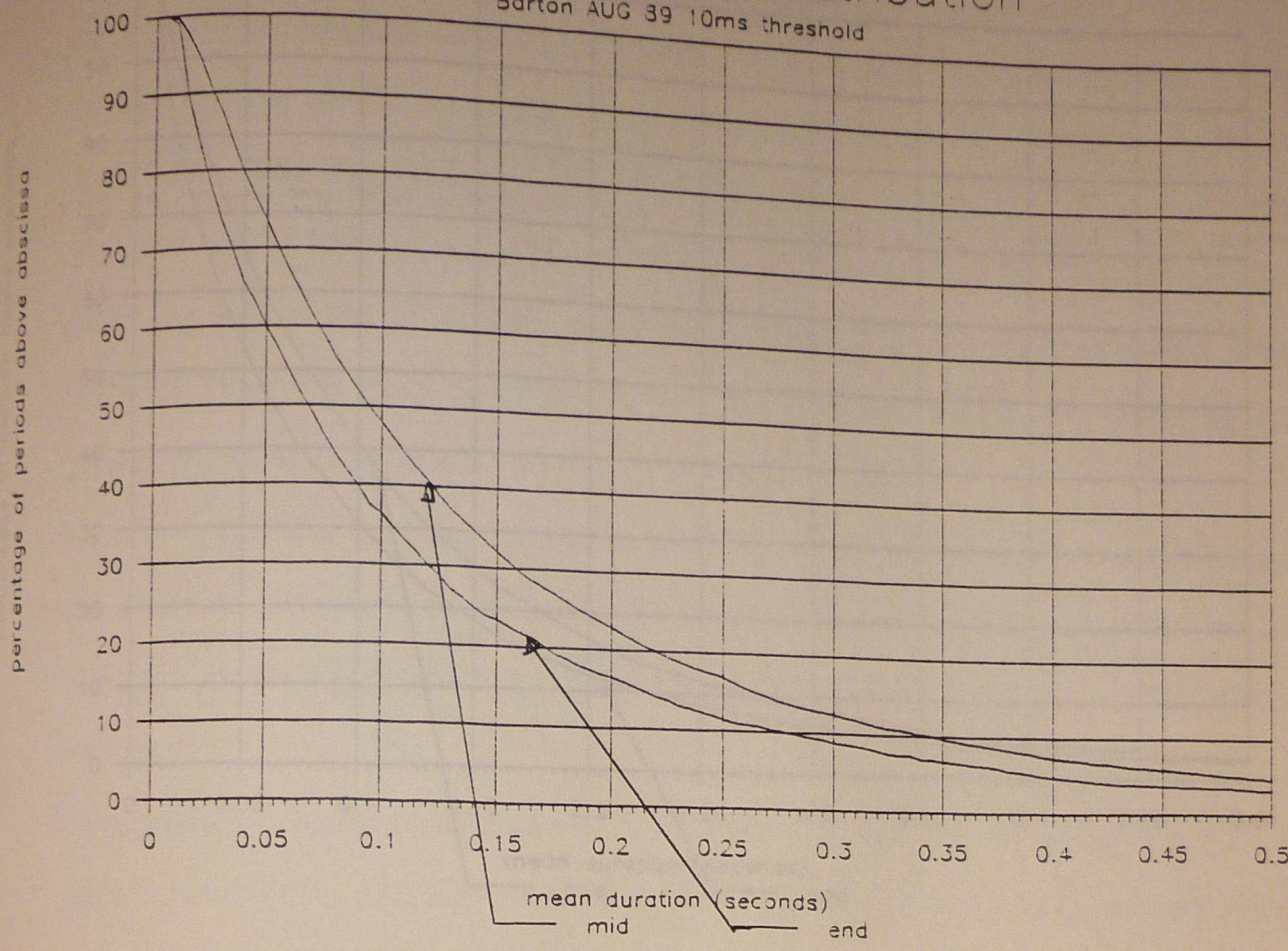

Fig 7.15 Duration distribution

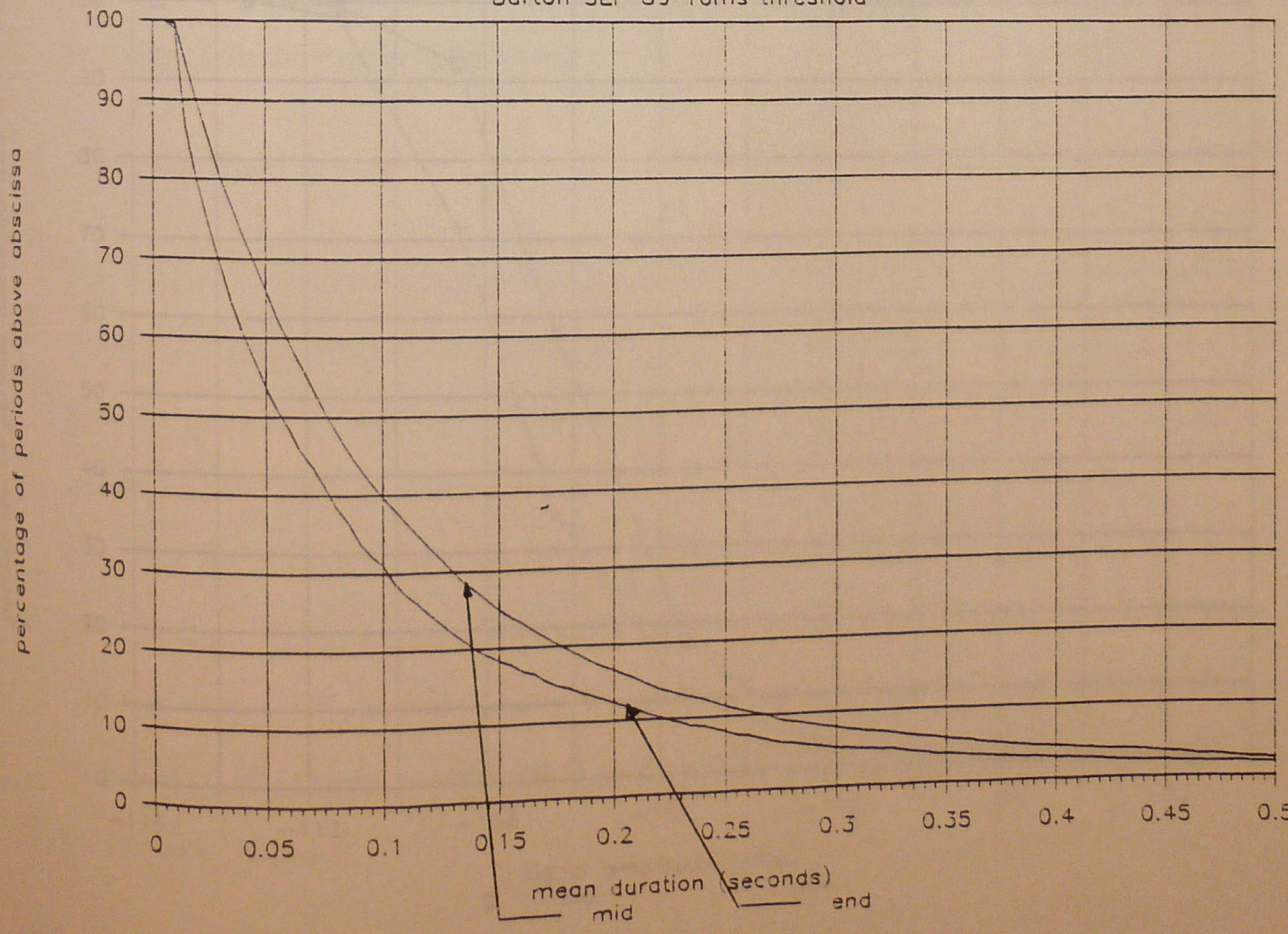

Fig 7.16 Duration distribution

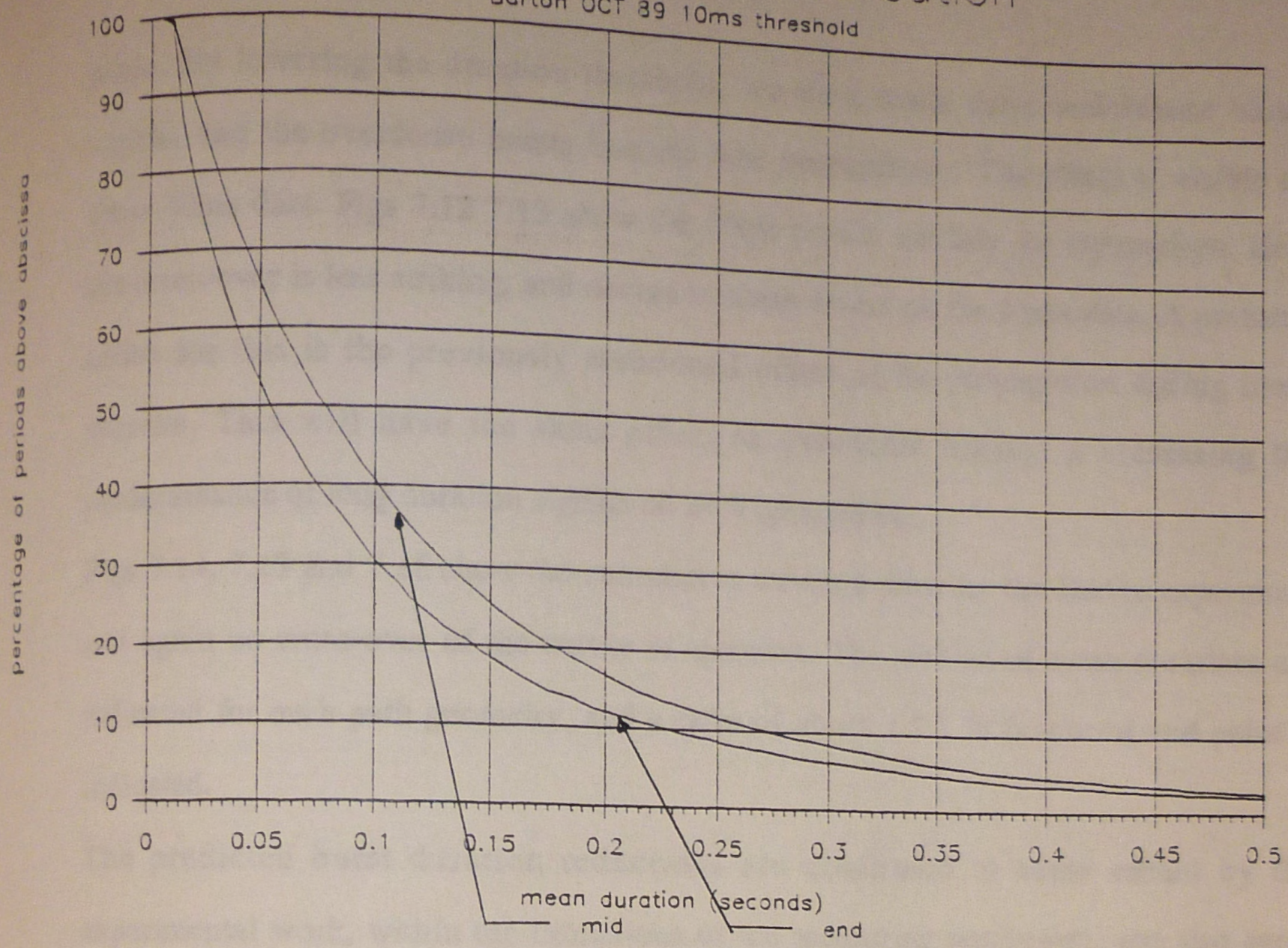

Fig 7.17 Amplitude distribution

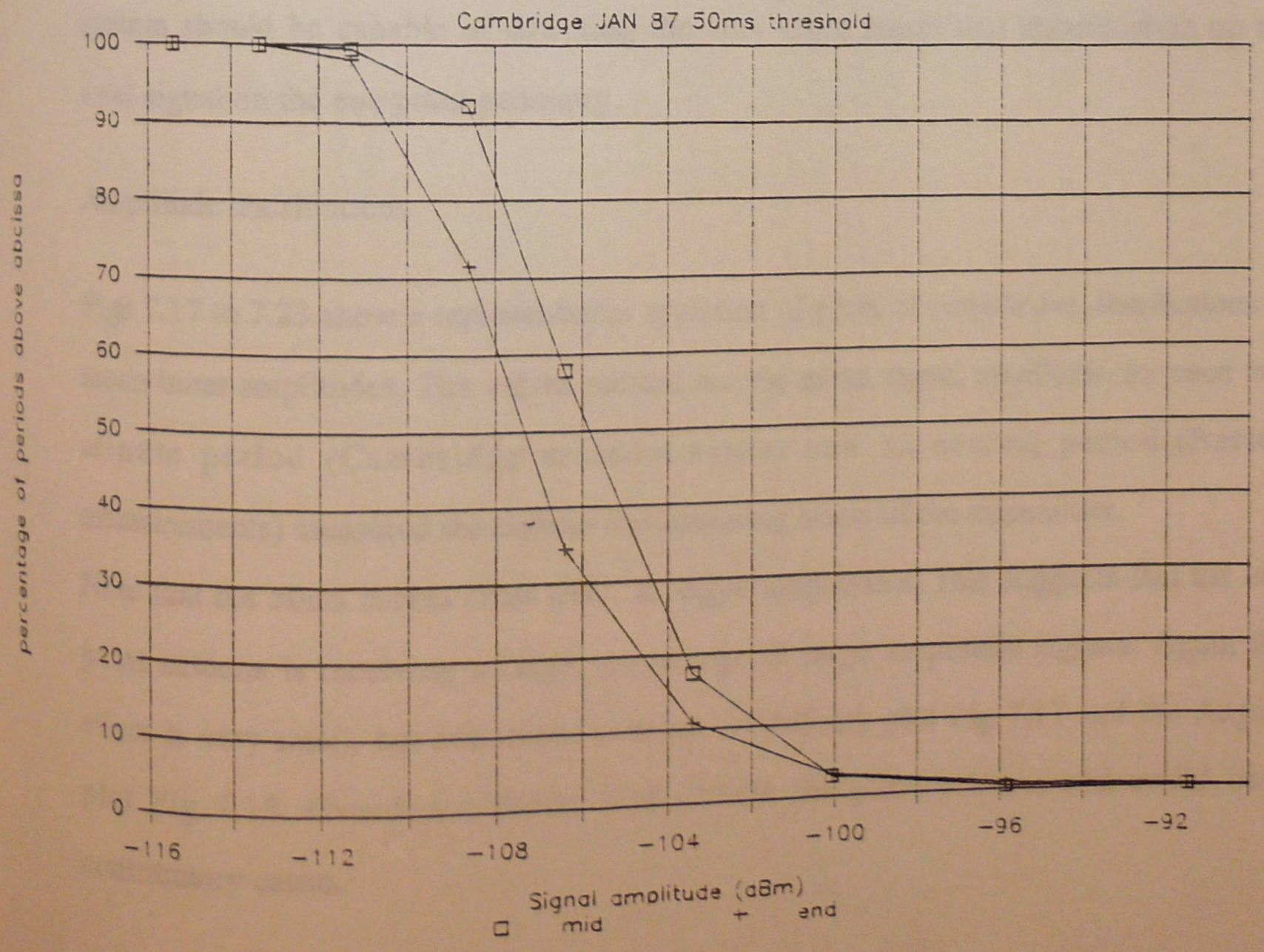

place. By lowering the duration threshold, we have made more underdense bursts visible, and the overdense bursts become less predominant. The effect is visible on other 50ms data. Figs 7.12 7.13 show the 50ms results for July for comparison. Here the cross-over is less striking, and occurs to some extent on the 15ms data. A probable cause for this is the previously mentioned effect of Es propagation during these months. This will have the same effect as overdense bursts, ie increasing the predominance of long duration signals on both geometries.

Figs 7.14, 7.15 and 7.16 show the cumulative duration plots for the Barton experiment and again no cross-over of the curves is apparent. The median of mean durations are indicated for each path geometry, and a ratio of about 1.5:1 in favour of mid point is indicated.

The predicted burst duration reductions are confirmed to some extent by the experimental work, within the limitations of the measuring equipment, and also agree with the extensive modelling work of Brown (33). To check the results, more experimental data needs to be obtained for a short path, probably of some 200Km. The system should be capable of detecting the very short bursts that should make up the total signal on the end point geometry.

Amplitude distributions

Figs 7.17 to 7.23 show a representative selection of plots of cumulative distributions of mean burst amplitudes. The values plotted are the mean signal amplitude for each two minute period (Cambridge measurements) and 12 second period,(Barton measurements) measured throughout the operating hours of the transmitter.

Note that the 50ms curves cross over, at larger amplitudes. This suggests that the end point antenna is receiving a larger percentage of large amplitude signals. Again the effect is very small, but noticeable both on the January plot Fig 7.17 and the August plot Fig 7.18. Overdense bursts will distort the picture here, and could be a contributory cause.

Fig 7.18 Amplitude distribution

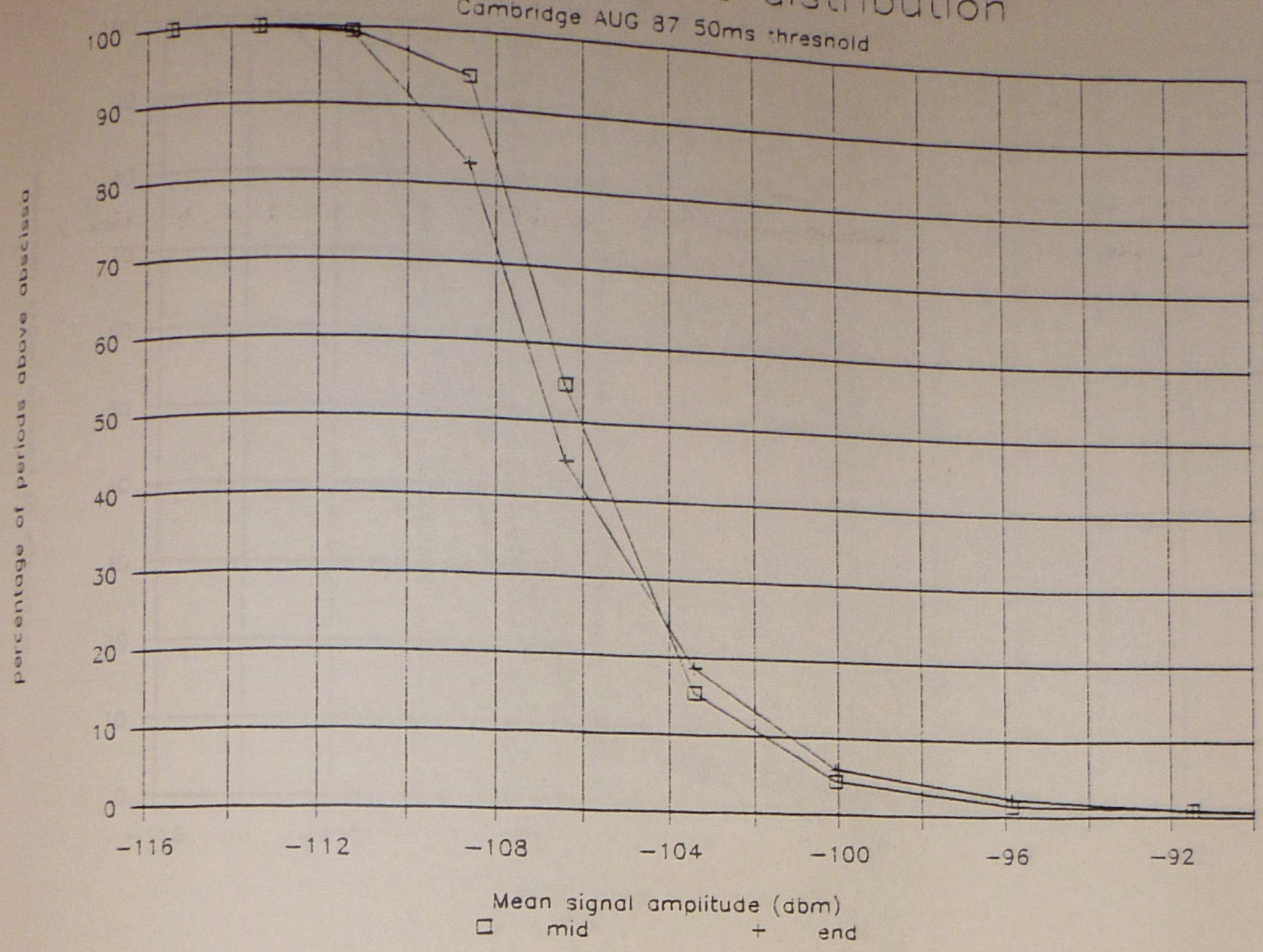

Fig 7.19 Amplitude distribution

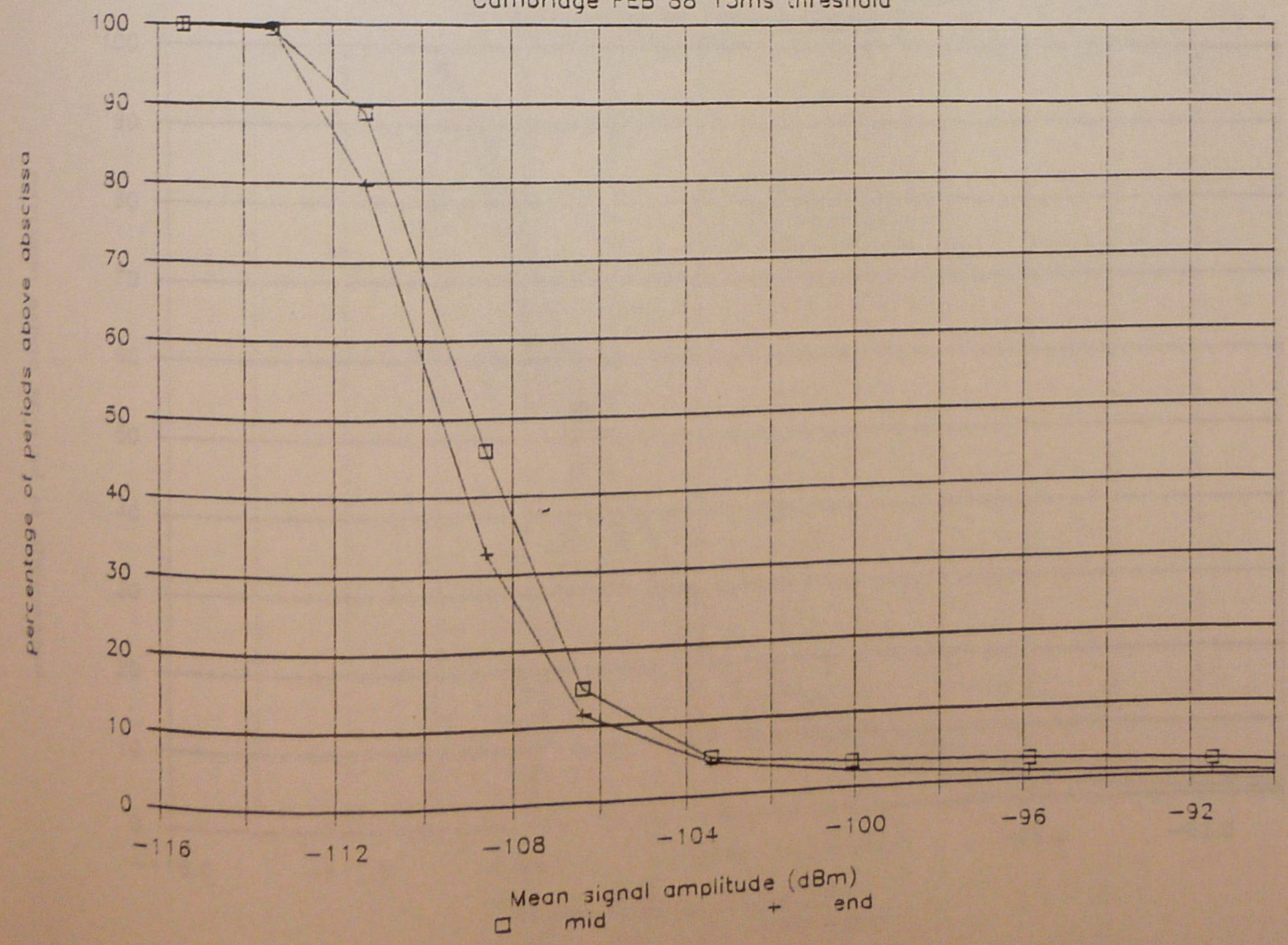

Fig 7.20 Amplitude distribution

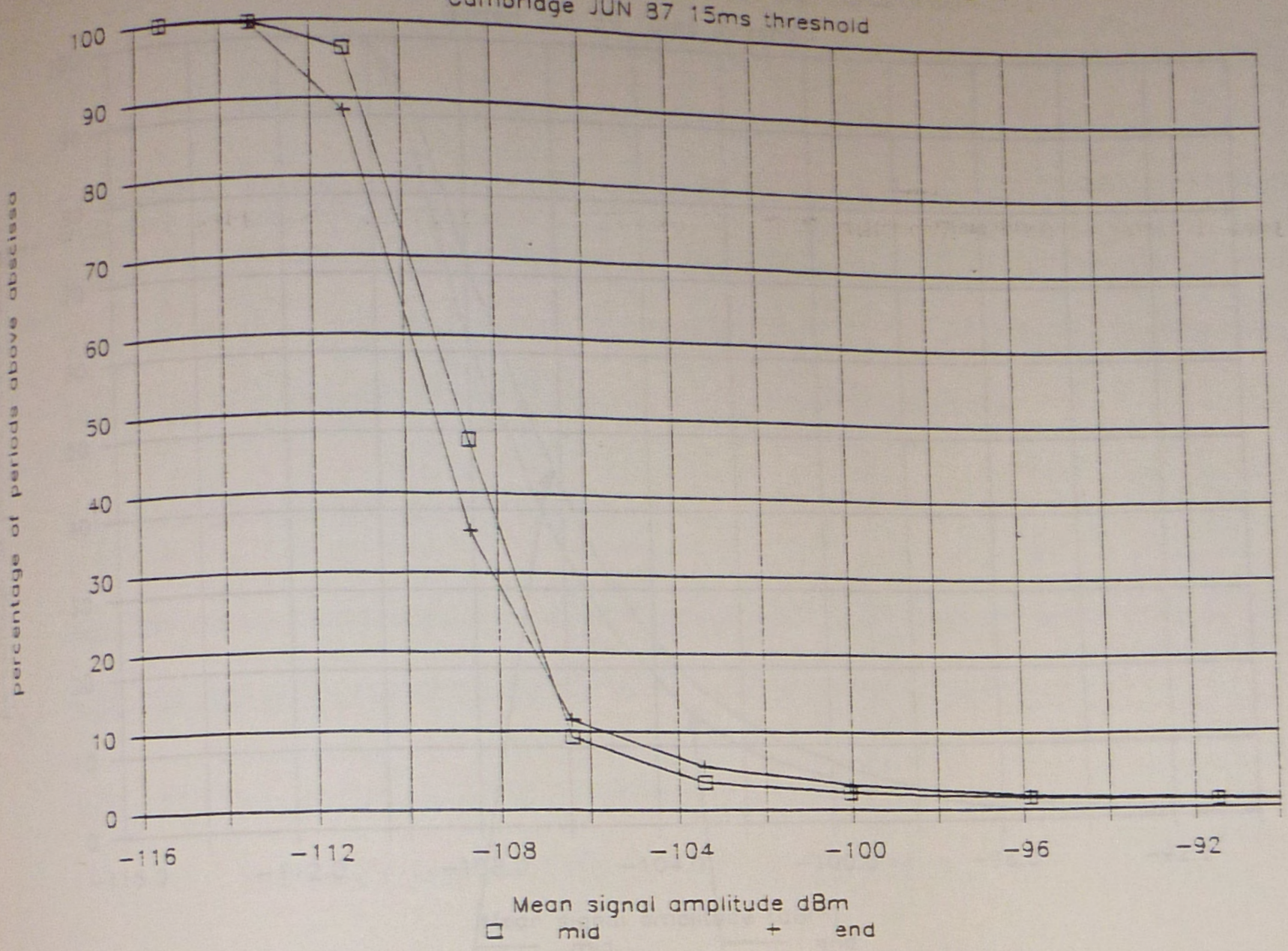

Fig 7.21 Amplitude distribution

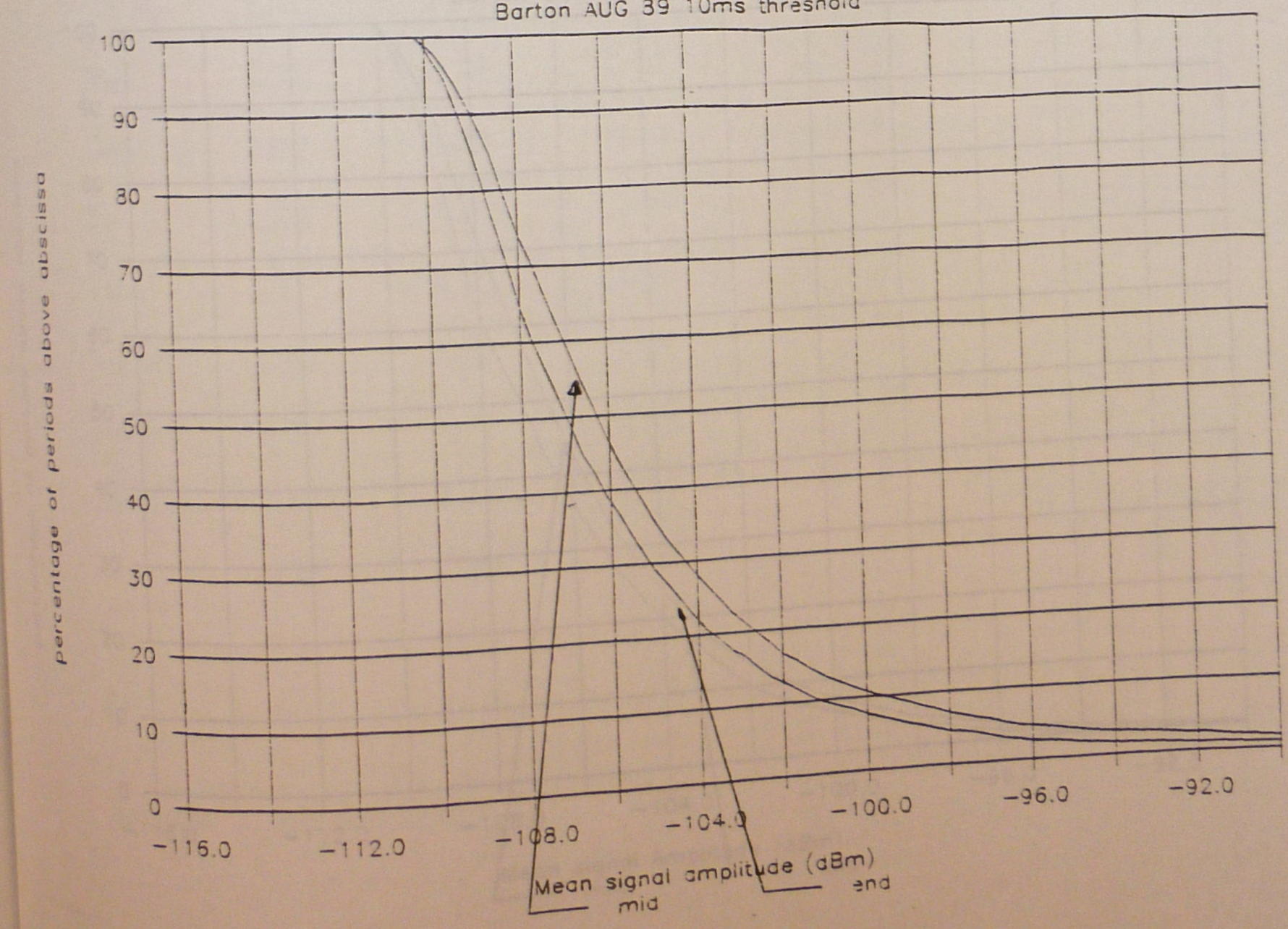

Fig 7.22 Amplitude distribution

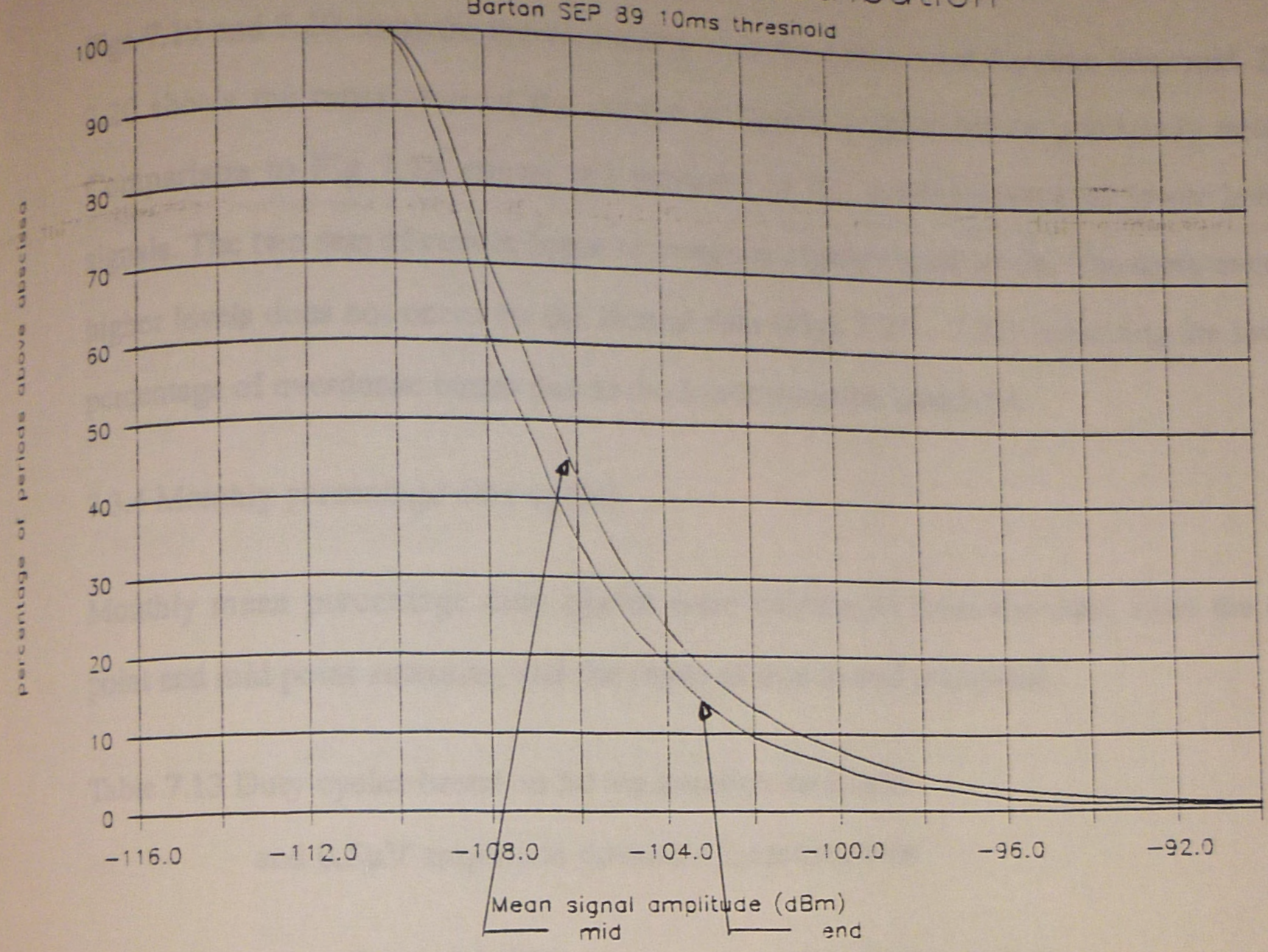

Fig 7.23 Amplitude distribution

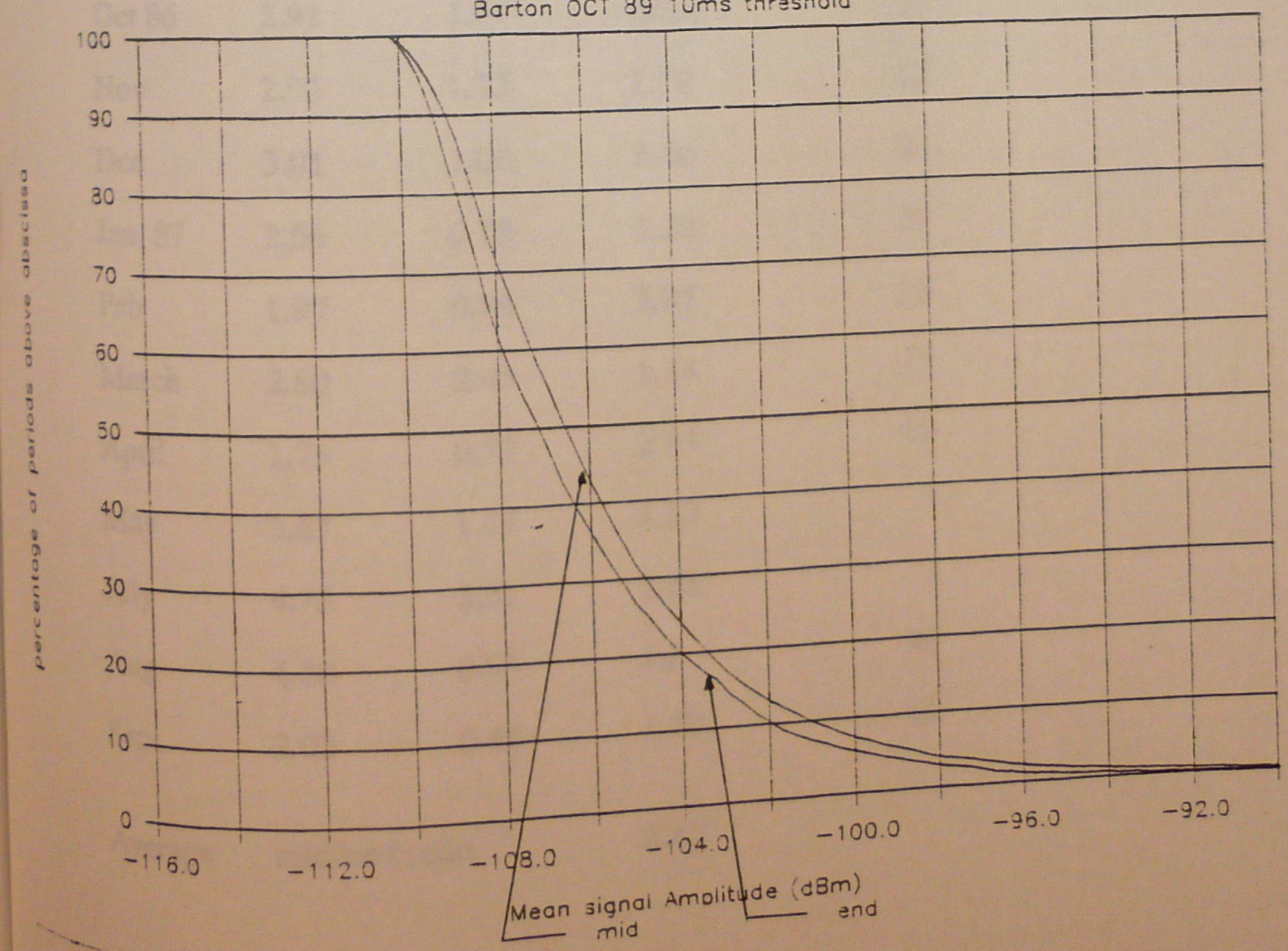

Figs 7.19 and 7.20 compare the data taken with the 15ms burst duration threshold. Fig 7.20 shows the cross-over of the curves at higher amplitudes as previously noted. Comparison to Fig 7.18 shows the increase in the predominance of lower levels signals. The two sets of curves begin to merge at higher signal levels. The cross-over at higher levels does not occur on the Barton data (Figs 7.21 – 7.23) indicating the lower percentage of overdense bursts due to the lower duration threshold.

7.3.4 Monthly percentage duty cycles

Monthly mean percentage duty cycles were calculated from the data, from the end point and mid point antennas, and the ratios of mid to end compared.

Table 7.13 Duty cycles based on 50 ms duration threshold
and 0.5μV amplitude threshold measurements

Month	duty cycle(%)			no of observations
	mid	end	mid/end	(days)
Oct 86	2.91	1.07	2.72	17
Nov	2.95	1.73	1.70	22
Dec	3.01	1.00	3.40	23
Jan 87	2.56	0.78	3.28	20
Feb	1.97	0.96	2.05	15
March	2.80	2.45	1.14	12
April	1.75	0.72	2.43	15
May	3.67	1.17	3.13	7
July	4.75	2.31	2.06	7
Aug	4.18	0.93	4.5	22
Sept	2.02	0.46	4.39	12
Average	mid/end ratio		2.82	

Table 7.14 Duty cycles based on 15ms duration threshold and 0.5μV amplitude threshold measurements

Month	duty cycle(%)			no of observations
	mid	end	mid/end	(days)
July 87	3.88	1.55	2.50	5
Jan 88	2.84	0.48	5.92	3
Average	mid/end ratio		4.21	

Table 7.15 Duty cycles based on 15ms duration threshold and 1.05μV amplitude threshold measurements

Month	duty cycle(%)			no of observations
	mid	end	mid/end	(days)
July 87	1.46	0.23	6.35	8
Nov 87	0.72	0.18	4.00	27
Jan 88	0.68	0.15	4.53	12
Average	mid/end ratio		4.96	

Table 7.16 Duty cycles : 10ms threshold for second experiment

Month	duty cycle(%)			no of observations
	mid	end	mid/end	(days)
June 89	3.74	0.67	5.6	6
July 89	2.81	0.56	5.02	3
Aug 89	5.96	1.36	4.38	8
Sep 89	2.13	0.48	4.44	10
Oct 89	2.59	0.81	3.2	11
Average	mid/end ratio		4.53	

Reference to Tables 7.13 to 7.15 shows that in all cases the mid point geometry gives a higher duty cycle by a factor varying between 1.14 to 6.36 with a mean value of 4.0. The Barton results of table 7.16 show a mean duty cycle advantage of 4.53 for mid point geometry. These compare favourably with the computer model result of 4.0. (Section 6.3.2).

These results are also consistent with the results calculated for 47 MHz by Brown (ref 33 Fig 6) using his computer model.

The daily duty cycle plots for the Barton experiment (Figs 7.24-7.26 show a tendency for this duty cycle improvement ratio to reduce at times of high shower activity (11-13 August, 6-10 October). This effect is not marked on the long term duty cycles with the higher duration threshold, (Fig 7.27) indicating that showers have a minority effect on this ratio. There is a tendency for the ratio to be higher in the summer months and December/January. A possible explanation for this is that the months noted are the main months for temperate zone Sporadic E (Es) propagation. Es propagation is less path geometry sensitive than meteor burst due to the wider area of the ionised region.

Fig 7.24 Daily duty cycle

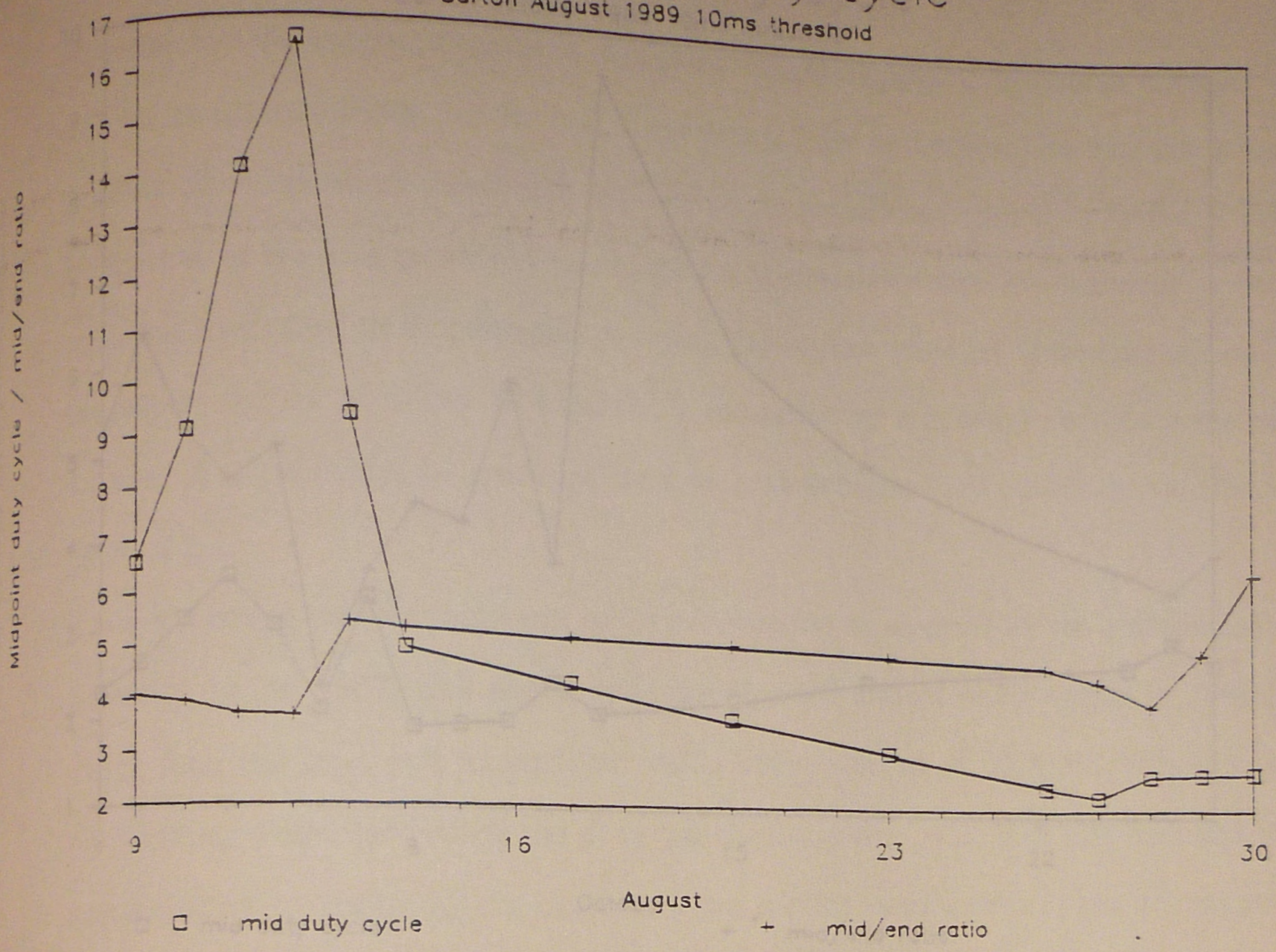

Fig 7.25 Daily duty cycle

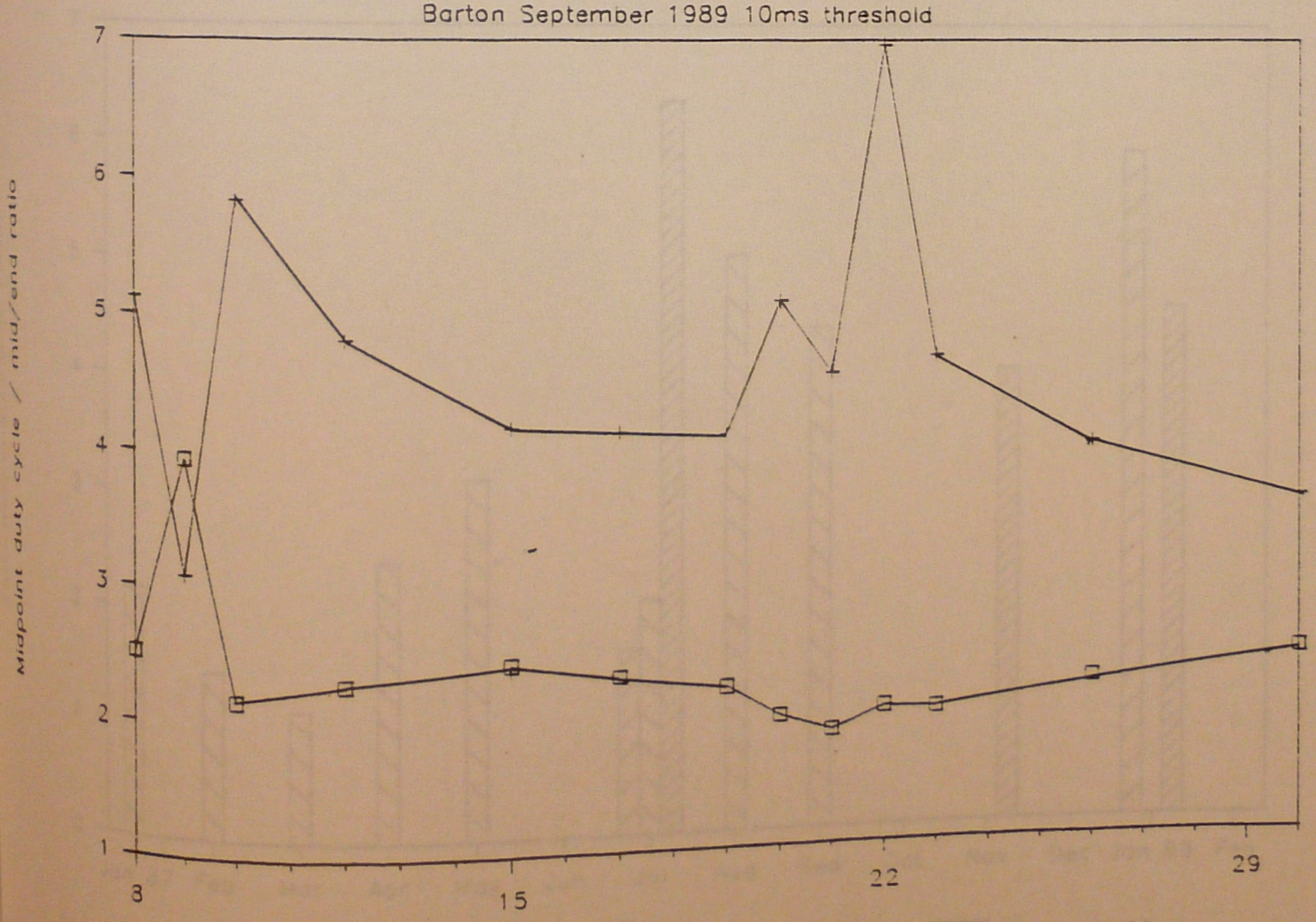

Fig 7.26 Daily duty cycle

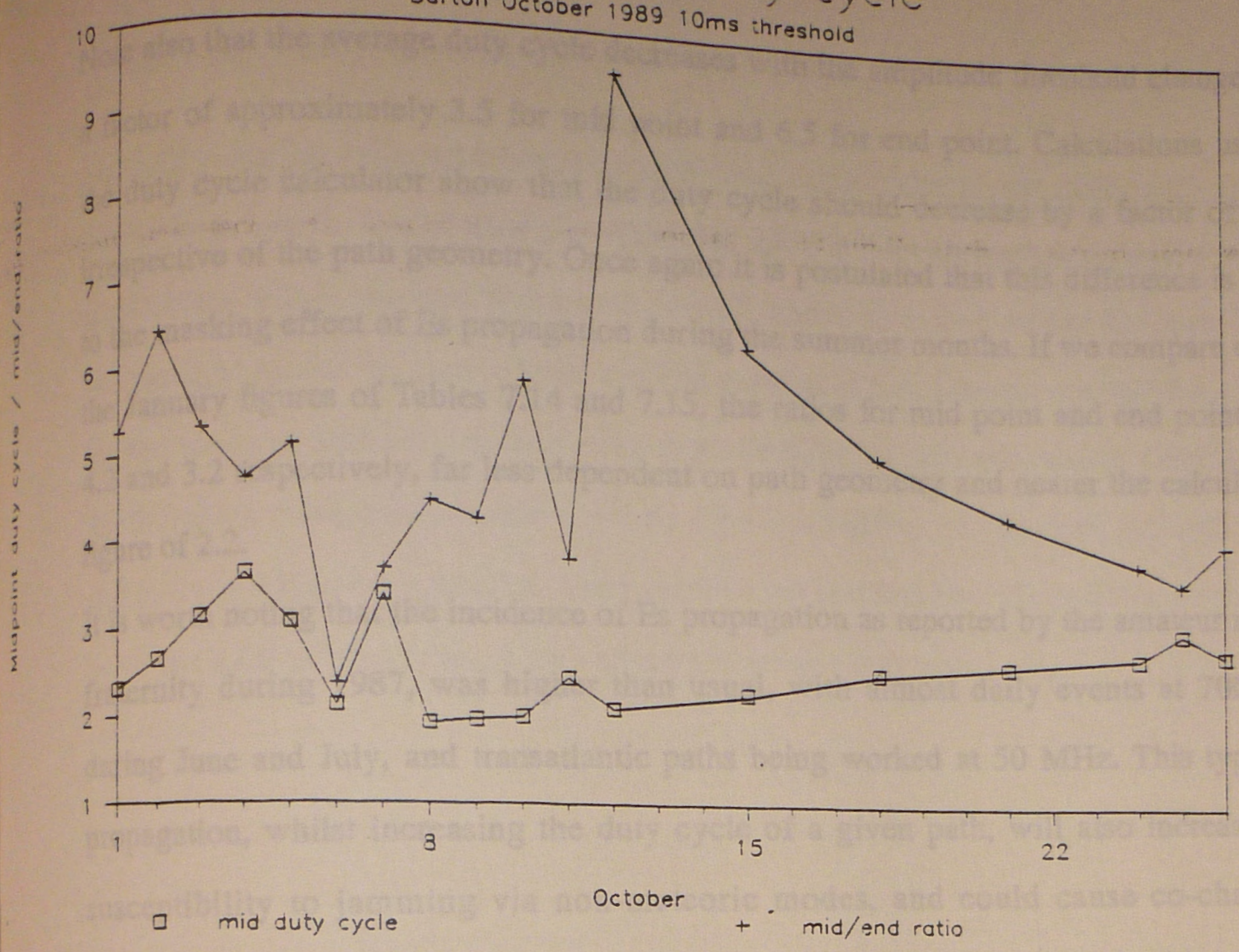

Fig 7.27 Mid point duty cycle advantage

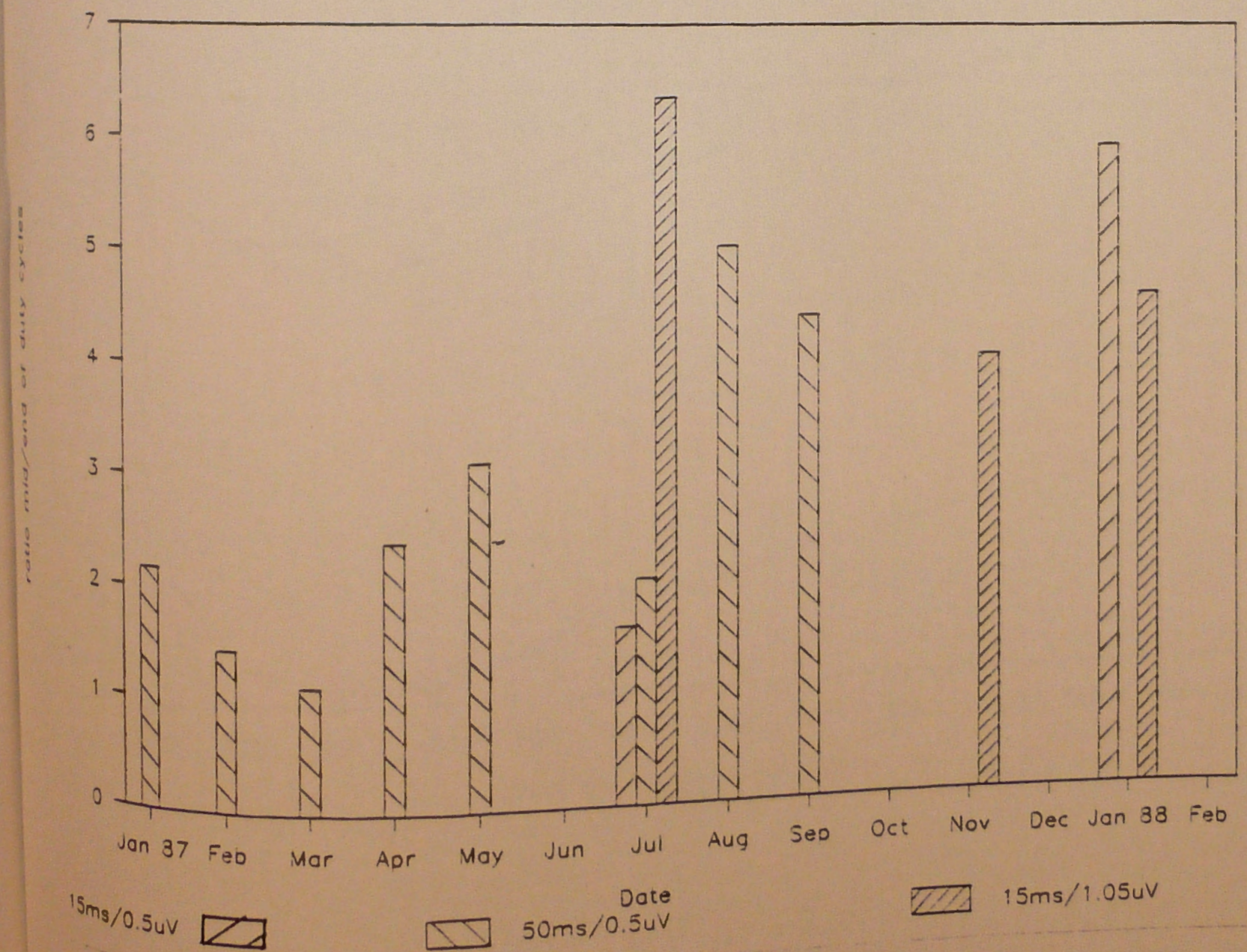

Note also that the average duty cycle decreases with the amplitude threshold change by a factor of approximately 3.5 for mid point and 6.5 for end point. Calculations using the duty cycle calculator show that the duty cycle should decrease by a factor of 2.2 irrespective of the path geometry. Once again it is postulated that this difference is due to the masking effect of Es propagation during the summer months. If we compare only the January figures of Tables 7.14 and 7.15, the ratios for mid point and end point are 4.2 and 3.2 respectively, far less dependent on path geometry and nearer the calculated figure of 2.2.

It is worth noting that the incidence of Es propagation as reported by the amateur radio fraternity during 1987, was higher than usual, with almost daily events at 70MHz during June and July, and transatlantic paths being worked at 50 MHz. This type of propagation, whilst increasing the duty cycle of a given path, will also increase its susceptibility to jamming via non-meteoric modes, and could cause co-channel interference problems due to the existence of large signals of long duration from distances up to 2500 km (35).

7.4 Effect of transition wavelength

Fig 7.28 plots the difference between theoretical end point and mid point path losses against path length. It is plotted for transverse trails at the experimental frequency and frequencies where the end point path is well above and well below the transition wavelength. As can be clearly seen, the end point path loss should be lower for a very limited range of path lengths, and even then the effect is only very small. Only below the transition wavelength should there be significant difference between the end point and mid point signal amplitudes. The experimental results show the received signals to be within a dB of each other, with a slight mid point advantage.

Fig 7.28 Mid/end point path loss ratio

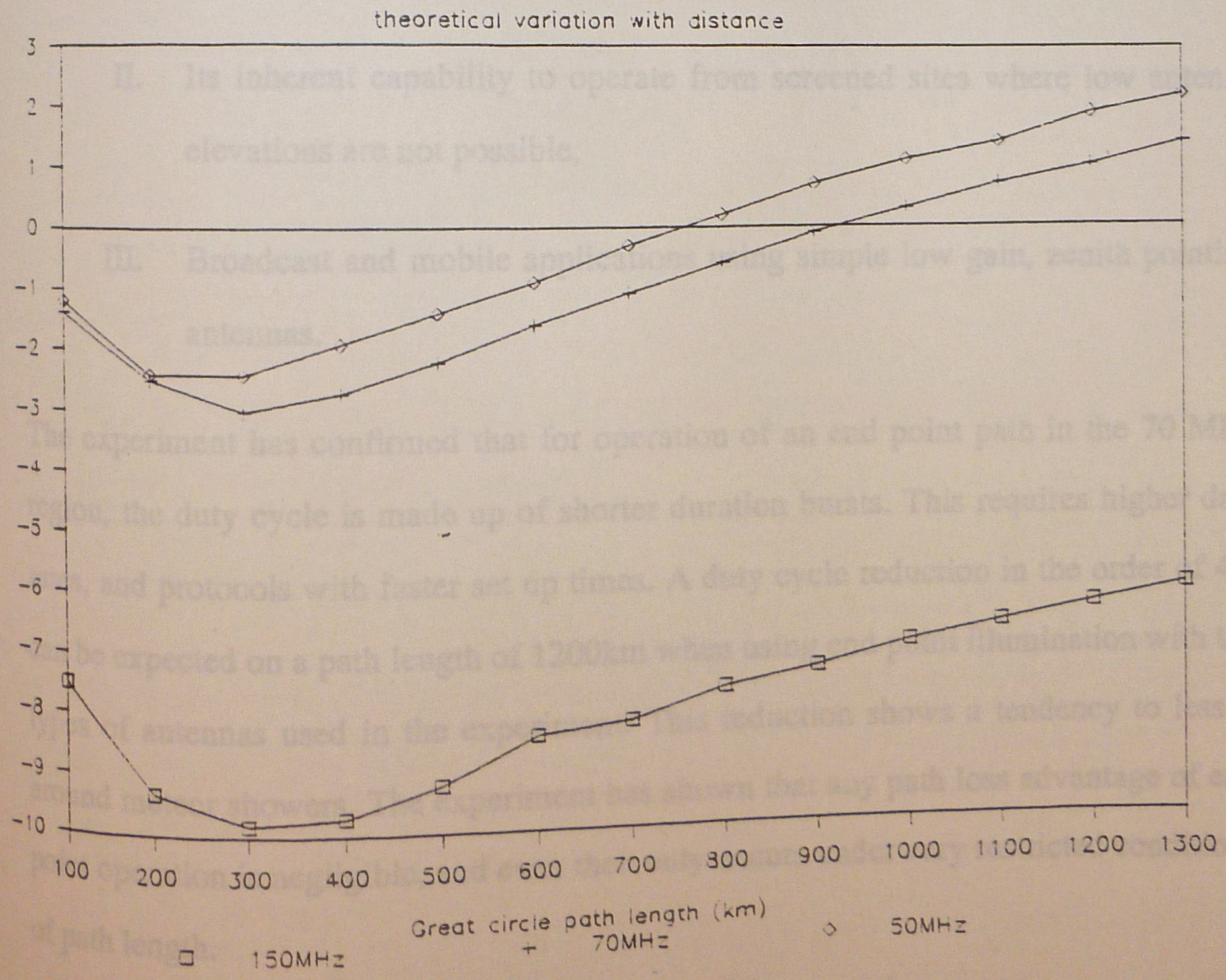

Section 8

Conclusions

8.1 Experimental results, and conclusions about the end point path geometry.

The experiment has shown that simple zenith pointing antenna systems can be used for meteor burst communications from "difficult" sites with a high level of noise. Received amplitudes have been shown not to significantly reduce, or increase when compared to mid point illumination, but duration and duty cycle are significantly reduced.

The attractions of "end point" path geometry are :

I. No requirement to carefully aim the antenna in azimuth or elevation,

II. Its inherent capability to operate from screened sites where low antenna elevations are not possible,

III. Broadcast and mobile applications using simple low gain, zenith pointing antennas.

The experiment has confirmed that for operation of an end point path in the 70 MHz region, the duty cycle is made up of shorter duration bursts. This requires higher data rates, and protocols with faster set up times. A duty cycle reduction in the order of 4:1 can be expected on a path length of 1200km when using end point illumination with the types of antennas used in the experiment. This reduction shows a tendency to lessen around meteor showers. The experiment has shown that any path loss advantage of end point operation is negligible, and even then only occurs under very restricted conditions of path length.

The dependence of transition wavelength on path geometry has been highlighted, requiring more complicated models for basic path loss at higher frequencies.

Section 9

Recommendations for further work

9.1 The data logger.

This report has described the design and use of an inexpensive data logger to be used for monitoring meteor burst signals from a broadcast VHF FM radio source. The data gathered shows that the approach of using such a readily available signal source can provide a viable alternative to the expense of a dedicated link for basic research into the characteristics of meteor burst propagation.

9.1.1 Limitations

Limitations upon the quality of the results were due to four main factors.

I. Insufficient memory in the microcomputer to allow storage of data without averaging.

II. The high level of noise at the receiving site, in the first experiment limiting the absolute signal sensitivity of the receiving equipment.

III. The four hour closedown of the source transmitter.

IV. The presence of frequency modulation on the transmission combined with a narrow band receiver.

9.1.2 Recommendations for further development of the data logger

Many inexpensive microcomputers are now available with at least 20 times the available random access memory as that available to the author at the start of the project in 1984. This would allow the capability to sample for considerably more than 12 seconds out of 30 on each antenna. This combined with a hard disc for archive

storage, would allow a far better and more accurate data logger to be designed around a modern microcomputer.

The problem of noise on the site was overcome by moving the experiment to a "quiet" site, away from sources of man made noise. From the point of view of fundamental research into the basic properties of the meteor burst mode this was essential, but the aims of this experiment were to try and study the performance of meteor burst circuits in a "practical" environment. The system designer may not always have the luxury of a quiet site, or have the capability of erecting large antenna systems in optimum locations. He is therefore faced with the problem of using a higher receiver threshold, and its consequent effect on duty cycle.

The second limitation in section 9.1.1 can therefore be used to some advantage to draw conclusions about a practical meteor burst path.

The problem of the modulation on the broadcast signal could be overcome by using a receiver with a bandwidth large enough to contain the majority of the available power. This though would have reduced the system sensitivity due to the degradation of received signal to noise ratio. One alternative approach to this problem is described below.

If the statistical distribution of power in the carrier and sidebands for typical modulation could be defined, then the ratio of power in the actual receiver bandwidth to the total power available to the receiver could be estimated, and a correction factor applied, by the data logger software, to the long term calculated values of amplitude, and hence duration and duty cycle. As this project was concerned more with the ratios between these quantities than absolute values, it was decided that the extra complication of such an approach was unnecessary.

9.2 Possible further work into end point geometry

Further experiments should be made from a quiet site with a shorter, dedicated path, where the uncertainties of the characteristics of a commercial broadcast source are removed. Absolute signal amplitudes and durations could then be monitored, with an improved data logger capable of discerning very short bursts from noise and to a higher degree of accuracy both in amplitude and duration. With a system with a larger storage capacity, the actual amplitudes and durations of the individual bursts could be stored. This would allow distributions to be compared to theory. On such a short path the duty cycle could be investigated and compared to a fuller model of the type used by Weitzen (38).

There is still more practical work to be performed to determine the optimum transmit and receive antenna patterns for a given path, or receiving location. It should take into account not only the need to optimise the duty cycle, but should also consider other factors such as antenna size, required transmitter power and local terrain.

When faced with communicating from deep valleys, end point illumination via meteor burst could provide an option. Such a "worst case" would be only accessible otherwise by HF, intermediate repeaters, or orbiting satellites using store and forward techniques. Data from such an experimental link would provide further useful information for system designers.

End point geometry also has applications to mobile receiving situations where size limitations will rule out high gain low radiation angle antennae. Further research could possibly be pursued into zenith oriented, roof mounted microstrip antennae, with the vehicle body used as ground plane.

The effect of overdense bursts has not been studied in any depth, and much theoretical work in this area remains to be done. Such bursts may prove to be the major contribution to the type of "worst case" link described above, and therefore good models are required, and good experimental data.

Universities, Polytechnics and Colleges could contribute to this in a small way by encouraging the Amateur Radio enthusiasts amongst their ranks to undertake projects to keep careful records of their use of the 144MHz band for communication via meteor burst with relatively simple equipment. The majority of these contacts rely on overdense bursts due to the relatively high frequency used. Such records could provide an inexpensive source of data on overdense bursts.

References

1. Nagaoka H "Possibility of the radio transmissions being disturbed by meteoric showers" Proc Imp Acad Tokyo vol 5 No 6 1929.

2. Pickard GW "A note on the relation of meteor showers and radio reception" Proc IRE vol 19 No 7 1931.

3. Lovell ACB and Clegg JA "Characteristics of the radio echoes from meteor trails" Proc Phys Soc vol 60 1948.

4. Von Eshelman R and Manning LA "Radio communication by scattering from meteoric ionisation" Proc IRE vol 42 1954

5. Forsyth PA, Vogan EL et al " The principles of JANET – a meteor burst communication system" Proc IRE Vol 45 1957

6. Sites FJ "Communications via meteor trails" AGARD conf proc 244 paper 19 1978

7. Rycroft CMD "An investigation into the optimum antenna azimuth and elevation angles for meteor scatter comms syst design" Unpublished undergraduate project report Dept of Communication Engineering Plymouth Polytechnic 1982

8. World Radio TV Handbook 1985 p109

9. Oetting JD "An analysis of meteor burst communications for military applications" IEEE trans comms syst vol 28 no 9 Sept 1980

10. "Communications by meteor burst propagation" CCIR report 893 251-3 1982 pp 166 – 174

11. Opie C "Interfacing the BBC microcomputer" McGraw Hill 1984 ISBN 0-07084-724-X

12. Birnbaum I "Assembly Language programming for the BBC microcomputer" 2nd ed 1984 ISBN 0-333-37096-1

13. Coll J and Allen D BBC microcomputer system User Guide

14. The Advanced user Guide for the BBC microcomputer

15. Von Eshleman R "On the wavelength dependence of the information capacity of meteor burst propagation" Proc IRE vol 45 1957 p 1710

16. Vincent W et al "Analysis of oblique path meteor propagation data from the communications viewpoint". Proc IRE vol 45 1957 p1701

17. Vincent W et al A meteor burst system for extended range VHF communications". Proc IRE vol 45 1957 p 1693

18. Hannum AJ et al "Air to ground meteoric scatter communications system" IRE trans. comms. syst. June 1960

19. Bartholome PJ and Vogt I "COMET – a new meteor burst system incorporating ARQ and diversity IEEE trans. Comm. vol COM-16 pp 268,278

20. Sugar GR " Radio propagation by reflection from meteor trails" Proc IEEE Feb 1964 p 116

21. Brown DW and Williams HP "The performance of meteor burst systems at different frequencies" AGARD Conf Proc 244 pp 24-1 to 24-26

22. Nes H "Dimensioning technique for meteor burst communications systems" Proc IEE pt F vol 132 no 6 Oct 1985

23. Meeks ML and James JC "On the influence of meteor radiant distributions in meteor scatter communications" Proc IRE vol 45 1957 pp 1724-1733

24. Willis K "4-2-70 VHF column" Radio Communication October 1983 p895

25. Eshleman VR and Mlodnosky RF "Directional characteristics of meteor propagation derived from radar measurements" Proc IRE vol 45 1957 p 1715

26. Grayer GH and Bartram CP "Meteor Scatter data" published 1980 by the Radio Society of Great Britain

27. Worsnop JC "Reduction of rf breakthrough from the BBC Computer " Radio Communication December 1987

28. Eshleman VR "Theory of radio reflections from electron-ion clouds" IRE trans on Antennas and Propagation vol AP3 Jan 1955 pp32-39

29. Viezbicke PP "Yagi antenna design" NBS technical note 688 US Dept of Commerce December 1976

30. "The effect of metal support structures on the performance of VHF and UHF antennas." Pye Telecommunications Ltd Engineering notes publication Ref No TSP485/1 1978.

31. Lovell AC " Meteor Astronomy " Oxford University Press 1954

32. Greenhow JS and Hall JE "The importance of initial trail radius on the apparent height and number distributions of meteor echoes" Monthly notices Royal Astron Soc 1960 Vol 121 p 183

33. Brown DW "A physical meteor burst model and some significant results for communication systems design." IEEE Journal on selected areas in communications vol Sac – 3 no 5 Sept 1985.

34. Hines CO and PughR E " The Spatial distribution of signal sources in meteoric forward scattering " Canadian Journal of Phys 1956 34 pp 1005-1015

35. Tagholm LF, Bell CP and Knight P "Ionospheric propagation in VHF television Band 1." BBC Research Dept document BBC RD 1975/17 June 1975

36. Davies JG "Radio Observations of meteors," Advances in Electronics and Electron Physics, Vol.9, Academic press, Inc., New York 1957.

37. Rudie NH "The relative distribution of observable meteor trails in forward scatter meteor communications" PhD thesis University of Montana 1967.

38. Weitzen JA "Communicating via meteor burst at short ranges" IEEE trans. on Comms. vol. com-35, No 11, November 1987.

39. Davidovici S and Kanterakis EG "Performance of a meteor burst communication system using packet messages with variable data rates". IEEE trans on Comms. vol. 37, No 1, January 1989.

40. Cannon PS "Polarisation rotation in meteor burst communication systems" Radio Science vol. 21, No. 3, May-June 1986.

41. Krauss JD "Antennas" McGraw-Hill, New York 1950

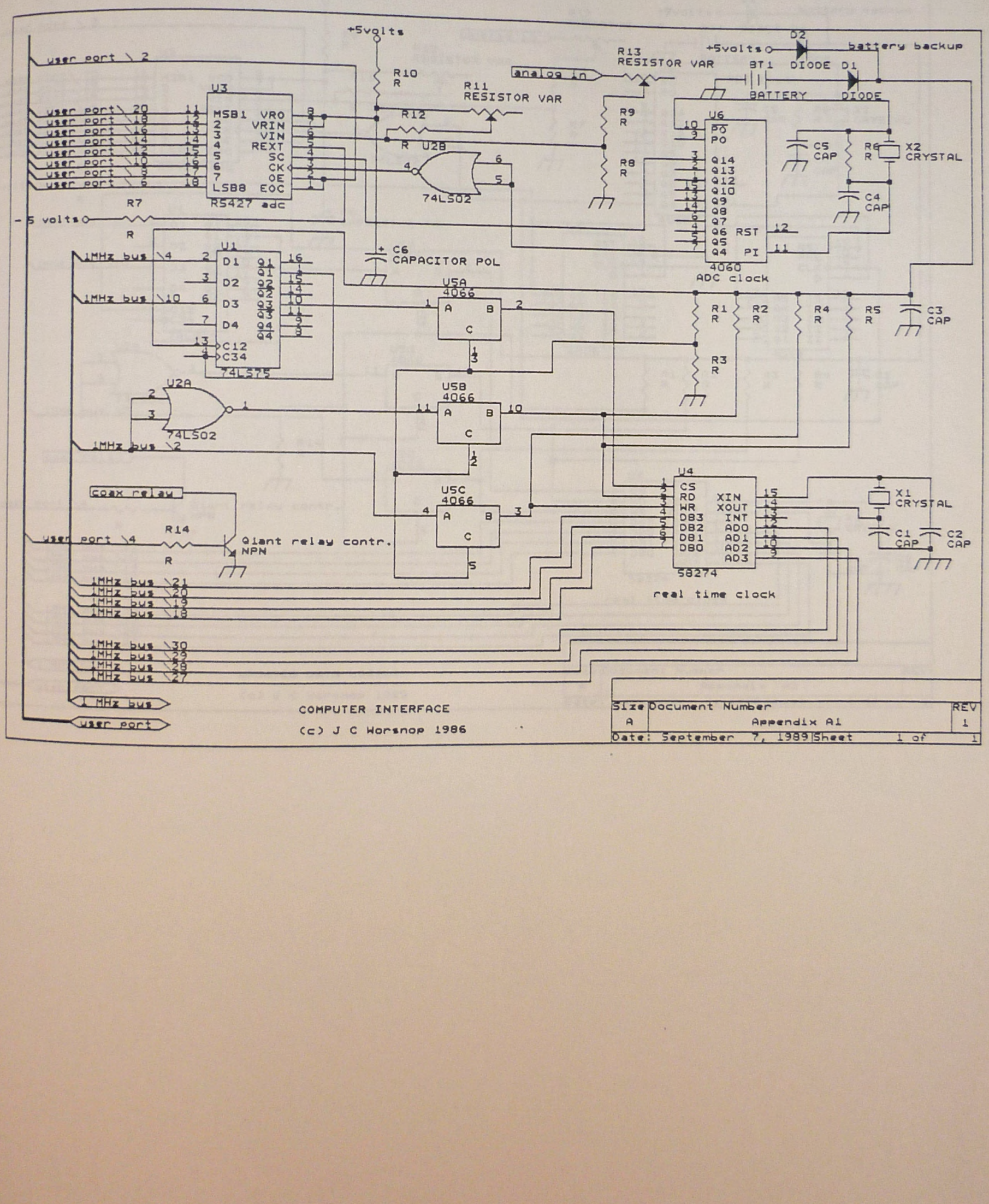
+5volts
user port \ 2
R10
R
R11
RESISTOR VAR
R12
R
analog in
R13
RESISTOR VAR
+5volts
D2
battery backup
BT1
BATTERY
DIODE D1
DIODE
U3
MSB1 VRO
VRIN
VIN
REXT
SC
CK
OE
LSB8 EOC
R5427 adc
user port \ 20
user port \ 18
user port \ 16
user port \ 14
user port \ 12
user port \ 10
user port \ 8
user port \ 6
U2B
74LS02
R9
R
R8
R
U6
PO
PO
Q14
Q13
Q12
Q10
Q9
Q8
Q7
Q6 RST
Q5
Q4 PI
4060
ADC clock
C5
CAP
R6
R
X2
CRYSTAL
C4
CAP
R7
R
- 5 volts
+ C6
CAPACITOR POL
U1
D1 Q1
D2 Q2
D3 Q3
D4 Q4
C12
C34
74LS75
1MHz bus \4
1MHz bus \10
U5A
4066
A B
C
U5B
4066
U5C
4066
U2A
74LS02
1MHz bus \2
R1
R
R2
R
R4
R
R5
R
C3
CAP
R3
R
coax relay
R14
R
user port \4
Qiant relay contr.
NPN
U4
CS
RD
WR
DB3
DB2
DB1
DB0
XIN
XOUT
INT
AD0
AD1
AD2
AD3
58274
real time clock
X1
CRYSTAL
C1
CAP
C2
CAP
1MHz bus \21
1MHz bus \20
1MHz bus \19
1MHz bus \18
1MHz bus \30
1MHz bus \29
1MHz bus \28
1MHz bus \27
1 MHz bus
user port
COMPUTER INTERFACE
(c) J C Worsnop 1986
Size
A
Document Number
Appendix A1
REV
1
Date: September 7, 1989
Sheet 1 of 1

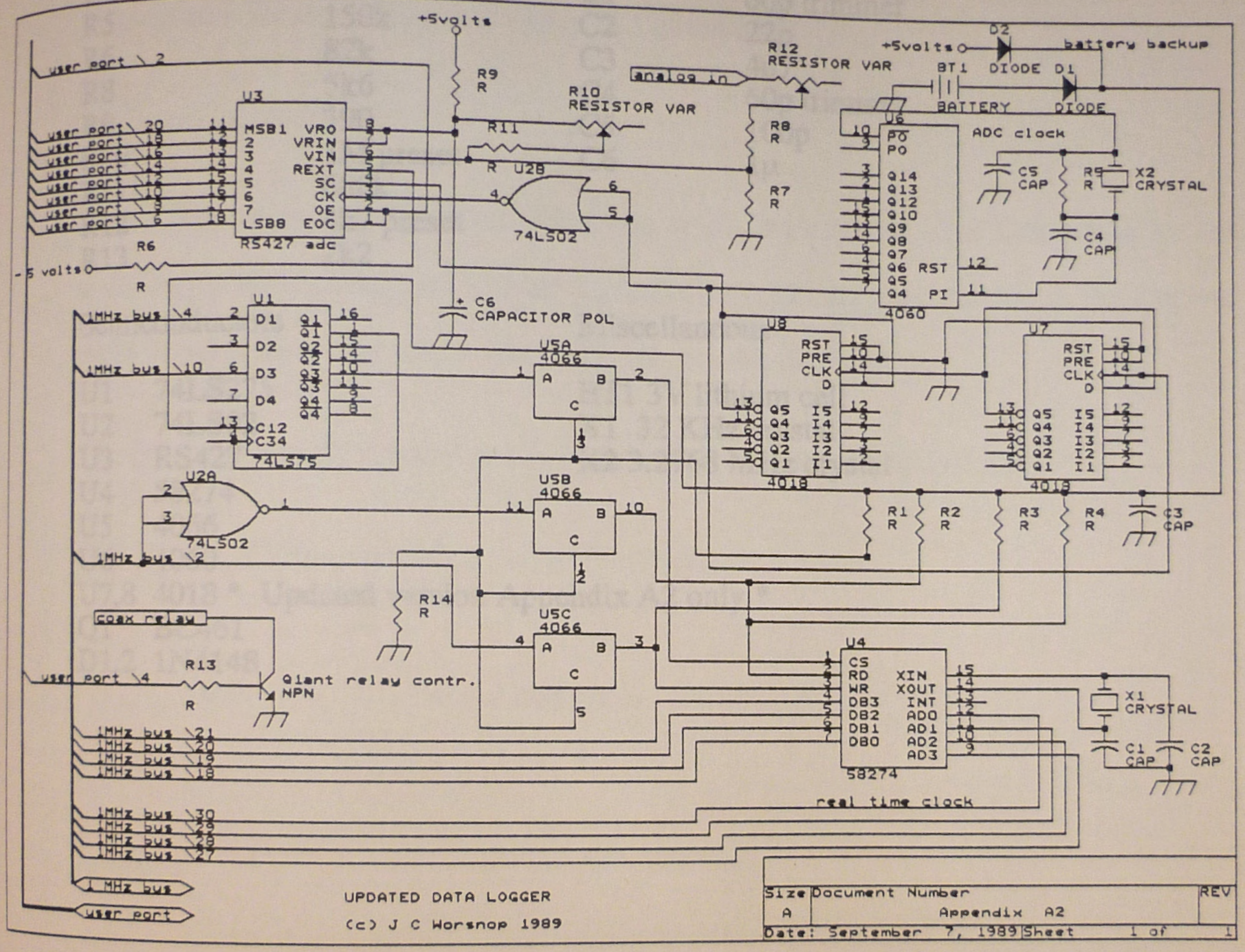
+5volts
user port \ 2
R9
R
R12
RESISTOR VAR
analog in
R10
RESISTOR VAR
D2
+5volts
battery backup
BT1
BATTERY
DIODE D1
DIODE
U3
MSB1
VRO
VRIN
VIN
REXT
SC
CK
OE
EOC
LSB8
RS427 adc
R11
R
U2B
74LS02
R8
R
R7
R
U6
ADC clock
C5
CAP
R9
R
X2
CRYSTAL
C4
CAP
4060
-5 volts
R6
R
+ C6
CAPACITOR POL
1MHz bus
U1
D1
D2
D3
D4
C12
C34
74LS75
U5A
4066
U8
RST
PRE
CLK
D
4018
U7
4018
R1
R
R2
R
R3
R
R4
R
C3
CAP
U2A
74LS02
U5B
4066
R14
R
coax relay
U5C
4066
U4
CS
RD
WR
DB3
DB2
DB1
DB0
XIN
XOUT
INT
AD0
AD1
AD2
AD3
58274
real time clock
X1
CRYSTAL
C1
CAP
C2
CAP
R13
Qiant relay contr.
NPN
1 MHz bus
user port
UPDATED DATA LOGGER
(c) J C Worsnop 1989
Size
A
Document Number
Appendix A2
REV
Date: September 7, 1989
Sheet 1 of 1

Appendix A3
Computer to receiver interface

Components list

Resistors (ohms)

R1-4,14,7	120k
R5	150k
R6	82k
R8	5k6
R9	390
R10	1M preset
R11	680k
R12	4k7 preset
R13	2k2

Capacitors (Farads)

C1	60p trimmer
C2	22p
C3	4n7
C4	60p trimmer
C5	100p
C6	1µ

Semiconductors

U1	74LS275
U2	74LS02
U3	RS427
U4	58274
U5	4066
U6	4060
U7,8	4018 * Updated version Appendix A2 only *
Q1	BC461
D1,2	1N4148

Miscellaneous

BT1 3V lithium cell
X1 32 KHz crystal
X2 3.2768 MHz crystal

Appendix (b)

1.Antenna models

The computer program for the calculation of link duty cycle described in appendix (e) requires information in the form of a gain function in azimuth and elevation about the polar pattern for the antennas at either end of the link.

1.1 Receiving antennae

Both antennae in use at the receiving site were five element Yagi Uda arrays on 0.8 wavelength booms designed to NBS specification (29) designed for use in the amateur radio 70MHz band. Section 5 details the reasons for their choice.

The first gain function model to be considered was that used by Nes (22)

$$G_r(a,b) = \frac{G_o \, EXP(-(a^2+b^2)G_o)}{4} \qquad b > 3 \text{ degrees}$$

$$= 0 \qquad b < 3 \text{ degrees} \ldots\ldots\ldots\text{(i)}$$

where G_r = the gain function

a,b = the azimuth and elevation angles respectively

G_o = the maximum gain = 8.91

This was initially compared over the range a,b = +- 90 degrees with the published plots (29), but did not take into account the differing azimuth and elevation beamwidths. After a little trial and error, the following expression was deemed suitable to describe the free space polar pattern.

$$G_r(a,b) = G_o \, EXP(-(a^2/3.5 + b^2/4)G_o) \ldots\ldots\text{(ii)}$$

Fig Ab1 Antenna model: E plane

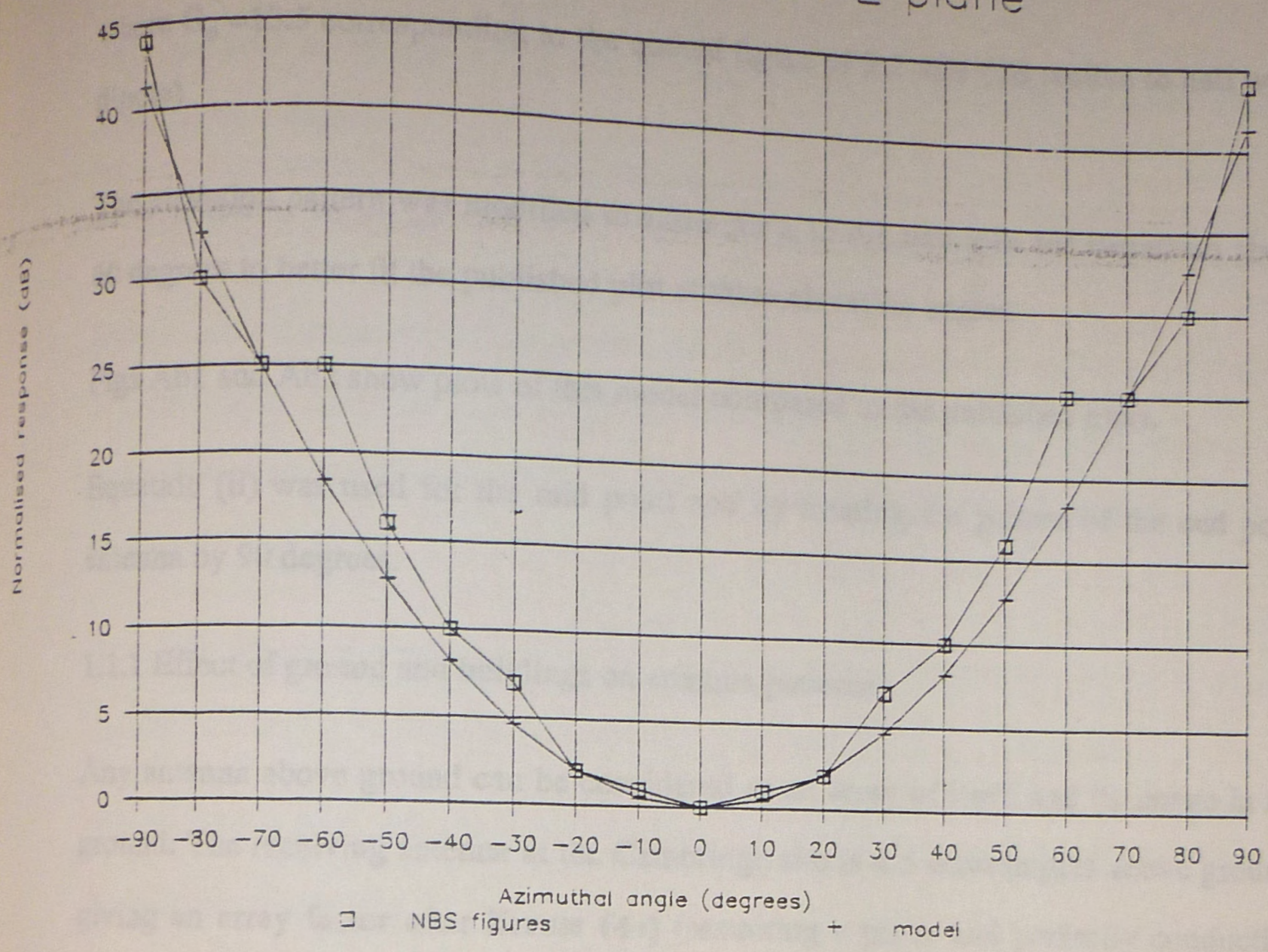

Fig Ab2 Antenna model: h plane

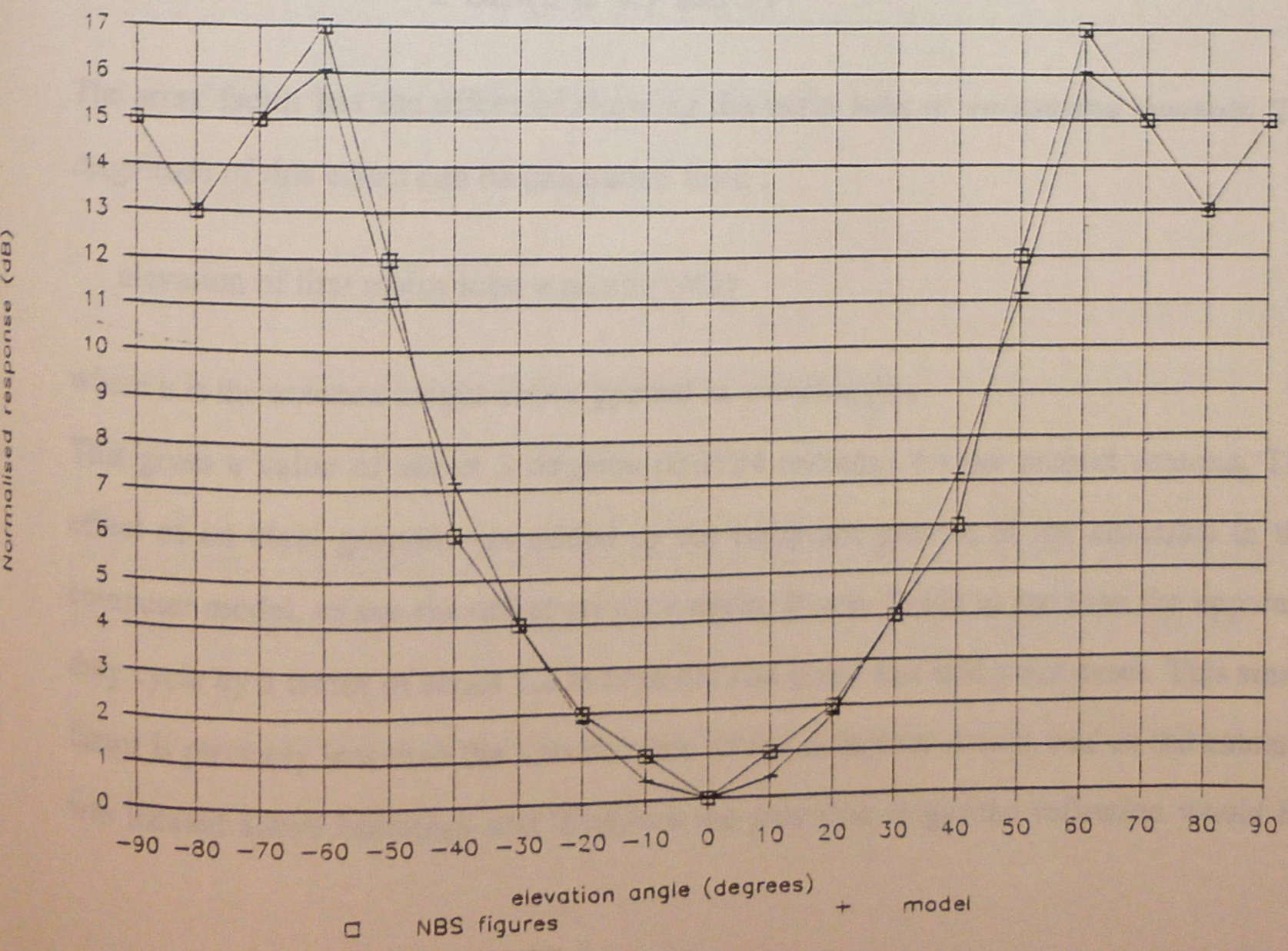

where G_o =13.5 corresponding to the quoted figure of 9.2 dBd (dB reative to half wave dipole)

The elevation pattern was modified to allow for a 15 dB side lobe for elevations above 60 degrees to better fit the published plot at these elevation angles.

Figs Ab1 and Ab2 show plots of this model compared to the published plots.

Equation (ii) was used for the mid point and by rotating the pattern of the end point antenna by 90 degrees.

1.1.1 Effect of ground and buildings on antenna patterns

Any antenna above ground can be considered as an array of itself and its image in the ground. The receiving antenna at the Cambridge site is 4.5 wavelengths above ground, giving an array factor after Krauss (41) (assuming a plane and perfectly conducting ground) of:

$$2*SIN(2*\pi*4.5*\sin(b))$$

The array factor has the effect of skewing the main lobe of an antenna upwards. The magnitude of this effect can be calculated from :

elevation of first major lobe = arcsin(1/4h)

where h is the antenna height above ground in wavelengths

This gives a value of about 3 degrees (0.0524 radians) for the project antenna. The effect of an ideal ground was added to the radiation pattern of the antennae in the computer model, to see the effect on duty cycle. It was found to increase the apparent duty cycle by a factor of about 1.2 in both the end point and mid point cases. This small factor is probably less than the uncertainties of the computer model, and as the antenna was located above buildings and therefore the gain due to ground reflection would be

very unlikely to be realised, it was decided to simply skew the free space pattern upwards by 3 degrees.

1.2 Transmitting antenna.

Detailed information proved impossible to obtain for the antenna system used at Radio Wroclaw, apart from the broad statement that they were high gain, omnidirectional and had a low vertical radiation angle. It was therefore decided to use a model that fitted commonly used Band 1 and 2 broadcast antennas used in Europe.

Reference 35 gives measured plots for a number of television transmitters in Band 1 and they all have a vertical 3dB beamwidth in the order of 5 to 10 degrees.

The model for the elevation pattern used in the duty cycle calculations was based on the following formula :

$$G_t = EXP(-kb^2) \ldots\ldots\ldots (iii)$$

where k is a constant (as the EIRP of the transmitter was known, the antenna model was normalised to the gain of an isotropic radiator)

3. Model testing

Due to the lack of hard information it was decided to run the duty cycle model with a number of different transmit antenna configurations. This would determine the magnitude of its effect on the duty cycle.

The reference run used an isotropic radiator, followed by equation (iii) with k=25 representing elevation 3dB points of 10 degrees and k=35 representing 7.5 degrees.

The runs were carried out with both mid point and end point illumination at the receiving site, using the 5 element yagi model of equation (ii).

It was found that the calculated duty cycle fell by a factor of 1.7 when going from an isotropic source to either of the two realistic models, with no noticeable change between k=25 and k=35. This change was confirmed both with the end point and mid point calculations.

It was therefore decided to use k=25 in all calculations.

To try and model any secondary lobes on the azimuth pattern of the antennas, a secondary lobe of –20dB down on main lobe was added to the antenna patterns outside the range modelled by the forward lobe. This was found to make negligible difference to the calculated duty cycles and was therefore abandoned.

program description "RUNPROG"

This is the main program controlling the experiment timing.
It calls the assembler code sampling routine "METOR12".
CONSTANTS
TIMER
SAMPLE
SETUP.....locations in assembly code program
BNUM
LSBL
MSBL
LSBA
MSBA.....locations for results of METOR12
VARIABLES
BLENGTH.....cumulative burst length in tenths of seconds
ALEN.....average burst length
AMPL.....cumulative burst amplitude
AAMP.....average burst amplitude
BNUM.....number of bursts over 2 min period
tenhour.....tens of hours
hour.....units of hours
tenminute.....tens of minutes
minute.....units of minutes
month.....units of month
tenmonth.....tens of month
tenday.....tens of days
day.....units of days
hourno$.....hour header for disc file
PROCEDURES
time.....returns day,date,time
midnight.....creates a new day file
divide.....works out average data values
storedata.....puts 1 hrs averaged data to disc
ARRAYS
STORE.....stores sorted 2 min data

MAIN PROGRAM

```
Set up user memory and load assembler code
Allocate memory locations for assembler
code,results of METOR12
Find out what time and date is.
Create a day file for data storage with title
"datemonth"
Call assembler code sampling routine to gather an
hour's data
Create array "STORE"
REPEAT forever
        work out averaged amplitude and duration
        over each two minute period.
        store in array named "STORE"
        Find out what time is
        Write contents of "STORE" to dayfile disc
        IF midnight
        THEN create new day file
        Call assembler code routine to gather
        another hour's data
END PROGRAM
```

LISTING

```
10 REM running program for MPhil project
20 REM version 14   15/2/87  (c) J C Worsnop
30 REM  program structure identical  to  "WHOLE13"  with
       added comments
35 REM name of PROCdisc changed to PROCtime for clarity
60 REM variable declarations
100 HIMEM=&7FFF : REM allocates more space to program
150 REM loads sampler code from disc
200 *LOAD meteo12 0900
300 *DR.2
350 REM the following lines point to parts of sampler code
400 TIMER=&0907
420 SAMPLE=&0948
430 SETUP=&900
450 REM  the following lines allocate memory locations to
     results of  SAMPLE
500 BNUM=&2100
600 LSBL=&210D
700 MSBL=&211A
800 LSBA=&2126
900 MSBA=&2132
1150 REM main program starts here
1200 PROCtime
1300 PROCmidnight
1400 CALL SETUP
1500 DIM STORE(3,12) : REM array to store sorted 2 minute data  1600  REPEAT
1700   PROCdivide
1800   PROCtime
1900   PROCstoredata
2000   CALL SAMPLE : REM returns total amplitude duration
```

```
                                and number of valid bursts
2100   UNTIL FALSE
2200 END
2300 REM end of main program
2360 :================================================================
2400 DEF PROCdivide : REM works out average amplitude and
                                duration for 2  mins
2450 REM and stores away in hour array "STORE"
2500 N=0
2600 REPEAT
2700   BLENGTH=((MSBL?N)*256+(LSBL?N))*5E-2
2800   IF BNUM?N=0 THEN ALEN=0 ELSE ALEN=BLENGTH/(BNUM?N)
2900   N=N+1  3000    STORE(1,N)=ALEN
3100   UNTIL N=12
3200 N=0  3300  REPEAT
3400   AMPL=(256*(MSBA?N)+(LSBA?N))
3500   IF BNUM?N=0 THEN AAMP=0 ELSE AAMP=AMPL/(BNUM?N)
3600   N=N+1
3700   STORE(2,N)=AAMP
3800   UNTIL N=12
3900 N=0
4000 REPEAT
4100   N=N+1
4200   STORE(3,N)=(BNUM?(N-1))
4300   UNTIL N=12
4400 ENDPROC
4500
:================================================================
4600 DEF PROCtime : REM looks to see what day, date, and
                                        time it is
4700 tenhour=FNrtime(&C7)
4800 hour=FNrtime(&C6)
4900 tenminute=FNrtime(&C5)
5000 minute=FNrtime(&C4)
5100 month=FNrtime(&CA)
5200 tenday=FNrtime(&C9)
5300 tenmonth=FNrtime(&CB)
5400 day=FNrtime(&C8)
5500 tenday=FNrtime(&C9)
5600 ENDPROC
5650 :
5700 :================================================================
5800 DEF FNrtime(address%) : REM real time clock access routine     5900  LOCAL
r%
6000 address%=address%AND &FF
6100 IF(address%<&C0) OR (address%>&FE) THEN=0
6200 A%=&92:X%=address%:r%=USR(&FFF4)
6300 =(r% AND &F0000) DIV &10000
6350 :
6400 :================================================================
6500 DEF PROCmidnight : REM creates new day file at midnight   6600  CLOSE#0
6700 filenam$=STR$(tenday)+STR$(day)+STR$(tenmonth)+STR$(month)    6800
X=OPENOUT(filenam$)
6900 ENDPROC
6950 :
```

```
7000 :=============================================================
7100 DEF PROCstoredata : REM  puts one hour's average
                              data to disc day file
7200 hourno$=STR$(tenhour)+STR$(hour)
7300 PRINT#X, VAL(hourno$)
7400 FOR COLUMN=1 TO 12
7500  FOR ROW=1 TO 3
7600   PRINT#X, STORE(ROW,COLUMN)
7700   NEXT ROW
7800  NEXT COLUMN
7900 IF hour=0 AND tenhour=0 AND minute=0 AND tenminute=0
     THEN PROCmidnight
8000 ENDPROC
```

Appendix (c) (ii)

This is the 6502 assembler code routine which controls the reading of the data from the ADC connected to the user port of the BBC micro.

The purpose of this software is to allow the system to look at the received signal amplitude from each antenna for two minutes out of every ten. All sampling starts at multiples of five minutes past the hour.

At hour + 0 minutes the software switches the mid point antenna to the receiver and stores five millisecond samples of data to the machine's RAM (the "scratch pad")for two minutes.

From hour +2 to hour +5, the software sorts through the data and counts the number of valid bursts, and their cumulative amplitudes and durations. These are stored as 2 bytes for total amplitude, 2 bytes for total duration, and 1 byte for the number of valid bursts in the period. The software then goes back to checking the clock and when hour +5 is reached the end point antenna is switched to the receiver and the whole process repeats for two minutes of end point data.

This process of changing antennas and logging data continues until the hour is reached, when the routine returns control to "RUNPROG". At the end of the hour the program has stored 30 bytes of data from each antenna representing the number of bursts logged, and their cumulative amplitude and duration.

Program description "METOR12"

Initialise user port on BBC for all lines inputs
put 0 in zero page location &79 (used later)
check minutes of clock
IF minutes = 0 THEN switch to midpoint antenna
AND check tens of minutes
If tens of minutes = 0 THEN return to RUNPROG
ELSE start sampling
ELSEIF minutes = 5 THEN switch to endpoint antenna and
start sampling

Sampling routine
.sample
set up user port
initialise scratch pad to location &2140
REPEAT
wait for data ready from ADC
store sample
UNTIL scratch pad full to &7F00

The RAM now contains 24K samples representing 2 minutes of data

Sorting routine for detecting bursts
.sift
Initialise temporary storage locations
set sort start location to &2140
REPEAT
look at sample
IF sample above threshold branch to routine ".ping"
ELSE increment sample location
UNTIL sample location = &7F00
call routine ".array"
Sample above threshold routine
.ping
store this sample as current maximum
set sample count to zero
REPEAT
add 1 to sample count
increment sample location
IF next sample > current maximum THEN make it
current maximum AND
increment sample count
ELSEIF next sample > threshold THEN increment sample
count
ELSEIF sample count > 3 THEN add sample count and
current maximum to running tally and increment burst count
(routine ".incr")
UNTIL sample location = &7F00 OR sample count < 3
branch back to .sift routine at .retrn

one hour storage routine
.array
This routine stores the reduced data from .sift as 60 bytes per hour starting at location &2100 .(See memory allocation table)

PROGRAM LISTING "METEO12" (program for 1st main experiment)

```
10  REM source code for meteo12  for MPhil project
20  REM (c) J C Worsnop 1986
30  REM further comments added 15/2/87
40  REM restructured slightly and  more comments added for
                writeup      25/6/87
50  :
60  DIM PASS 450
70  FOR I%=0 TO 3 STEP 3:P%=PASS
80    :
90    REM   start of code
100    [OPT I%
110   :
120   .setup      \ Initialise Port
130   LDA#&00 : STA&FE62 : STA&79
140   :
170   .timer      \ finds out if minutes 0 or 5
180   LDX#&C4
190   JSR r.time   \ returns minutes in Y register
200   CPY #&00 : BEQ str0 : CPY#05 : BEQ str5
240   JMP timer    \ loops if not 0 or 5
250   :
260   .str0  \ switches to  mid  an  checks  if top of
                              hour then starts sampling
270   LDA#&CE : STA&FE6C : STA&FE60 : LDX#&C5
310    JSR r.time   \ returns tens of minutes in Y register  320    CPY#0 : BEQ disc :
JMP sample
360   :
370   .str5       \ switches end ant then starts
                                      sampling
380   LDA#&EE : STA&FE6C : STA&FE60 : JMP sample
420   :
430   .disc       \                   top of  hour routine , returns to
                                      BASIC prog to disc dump
440   LDA#0  : STA&79 : RTS
470   :
480   .sample      \ ADC sampling routine
490   LDA#&90 : ORA&FE6C : STA&FE6C : LDX#0 : LDX&77
540     LDX#&21          \ sets start of "scratch pad" to &2140  550    STX&78 :
LDY#&40
560   :
570   .begin
580   LDA#&10
590   .wait        \ waits for data ready signal from ADC  600   BIT&FE6D : BEQ wait
: LDA&FE60
610   STA(&77),Y    \ stores sample in RAM
640   INY : CPY#0 : BNE begin : INC&78
650   LDA#&7F : CMP&78      \ checks for  end of 2 minutes
                                          (scratch pad full to
                                          &7FFF)

700   BNE begin
710   :
720   .sift       \                   sorts through  stored  RAM data
                                      and detects bursts
```

```
730  LDA#0 : STA&72 : STA&73 : STA&74 : STA&75 : STA&76
790  TAX : STX&77
800  LDX#&21 : STX&78 : LDX#&40 : LDY#&40  \ sets start
                                           location for sort to
                                           &2140
850  :
860  .sort
870   LDA(&77),Y      \ checks if sample above threshold  880    CMP#&A0 : BCS
ping
900  :
910  .retrn
920  INY          \ if not moves to next sample
930  CPY#0 : BNE sort
940  INC&78 : LDA#&7F : CMP&78  \ checks for end of
                                  scratch pad at 7FFF
980  BNE sort : JSR array : JMP timer      \ end of main
                                                    program
1010  :
1020  .ping              \ sample above threshold routine
1030  STA&74            \ stores sample in location &74
                        (this stores the burst maximum value) 1040    LDA#0 :
STA&70 : STA&71
1070  :
1080  .burst        \ increments sample count
1090  INC&70 : LDA#0 : CMP&70 : BEQ pag
1130  :
1140  .back                          \ moves on to look at next sample
                                     value
1150  INY : CPY#0 : BEQ paje
1180  :
1190  .test
1200  LDA(&77),Y : CMP&74       \ checks if above
                                                 current maximum
1220  BCC less : STA&74
1240  :
1250  .less
1260  CMP#&A0       \ if not  checks  if still above
                                threshold and returns if so
1270  BCS burst : LDA&71 : CMP#0 : BNE incr : LDA&70
1320  CMP#&03 : BCC retrn     \ checks if burst>3
        samples, if not ignores and looks for next
        sample
1340  :       \ if burst  >  3  samples  adds length
                          and amplitude  to running tally and
                          increments burst count
1350  .incr : LDA&74 : CLC : ADC&75 : STA&75 : LDA#0
1410  ADC&76 : STA&76 : LDA&70 : CLC : ADC&72 : STA&72
1470  LDA&71 : ADC&73 : STA&73 : INX : JMP retrn
1520  :
1530  .pag
1540  INC&71         \ sample count paging routine
1550  JMP back : RTS
1570  :
1580  .paje          \ scratch pad pointer paging routine 1590    INC&78 : LDA#&7F :
CMP&78 : BNE test : JSR array
```

```
1640  JMP timer
1650  :
1660  .r.time       \ reads time from realtime clock 1670   LDA#&92 : JSR&FFF4 :
STY&60 : LDA#&0F
1680  AND&60 : TAY : RTS
1740  .array        \stores sorted  data  in  5 byte by
                                    12 array ready for disc dump
1750  TXA : LDX#0 : STX&77 : LDX#&21 : STX&78 : LDY&79
1810  STA(&77),Y : LDX#&0D : STX&77 : LDA&72 : STA(&77),Y
1860  LDX#&1A : STX&77 : LDA&73 : STA(&77),Y : LDX#&26
1910  STX&77 : LDA&75 : STA(&77),Y : LDX#&32 : STX&77
1960  LDA&76 : STA(&77),Y : INC&79  : RTS
2000  :
2010  ]:NEXTI%
2020 CALL setup
```

Modified Program "PHDCD6D" for second experiment

```
10  REM source code for Phd project
20  REM (c) J C Worsnop 1989  7/9/89
30  REM version 6D (FF mod long burst mod + hysteresis)
40  REM modified to start at seconds 0 and 30
50  :
60  FOR I%=0 TO 3 STEP 3:P%=&900
70   :
71  space =&14
80  counter = &7A
90  threshold = &90
100   REM   start of code
110   [OPT I%
120   :
130   .setup      \ Initialise Port
140   LDA#&00 : STA&FE62 : STA&79
170   :
180   .timer      \ finds out if seconds 0 or 30
190   LDX#&C2 : JSR r.time  \ returns seconds in
                                                  register
210   CPY#0 : BEQ continue : JMP timer
240   .continue
250   LDX#&C3 : JSR r.time   \ returns tens of seconds in
                                                    Y register
270   CPY #&00 : BEQ str0 : CPY#03 : BEQ str30
310   JMP timer    \ loops if not 0 or 30
320   :
330   .str0   \ switches to mid and checks if end of ten
                        minutes then
340   LDA#&CE : STA&FE6C : STA&FE60 : LDX#&C4
380   JSR r.time   \ returns minutes in Y register
390   CPY#0 : BEQ disc : JMP sample
430   :
440   .str30        \ switches end ant then starts
                                    sampling
450   LDA#&EE : STA&FE6C : STA&FE60 : JMP sample
490   :
500   .disc     \ ten minute routine, returns to BASIC prog
```

```
510  LDA#0 : STA&79 : RTS
540  :
550  .sample       \ ADC sampling routine
560  LDA#&90 : ORA&FE6C : STA&FE6C : LDX#0 : STX&77
610  LDX#&21       \ sets start of "scratch pad" to &2140
620  STX&78 : LDY#&40
640  .begin
650  LDA#&10
660  .wait         \ waits for data ready signal from ADC
670  BIT&FE6D : BEQ wait : LDA&FE60
700  STA(&77),Y    \ stores sample in RAM
710  INY : CPY#0 : BNE begin : INC&78 : LDA#&7F
760  CMP&78        \ checks for end of twelve seconds
                                (scratch pad full)
770  BNE begin
780  :
790  .sift         \ sorts through stored RAM data and
                                detects
800  LDA#0 : STA&72 : STA&73 : STA&74 : STA&75 : STA&76
860  TAX : STX&77 : LDX#&21 : STX&78 : LDX#0
910  LDY#&40       \ sets start location for sort to &2140
920  :
930  .sort
940  LDA(&77),Y    \ checks if sample above threshold
950  CMP#&FF       \ or FF
960  BEQ retrn : CMP# threshold
980  BCS ping      \ if > A0 go to ping
990  :
1000 .retrn
1010 INY           \ if not moves to next sample
1020 CPY#0 : BNE sort
1040 INC&78 : LDA#&7F
1060 CMP&78        \ checks for end of scratch pad at
                                &7F00
1070 BNE sort
1080 .finish
1090 JSR array
1100 JMP timer     \ end of main program
1110 :
1120 .ping         \ sample above threshold routine
1130 STA&74        \ stores sample in location &74
1140 LDA#0         \ (this stores running maximum)
1150 STA&70 : STA&71 \ sets sample counter to zero
1170 :
1180 .burst        \ increments sample count
1190 INC&70 : LDA#0 : CMP&70       \ checks for paging
1220 BNE back : INC &71
1240 :
1250 .back         \ moves on to look at next sample value
1260 INY : CPY#0 : BEQ paje
1290 :
1300 .test
1310 LDA(&77),Y    \ gets next sample
1320 CMP#&FF : BEQ less
1330 CMP&74        \ checks if above current maximum
```

```
1350  BCC less : STA&74
1370  :
1380  .less       \ comes here if =FF or < current maxm
1390  CMP# threshold     \ if not checks if still above
                                                  threshold
1400  BCS burst                                   \ if so burst still
                                                   on..loops back to burst
1410  .spacevalid    \ if < threshold or FF
1420  LDA#1 : STA counter
1440  .getsample
1450  INY : CPY#0 : BNE go_on
1480  .paj        \ only if Y=0 incs MSB and checks
                                        for 7F00
1490  INC &78 : LDA#&7F : CMP &78
1520  BNE go_on      \ burst over, checking for spaces
1530  JMP lenvalid2   \ if end of scratch pad
1540  .out2
1550  JSR incr : JSR array : JMP timer
1580  :
1590  .go_on
1600  LDA(&77),Y          \ gets next sample
1610  STA &7B             \ stores in &7B
1620  CMP # threshold     \ checks if above threshold
1630  BCS more
1640  .counterinc         \ increments 20counter
1650  INC counter : LDA #space
1670  CMP counter         \ checks if 20
1680  BEQ valid           \ if so finishes
1690  JMP getsample
1700  .more
1701  LDAcounter : CLC : ADC&70 : STA&70 : LDA#0
1706  ADC&71 : STA&71 : LDA&7B \ compares to present max
1771  CMP#&FF : BEQ less : CMP &74 : BCC less
1800  LDA &7B             \ replaces if greater
1810  STA &74 : JMP less
1820  .inc                \ length ok
1840  JSR incr : JMP retrn
1860  :
1870  .valid
1880  JMP allvalid
1890  .exit
1900  JMP retrn
1910  :
1920  .paje       \ scratch pad pointer paging routine
1930  INC&78 : LDA#&7F
1940   CMP&78          \ checks for end of scratch pad
1960  BNE test       \ if not goes to test and continues
1970  JMP lenvalid1    \ if so checks length only
1980  .out1
1990  JSR array : JMP timer
2010  :
2020  .lenvalid1
2040  LDA&71
2041  CMP#0  \ if not checks if MSB sample count = 0
2060  BNE fin      \ if not must be >255 ... burst valid
```

```
2070  LDA&70 : CMP#&0A
2090  BCS fin    \ checks if burst > 10 samples, if not,
                    inc
2100  JMP out1
2101  :
2110  .fin
2120  JSR incr : JMP finish
2140  :
2141  .lenvalid2
2142  LDA&71 : CMP #0 : BNE fin : LDA &70 : CMP#&0A
2147  BCS fin : JMP out2
2149  :
2150  .incr
2160  LDA&74 : CLC : ADC&75 : STA&75 : LDA#0 : ADC&76
2220  STA&76 : LDA&70 : CLC : ADC&72 : STA&72 : LDA&71
2280  ADC&73 : STA&73 : INX : RTS
2320  :
2330  .allvalid      \space ok checks length
2340  LDA&71 : CMP#0 : BNE inc : LDA&70 : CMP# &0A
2390  BCS inc : JMP exit
2410  :
2420  .r.time        \  reads time from realtime clock
2430  LDA#&92 : JSR&FFF4 : STY&60 : LDA#&0F: AND&60
2480  TAY : RTS
2500  :
2510  .array  \stores sorted data in 5 byte by 20 array
2520  TXA : LDX#&CA : STX&77 : LDX#&20 : STX&78 : LDY&79
2580  STA(&77),Y : LDX#&DE : STX&77 : LDA&72 : STA(&77),Y
2630  LDX#&F2 : STX&77 : LDA&73 : STA(&77),Y : LDX#&21
2684  STX&78 : LDX#&06 : STX&77 : LDA&75 : STA(&77),Y
2730  LDX#&1A : STX&77 : LDA&76 : STA(&77),Y : INC&79
2780  RTS
2790  :
2800  ]:NEXTI%
2810 CALL setup
```

The first three programs "NUMBERS", "AMPLTDE", and "DURATON" produce plots of number of bursts, average amplitude, and duration per two minute period against time for a selected day.

As they are all of the same basic format, differing only in the quantity read from the file, I will only describe the operation of "NUMBERS", the other two will be self explanatory.

Program description "NUMBERS"

CONSTANTS

mid,end..... pointer start values for reading burst number data

VARIABLES

filename$..... day file required

drive.....datasource drive

choice.....temporary store for pointer

counter.....end of file counter

tot .....loop counter

burst.....temporary store for input data byte

arraycount.....counts up by 6 to indicate end of a stored number

hop.....incremented by 6 each time stored number is read

column.....array pointer

PROCEDURES

axes.....draws axes

scales..... .....puts on scales

graph.....plots graph

midpoint.....reads data from file

initialise.....sets up drives and opens files

ARRAYS

midpoint.....holds required data from file

MAIN PROGRAM

Input wanted file details

Dimension array "midpoint" to hold extracted data

Draw graph axes and scales set pointer to read endpoint data

REPEAT (once)

Read data from disc into "midpoint"

plot data

set pointer to read endpoint data

END of program

```
Program listing "NUMBERS"
10 REM Number of bursts per 2-min period vs time"
20 REM version 1 22/11/86
21 REM further comments added 1/7/87
30 REM (c) J C Worsnop 1986
40 REM start of main program
50 mid=17
60 end=35
70 pointer=end
80 PRINT "PROGRAM TO PLOT BURSTNUMBERS"
90 PRINT
100 INPUT"WHAT IS THE FILENAME",filename$
110 INPUT"WHICH DRIVE IS IT IN",drive
120 DIM midpoint(144)
130 MODE1
140 PROCaxes
150 PROCscales
160 GCOL 0,3
170 tot=0
180 REPEAT
190   choice=pointer
200   PROCinitialise
210   pointer=choice
```

```
220   REPEAT
230     PROCmidpoint
240    UNTIL counter=288
250   CLOSE#0
260   PROCgraph
270   pointer=mid
280   tot=tot+1
290   GCOL 0,2
300  UNTIL tot=2
310 *DR.0
320 END
330 :
340 REM PROCEDURES
350 :=================================
360 REM SETS UP DRIVES AND OPENS FILES
370 DEF PROCinitialise
380 IF drive= 0 THEN *DR.0
390 IF drive= 1 THEN *DR.1
400 IF drive= 2 THEN *DR.2
410 IF drive= 3 THEN *DR.3
420 channel=OPENIN(filename$)
430 counter=0
440 arraycounter=0
450 hop=6
460 ENDPROC
470 :=================================
480 REM READS DATAFILES
490 DEF PROCmidpoint
500 REPEAT
510   PTR#channel=(pointer+18*counter)
520   INPUT#channel,burst
530   midpoint(arraycounter)=burst
540   counter=counter+2
550   arraycounter=arraycounter+1
560  UNTIL arraycounter=hop
570 pointer=pointer+5
580 hop=hop+6
590 ENDPROC
600 :=================================
610 REM PLOTS GRAPH
620 DEF PROCgraph
630 MOVE 50,150
640 FOR column=0 TO 143
650  DRAW 50+(column*8),150+(6*(midpoint(column)))    660   NEXT column
670 ENDPROC
680 :=================================
690 REM DRAWS AXES FOR GRAPH
700  DEF PROCaxes
710  GCOL 0,1
720  MOVE 50,150
730  FOR column=0 TO 143 STEP 6.217
740   MOVE 50+(column*8),918
750   DRAW 50+(column*8),150
760   NEXT column
770  MOVE 50,150
```

```
780  FOR row=0 TO 768 STEP 96
790   MOVE 50,(row+150)
800   DRAW 1194,(row+150)
810   NEXT row
820  ENDPROC
830  :================================
840  REM PUTS SCALES ON AXES
850  DEF PROCscales
860  VDU5
870  value=0
880  FOR X=30 TO 1204 STEP 50
890   MOVE X,130
900   IF value=0 OR value=1  OR value=3 OR value=5 OR
         value=7 OR value=9 OR value=11  OR  value=13 OR
         value=15 OR value=17 OR  value=19  OR  value=21
         OR value=23 THEN PRINT;value
910   value=value+1
920   NEXT X
930   MOVE 300,80
940  PRINT "Time GMT  Date ";filename$
950 yvalue=0
960  FOR yvalue=16 TO 128 STEP 16
970   MOVE 1194,160+(yvalue*6)
980   PRINT; yvalue
990   NEXT yvalue
1000    MOVE 600,1000
1010  PRINT"Bursts per minute"
1020  VDU4
1030  ENDPROC
```

Program listing "DURATON"

```
10 REM  Burst Duration per 2-min period vs time
20 REM version 1 22/11/86
30 REM further comments added 1/7/87
40 REM (c) J C Worsnop 1986
50 mid=5
60 end=23
70 pointer=end
80 REM START OF MAIN PROGRAM
90 PRINT "PROGRAM TO PLOT BURST DURATIONS"
100 PRINT
110 INPUT"WHAT IS THE FILENAME",filename$
120 INPUT"WHICH DRIVE IS IT IN",drive
130 DIM midpoint(144)
140 MODE1
150 PROCaxes
160 PROCscales
170 GCOL 0,3
180 tot=0
190 REPEAT
200   choice=pointer
210   PROCinitialise
220   pointer=choice
230   REPEAT
```

```
240   PROCmidpoint
250  UNTIL counter=288
260  CLOSE#0
270  PROCgraph
280  pointer=mid
290  tot=tot+1
300  GCOL 0,1
310 UNTIL tot=2
320 *DR.0
330 END
340 REM PROCEDURES
350:================================
360 REM SETS UP DRIVES AND OPEN FILES
370 DEF PROCinitialise
380 IF drive= 0 THEN *DR.0
390 IF drive= 1 THEN *DR.1
400 IF drive= 2 THEN *DR.2
410 IF drive= 3 THEN *DR.3
420 channel=OPENIN(filename$)
430 counter=0
440 arraycounter=0
450 hop=6
460 ENDPROC
470:================================
480 REM READS DATAFILES
490 DEF PROCmidpoint
500 REPEAT
510  PTR#channel=(pointer+18*counter)
520  INPUT#channel,burst
530  midpoint(arraycounter)=burst
540  counter=counter+2
550  arraycounter=arraycounter+1
560 UNTIL arraycounter=hop
570 pointer=pointer+5
580 hop=hop+6
590 ENDPROC
600:================================
610 REM PLOTS GRAPH
620 DEF PROCgraph
630 MOVE 50,150
640 FOR column=0 TO 143
650 DRAW 50+(column*8),150+(192*(midpoint(column)))
660 NEXT column
670 ENDPROC
680:================================
690 DEF PROCaxes
700 REM DRAWS AXES FOR GRAPH
710 GCOL 0,3
720 MOVE 50,150
730 FOR column=0 TO 143 STEP 6.217
740 MOVE 50+(column*8),918
750 DRAW 50+(column*8),150
760 NEXT column
770 MOVE 50,150
780 FOR row=0 TO 768 STEP 96
```

```
790 MOVE 50,(row+150)
800 DRAW 1194,(row+150)
810 NEXT row
820 ENDPROC
830:================================
840 REM PUTS SCALES ON AXES
850 DEF PROCscales
860 VDU5
870 value=0
880 FOR X=30 TO 1204 STEP 50
890 MOVE X,130
900 IF value=0 OR value=1  OR  value=3  OR  value=5  OR
    value=7  OR  value=9  OR value=11  OR  value=13  OR
    value=15 OR value=17 OR value=19  OR  value=21  OR
    value=23 THEN PRINT;value
910 value=value+1
920 NEXT X
930 MOVE 300,80
940 PRINT "Time GMT  Date ";filename$
950 yvalue=0
960 FOR yvalue=0.5 TO 2.0 STEP 0.5
970 MOVE 1194,160+(yvalue*384)
980 PRINT; yvalue*200
990 NEXT yvalue
1000 MOVE 350,1000
1010 PRINT"Average burst Duration (msec)"
1020 VDU4
1030 ENDPROC
```

Program listing "AMPLTDE"

```
10 REM Burst Amplitude per 2-min period vs time
20 REM Version 1  22/11/86
30 REM Further comments added 1/7/87
40 REM (c) J C Worsnop 1986
50 mid=11
60 end=29
70 pointer=end
80 REM START OF MAIN PROGRAM
90 PRINT "PROGRAM TO PLOT BURST AMPLITUDES"
100 PRINT
110 INPUT"WHAT IS THE FILENAME",filename$
120 INPUT"WHICH DRIVE IS IT IN", drive
130 DIM midpoint(144)
140 MODE1
150 PROCaxes
160 PROCscales
170 GCOL 0,1
180 tot=0
190 REPEAT
200   choice=pointer
210   PROCinitialise
220   pointer=choice
230   REPEAT
```

```
240    PROCmidpoint
250  UNTIL counter=288
260  CLOSE#0
270  PROCgraph
280  pointer=mid
290  tot=tot+1
300  GCOL 0,2
310 UNTIL tot=2
320 *DR.0
330 END
340:
350:=================================
360 REM  SETS  UP DRIVES AND OPENS FILES
370 DEF PROCinitialise
380 IF drive =1 THEN *DR.1
390 IF drive =2 THEN *DR.2
400 IF drive =3 THEN *DR.3
410 IF drive =0 THEN *DR.0
420 channel=OPENIN(filename$)
430 counter=0
440 arraycounter=0
450 hop=6
460 ENDPROC
470:=================================
471 REM  READS  DATA FILES
480 DEF PROCmidpoint
490 REPEAT
500  PTR#channel=(pointer+18*counter)
510  INPUT#channel,burst
520  midpoint(arraycounter)=burst
530  counter=counter+2
540 arraycounter=arraycounter+1
550 UNTIL arraycounter=hop
560 pointer=pointer+5
570 hop=hop+6
580 ENDPROC
590:=================================
591 REM PLOTS GRAPH
600 DEF PROCgraph
610 MOVE 50,150
620 FOR column=0 TO 143
630  IF  midpoint(column)=0 OR midpoint(column)>256 THEN
       650
640 DRAW 50+(column*8),150+(3*(midpoint(column)))
650 NEXT column
660 ENDPROC
670:=================================
671 DRAWS AXES FOR GRAPH
680 DEF PROCaxes
690 GCOL 0,3
700 MOVE 50,150
710 FOR column=0 TO 143 STEP 6.217
720 MOVE 50+(column*8),918
730 DRAW 50+(column*8),150
740 NEXT column
```

```
750 MOVE 50,150
760 FOR row=0 TO
768 STEP 96
770 MOVE 50,(row+150)
780 DRAW 1194,(row+150)
790 NEXT row
800 ENDPROC
810:================================
811 REM PUTS SCALES ON AXES
820 DEF PROCscales
830 VDU5
840 value=0
850 FOR X=30 TO 1204 STEP 50
860 MOVE X,130
870  IF value=0 OR value=1  OR  value=3  OR  value=5  OR
      value=7  OR  value=9  OR value=11  OR  value=13  OR
      value=15 OR value=17 OR value=19  OR  value=21  OR
      value=23 THEN PRINT;value
880 value=value+1
890 NEXT X
900  MOVE 300,80
910 PRINT "Time GMT  Date ";filename$
920 yvalue=0
930 FOR yvalue=16 TO 128 STEP 16
940 MOVE 1194,160+(yvalue*6)
950 PRINT; 2*yvalue
960 NEXT yvalue
970 MOVE 600,1000
980 PRINT"Burst Amplitude"
990 VDU4
1000 ENDPROC
```

Appendix (c)(iv)

The programs GRANAM5 and GRANKS8 are also very similar in structure and they produce cumulative distributions of amplitude and burst duration respectively.I will therfore only describe the first in detail and the second should be self explanatory.

Program description "GRANAM5" This program sorts the burst amplitudes in rank order and produces a cumulative distribution of amplitudes in graphical form. It uses some common procedures, constants, arrays and variables from "NUMBERS" so these will not be defined again.

CONSTANTS

next.....pointer start value

first.....first file to be read

last.....last file to be read

VARIABLES

date.....current file being processed

box.....pointer to required value in
array "bucket"

PROCEDURES

clear.....sets all locations in "bucket"
to zero

main.....main program

rank.....sorts amplitudes into rank order

error.....error trap for missing files

ARRAYS

bucket.....store for sorted amplitudes

MAIN PROGRAM

constants declaration

setup arrays

enter wanted data details

draw axes and scales for graph

REPEAT for midpoint and endpoint data

read in data

sort into rank order

plot graph on screen

plot graph to printer

END

Program listing"GRANAM5"

```
10 REM  Burst Amplitude sorter
30 REM version   1/6/87
40 REM (c)  J C Worsnop 1987
50 REM cumulative distribution GRAPHICAL OUTPUT
60 ON ERROR GOTO 960
70 VDU15
80 CLS
90 PRINT "PROGRAM TO SORT BURST AMPLITUDES"
100 mid=11
110 end=29
120 next=mid
130 DIM midpoint(144)
140 DIM bucket(255)
150 PRINT
160 INPUT"WHICH DRIVE CONTAINS THE DATA DISC",drive
170 PRINT
180 INPUT"ENTER FIRST DAY",first
190 PRINT
200 INPUT"ENTER LAST DAY",last
210 MODE1
220 PROCaxes
230 PROCscales
240  GCOL 0,1
250  date = first-100
260  PROCmain(next)
270   GCOL 0,3
280   PROCclear
290   date = first-100
300   PROCmain(next)
310 *DR.0
330 *GDUMP
340 END
```

```
350 :=============================================================
360 DEF PROCclear
370 FOR I =0 TO 255
380  bucket(I)=0
390  NEXT I
400 ENDPROC
420  DEF PROCmain(pointer)
430      REPEAT
440        date =date+100
441        IF date>last THEN 570
450        filename$ =STR$(date)
460        IF LEN(filename$)=3 THEN filename$
                 ="0"+filename$
470       choice=pointer
480       PROCinitialise
490       pointer=choice
500         REPEAT
510           PROCmidpoint
520          UNTIL counter=288
530       CLOSE#0
540       PROCrank
550       pointer=choice
560      UNTIL date = last
570     PROCgraph
580     next=end
590 ENDPROC
600 :================================
610  REM SETS UP DRIVES AND OPENS FILE
620 DEF PROCinitialise
630  IF drive= 0 THEN *DR.0
640  IF drive= 1 THEN *DR.1
650  IF drive= 2 THEN *DR.2
660  IF drive= 3 THEN *DR.3
670 channel=OPENIN(filename$)
680  counter=0
690 arraycounter=0
700 hop=6
710 ENDPROC
720 :================================
730  REM READS DATAFILES
740  DEF PROCmidpoint
750  REPEAT
760    PTR#channel=(pointer+18*counter)
770    INPUT#channel,burst
780    midpoint(arraycounter)=burst
790    counter=counter+2
800   arraycounter=arraycounter+1
810   UNTIL arraycounter=hop
820 pointer=pointer+5
830 hop=hop+6
840 ENDPROC
850 :================================
860  REM SORTS AMPLITUDES INTO RANK ORDER
870  DEF PROCrank
880  REM FOR column = 25 TO 83
```

```
890 FOR column = 83 TO 143
900  FOR box =160 TO 200 STEP 2
910  IF  midpoint(column)>=box  THEN bucket(box)=bucket(box)+1 :       NEXT
box
920  NEXT column
930 ENDPROC
940 :=============================================================
950 DEF PROCerror
960 REM ERROR TRAP FOR MISSING DATES
970 CLOSE#0
1020 IF next=mid THEN  GOTO
260 ELSE GOTO 300
1030 END
1040 ENDPROC
1050 :=================================
1060 DEF PROCgraph
1070 MOVE 50,150
1080 FOR box=0 TO 20
1090 DRAW 50+(box*57.2),150+7.68*((bucket(160+box*2)/
     bucket(160))*100)
1100  NEXT box
1110 ENDPROC
1120
1130 :=================================
1140 DEF PROCaxes
1150 GCOL 0,2
1160 MOVE 50,150
1170 FOR column=0 TO 20
1180   MOVE 50+(column*57.2),918
1190   DRAW 50+(column*57.2),150
1200   NEXT column                    :REM vertical lines
1210 MOVE 50,150
1220 FOR row=0 TO 100 STEP 10
1230   MOVE 50,(150+row*7.68)
1240   DRAW 1194,(150+row*7.68)
1250    NEXT  row                    :REM  horizontal lines
1260 ENDPROC
1270 :=============================
1280 DEF PROCscales
1290 VDU5  1300  value=0
1310 FOR X=0 TO 1194 STEP 57.5
1320   MOVE X,130
1330   IF value=0 OR value=4  OR  value=8 OR value=12 OR
         value=16 OR value=20 OR value=24  OR  value=28 OR
         value=32   OR   value=36  OR  value=40  THEN
         PRINT;value+160
1340   value=value+2
1350   NEXT X
1360 MOVE 300,80
1370 PRINT "Amplitude number"
1380 yvalue=0
1390 FOR yvalue=1 TO 10
1400   MOVE 1196,160+(yvalue*76.8)
1410   PRINT; yvalue*10
1420   NEXT yvalue
```

```
1430 MOVE 200,40
1440 PRINT"date ";first"  to  ";last
1450 MOVE 40,1000
1460 PRINT"Cumulative distribution of amplitudes"
1470 VDU4
1480 ENDPROC
```

Program listing "GRANKS8"

```
10 REM  Burst Duration sorter
20 REM version  1/7/87
30 REM (c)  J C Worsnop 1987
40 REM cumulative distribution GRAPHICAL OUTPUT
50 ON ERROR GOTO 950
60 VDU15
70 mid=5
80 end=23
90 CLS
100 PRINT "PROGRAM TO SORT BURST AMPLITUDES"
110 next=mid
120 DIM midpoint(144)
130 DIM bucket(255)
140 PRINT
150 INPUT"WHICH DRIVE CONTAINS THE DATA DISC",drive
160 PRINT
170 INPUT"ENTER FIRST DAY",first
180 PRINT
190 INPUT"ENTER LAST DAY",last
200 MODE1
210 PROCaxes
220 PROCscales
230  GCOL 0,1
240  date = first-100
250  PROCmain(next)
260    GCOL 0,3
270    PROCclear
280    date = first-100
290    PROCmain(next)
300 *DR.0
310 *GDUMP
320 END
330 :=================================================
340 DEF PROCclear
350 FOR I =0 TO 255
360  bucket(I)=0
370  NEXT I
380 ENDPROC
390 :=================================================
400 DEF PROCmain(pointer)
410      REPEAT
420      date =date+100
430      IF date>last THEN 560
440      filename$ =STR$(date)
450       IF  LEN(filename$)=3  THEN  filename$
                  ="0"+filename$
460      choice=pointer
```

```
        PROCinitialise
470     pointer=choice
480       REPEAT
490         PROCmidpoint
500         UNTIL counter=288
510     CLOSE#0
520     PROCrank
530     pointer=choice
540     UNTIL date = last
550   PROCgraph
560   next=end
570 ENDPROC
580 :=================================
590 REM SETS UP DRIVES AND OPENS FILE
600 DEF PROCinitialise
610 IF drive= 0 THEN *DR.0
620 IF drive= 1 THEN *DR.1
630 IF drive= 2 THEN *DR.2
640 IF drive= 3 THEN *DR.3
650 channel=OPENIN(filename$)
660 counter=0
670 arraycounter=0
680 hop=6
690 ENDPROC
700 :=================================
710 REM READS DATAFILES
720 DEF PROCmidpoint
730 REPEAT
740   PTR#channel=(pointer+18*counter)
750   INPUT#channel,burst
760   midpoint(arraycounter)=burst
770   counter=counter+2
780 arraycounter=arraycounter+1
790 UNTIL arraycounter=hop
800 pointer=pointer+5
810 hop=hop+6
820 ENDPROC
830 :=================================
840 REM SORTS DURATIONS INTO RANK ORDER
850 DEF PROCrank
860 FOR column = 0 TO 143
880  FOR box = 0 TO 20
890
892   IF midpoint(column)>=box/10 AND midpoint(column)>0THEN
900 bucket(box)=bucket(box)+1 : NEXT box
910  NEXT column
920 ENDPROC
930 :=================================================
940 DEF PROCerror
950 REM ERROR TRAP FOR MISSING DATES
960 CLOSE#0
970 IF next=mid THEN  GOTO 250 ELSE GOTO 290
980 END
990 ENDPROC
1000 :=================================
```

```
1010 DEF PROCgraph
1020 MOVE 50,150
1030  FOR box=0 TO 20
1040  DRAW50+(box*57.2),150+7.68*((bucket(box)/bucket(0))*100)
1050   NEXT box
1060 ENDPROC
1070
1080 :=================================
1090 DEF PROCaxes
1100 GCOL 0,2
1110 MOVE 50,150
1120 FOR column=0 TO 20
1130  MOVE 50+(column*57.2),918
1140  DRAW 50+(column*57.2),150
1150  NEXT column              :REM vertical lines
1160 MOVE 50,150
1170 FOR row=0 TO 100 STEP 10
1180  MOVE 50,(150+row*7.68)
1190  DRAW 1194,(150+row*7.68)
1200   NEXT  row               : REM  horizontal lines
1210 ENDPROC
1220 :==============================
1230 DEF PROCscales
1240 VDU5  1250  value=0
1260 FOR X=0 TO 1194 STEP 57.5
1270  MOVE X,130
1280  IF value=0 OR value=4  OR  value=8 OR value=12 OR
        value=16 OR value=20 OR value=24  OR  value=28 OR
        value=32   OR   value=36   OR val  ue=40   THEN
        PRINT;value*5  1290    value=value+2
1300   NEXT X
1310 MOVE 300,80
1320 PRINT "duration (ms)"
1330 yvalue=0
1340 FOR yvalue=1 TO 10
1350   MOVE 1196,160+(yvalue*76.8)
1360   PRINT; yvalue*10
1370   NEXT yvalue
1380 MOVE 200,40
1390 PRINT"date ";first"   to   ";last
1400 MOVE 40,1000
1410 PRINT"Cumulative distribution of durations"
1420 VDU4
1430 ENDPROC
```

The three programs LOSITES, LOSJCW and MSLOS are all of the same structure and based on the formulae given in ref 10. The following description of one will be enough to understand all three. They differ in the following ways.

LOSITES assumes:

I. mid point and end point paths below the transition frequency

II. zero initial trail radius

III. average trail height fixed at 100Km

LOSJCW assumes

I. midpoint and end point paths below the transition frequency

II. initial trail radius and trail height as calculated from ref 10

MSLOS assumes

I. End point path only above transition frequency

II. initial trail height and radius as calculated in ref 10

Program description MSLOS

VARIABLES

beta.....angle between the trail axis and the plane of propagation

frequency.....system frequency in MHz

range.....great circle distance between transmitter
and receiver

lambda.....system wavelength in metres

pathloss.....normalised pathloss

trail_height.....trail height in Km

trail_radius.....initial radius if trail in metres

diffusion_constant..trail ambipolar diffusion constant

/velocity ratio

Rr.....distance from scattering point to

receiver in Km

D.....ambipolar diffusion constant ($m^2 s^{-1}$)

Rt.....distance from scattering point to

transmiter in Km

phi.....angle of incidence to meteor plane

peak.....pathloss at peak of burst

expon.....exponential decay term of burst

PROCEDURES

trail_height.....calculates trail height

diffusion_constant..calculates diffusion constant /velocity

ratio

trail_radius.....calculates initial trail radius

D.....calculates diffusion constant

midpathloss.....calculates normalised path loss for mid

point path geometry

endpathloss.....calculates normalised path loss for end

point path geometry

MAIN PROGRAM

enter required system data... beta value, frequency, path

length, path geometry

calculate wavelength

calculate trail height

calculate diffusion constant/velocity ratio

calculate initial trail radius

calculate diffusion constant

calculate normalised path loss

print results

END

Note that in "LOSITES" the procedures for calculating trail height and initial trail radius are replaced by the constant values described earlier.

Program listing

"LOSITES"

```
10 REM program for calculating path loss for meteor burst  systems
20 REM (c) J C Worsnop 1987
30 REM version 7 1/6/87 user defined beta,below Ft
40 CLS:PRINT:PRINT"program for comparing path losses
                                        in  meteor burst systems"
50 PRINT"assuming both paths below Ft"
70 PRINT
80 INPUT"enter beta value "beta
90 PRINT
100 INPUT"enter system frequency in MHz  "frequency
110 PRINT
130 INPUT"enter great circle range in Km " range
140 PRINT
150 INPUT"mid point or end point loss (M/E)",path$
170 PRINT
190 lambda=300/frequency
200 trail_height=100 :REM PROCtrail_height
210 PROCdiffusion_const
220 trail_radius =0 :REM PROCtrail_radius
230 IFpath$="M" THEN PROCmidpathloss ELSE PROCendpathloss
260 PRINT "the normalised path loss is " 10*LOG(pathloss)      " dB"

270 END
280 :
290 DEF PROCtrail_height
300 trail_height = -17*LOG(frequency) + 124
310 PRINT
320 PRINT"average trail height " trail_height "Km"
```

```
330 PRINT
340 ENDPROC
350 :
360 DEF PROCdiffusion_const
370 diffusion_const=(.0015*trail_height+.035+.0013*
    (trail_height-90)^2)*1E-3
380 ENDPROC
390 :
400 DEF PROCendpathloss
410 Rr=trail_height
420 PRINT"Rr= "Rr" Km"
430 Rt=SQR(6360^2+(6360+trail_height)^2-2*6360*
    (6360+trail_height)*COS(range/6360))
450 PRINT"Rt= "Rt" Km"
460 phi=(ASN(6360*SIN(range/6360)/Rt))/2
470 PRINT"phi= "phi" radians"
490 peak1=(lambda^3)*(2.8178E-15*1E14)^2
500 peak2=(1-(COS(RAD(beta)))^2*(SIN(phi))^2)*16*PI^2*
    (Rt*1000)*(Rr*1000)*1000*(Rt+Rr)
510 peak=peak1/peak2
520 expo1=-8*PI^2*trail_radius^2
530 expo2=(COS(phi))^2
540 expo3=lambda^2
550 expo4=(expo1*expo2)/expo3
560 expon=EXP(expo4)
570 pathloss=peak*expon
580 ENDPROC
590 :
600 DEF PROCmidpathloss
610 Rt=SQR((6360^2+(6360+trail_height)^2)-2*6360*
    (6360+trail_height)*COS(range/12720))
620 Rr=Rt
630 PRINT"Rt=Rr= "Rt
640 phi=ASN(6360*SIN(range/12720)/Rt)
650 PRINT"phi= "phi" radians"
660 peak1=(lambda^3)*(2.8178E-15*1E14)^2
670 peak2=(1-(COS(RAD(beta)))^2*(SIN(phi))^2)*16*PI^2*
    (Rt*1000)*(Rr*1000)*1000*(Rt+Rr)
680 peak=peak1/peak2
690 expo1=-8*PI^2*trail_radius^2
700 expo2=(COS(phi))^2
710 expo3=lambda^2
720 expo4=(expo1*expo2)/expo3
730 expon=EXP(expo4)
740 pathloss=peak*expon
750 ENDPROC
760 :
770 DEF PROCtrail_radius
780 trail_radius=10^((.035*trail_height)-3.45)
790 ENDPROC
```

Program listing "LOSJCW"

```
10 REM program for calculating path loss for meteor burst
     systems
```

```
20 REM (c) J C Worsnop 1987
30 REM version 7 1/6/87 user defined beta,below Ft
40 CLS:PRINT:PRINT"program for comparing path losses in
     meteor burst systems"
50 PRINT"assuming both paths below Ft"
70 PRINT
80 INPUT"enter beta value "beta
90 PRINT
100 INPUT"enter system frequency in MHz "frequency
110 PRINT
130 INPUT"enter great circle range in Km " range
140 PRINT
150 INPUT"mid point or end point loss (M/E)",path$
170 PRINT
190 lambda=300/frequency
200 PROCtrail_height
210 PROCdiffusion_const
220 PROCtrail_radius
230 IFpath$="M" THEN PROCmidpathloss ELSE PROCendpathloss
260 PRINT "the normalised path loss is " 10*LOG(pathloss)
      " dB"
270 END
280 :
290 DEF PROCtrail_height
300 trail_height = -17*LOG(frequency) + 124
310 PRINT
320 PRINT"average trail height " trail_height "Km"
330 PRINT
340 ENDPROC
350 :
360 DEF PROCdiffusion_const
370 diffusion_const=(.0015*trail_height+.035+.0013*
      (trail_height-90)^2)*1E-3
380 ENDPROC
390 :
400 DEF PROCendpathloss
410 Rr=trail_height
420 PRINT"Rr= "Rr" Km"
440 Rt=SQR(6360^2+(6360+trail_height)^2-2*6360*
      (6360+trail_height)*COS(range/6360))
450 PRINT"Rt= "Rt" Km"
460 phi=(ASN(6360*SIN(range/6360)/Rt))/2
470 PRINT"phi= "phi" radians"
490 peak1=(lambda^3)*(2.8178E-15*1E14)^2
500 peak2=(1-(COS(RAD(beta)))^2*(SIN(phi))^2)*16*PI^2*
      (Rt*1000)*(Rr*1000)*1000*(Rt+Rr)
510 peak=peak1/peak2
520 expo1=-8*PI^2*trail_radius^2
530 expo2=(COS(phi))^2
540 expo3=lambda^2
550 expo4=(expo1*expo2)/expo3
560 expon=EXP(expo4)
570 pathloss=peak*expon
580 ENDPROC
590 :
```

```
600 DEF PROCmidpathloss
610 Rt=SQR((6360^2+(6360+trail_height)^2)-2*6360*
    (6360+trail_height)*COS(range/12720))
620 Rr=Rt
630 PRINT"Rt=Rr= "Rt
640 phi=ASN(6360*SIN(range/12720)/Rt)
650 PRINT"phi= "phi" radians"
660 peak1=(lambda^3)*(2.8178E-15*1E14)^2
670 peak2=(1-(COS(RAD(beta)))^2*(SIN(phi))^2)*16*PI^2*
    (Rt*1000)*(Rr*1000)*1000*(Rt+Rr)
680 peak=peak1/peak2
690 expo1=-8*PI^2*trail_radius^2
700 expo2=(COS(phi))^2
710 expo3=lambda^2
720 expo4=(expo1*expo2)/expo3
730 expon=EXP(expo4)
740 pathloss=peak*expon
750 ENDPROC
760 :
770 DEF PROCtrail_radius
780 trail_radius=10^((.035*trail_height)-3.45)
790 ENDPROC
```

Program listing "MSLOS"

```
10 REM program for calculating path loss for meteor
    burst systems
20 REM (c) J C Worsnop 1987
30 REM version 6 1/5/87 user defined beta
40  CLS:PRINT:PRINT"program  for comparing path losses in meteor
burst systems"
41 PRINT"assuming end point path above Ft only"
50 PRINT
51 INPUT"enter beta value "beta
52 PRINT
60 INPUT"enter system frequency in MHz  "frequency
70 PRINT
90 INPUT"enter great circle range in Km " range
100 PRINT
110 INPUT"mid point or end point loss (M/E)",path$
130 PRINT
150 lambda=300/frequency
160 PROCtrail_height
170 PROCdiffusion_const
180 PROCtrail_radius
190 IFpath$="M" THEN PROCmidpathloss ELSE PROCendpathloss
220 PRINT "the normalised path loss is  "10*LOG(pathloss) " dB"  230  END
240 :
250 DEF PROCtrail_height
260 trail_height = –17*LOG(frequency) + 124
270 PRINT
280 PRINT"average trail height " trail_height "Km"
290 PRINT
300 ENDPROC
310 :
```

```
320 DEF PROCdiffusion_const
330 diffusion_const=(.0015*trail_height+.035+.0013*
    (trail_height-90)^2)*1E-3
340 ENDPROC
350 :
360 DEF PROCendpathloss
370 Rr=trail_height
380 PRINT"Rr= "Rr" Km"
400 Rt=SQR(6360^2+(6360+trail_height)^2-2*6360*(6360+
    trail_height)*COS(range/6360))
410 PRINT"Rt= "Rt" Km"
420 phi=(ASN(6360*SIN(range/6360)/Rt))/2
430 PRINT"phi= "phi" radians"
450 peak1=((1/diffusion_const)^2*(lambda^6)*(2.8178E-15
    *1E14)^2)
460 peak2=((COS(phi))^4)*(Rt*1000)^2*(Rr*1000)^2*4096*
    PI^6
470 peak=peak1/peak2
471 expo1=-8*PI^2*trail_radius^2
472 expo2=(COS(phi))^2
473 expo3=lambda^2
474 expo4=(expo1*expo2)/expo3
480 expon=EXP(expo4)
490 pathloss=peak*expon
500 ENDPROC
510 :
520 DEF PROCmidpathloss
530 Rt=SQR((6360^2+(6360+trail_height)^2)-2*6360*(6360
    +trail_height)*COS(range/12720))
540 Rr=Rt
550 PRINT"Rt=Rr= "Rt
560 phi=ASN(6360*SIN(range/12720)/Rt)
570 PRINT"phi= "phi" radians"
580 peak1=(lambda^3)*(2.8178E-15*1E14)^2
590 peak2=(1-(COS(RAD(beta)))^2*(SIN(phi))^2)*16*PI^2
    *(Rt*1000)*(Rr*1000)*1000*(Rt+Rr)
600 peak=peak1/peak2
610 expo1=-8*PI^2*trail_radius^2
611 expo2=(COS(phi))^2
612 expo3=lambda^2
613 expo4=(expo1*expo2)/expo3
614 expon=EXP(expo4)
620 pathloss=peak*expon
630 ENDPROC
640 :
650 DEF PROCtrail_radius
660 trail_radius=10^((.035*trail_height)-3.45)
670 ENDPROC
```

Appendix (c)(vi)

The two programs MSDUR and DURJCW use the same format as the path loss programs, and the formulae from ref 10. Consequently the descriptions will be limited to definition of variables and procedures that have not been defined earlier.

VARIABLES

duration.....burst duration to 0.288 of peak amplitude

PROCEDURES

miduration.....calculates burst duration for midpoint

path

enduration.....calculates burst duration for endpoint

path

The path losses calculated are normalised to isotropic sources at transmitter and receiver. The durations are calculated to the time where the signal power falls to 0.288 of its peak value. It should also be noted that the losses and durations assume mainly underdense bursts.(See chapter 3

Program listing "MSDUR"

```
10 REM program for calculating burst duration for meteor
       burst systems
20 REM (c) J C Worsnop 1987
30 REM version 1 10/5/87
40 CLS:PRINT:PRINT"program for comparing burst
   duration in meteor burst systems"
50 PRINT"assuming end point path above Ft only"
60 PRINT
70 INPUT"enter beta value "beta
80 PRINT
90 INPUT"enter system frequency in MHz  "frequency
100 PRINT
110 INPUT"enter great circle range in Km " range
120 PRINT
130 INPUT"mid point or end point duration (M/E)",path$  140 PRINT
150 lambda=300/frequency
160 PROCtrail_height
170 PROCdiffusion_const
```

```
180 PROCtrail_radius
190 PROCD
200  IFpath$="M“ THEN PROCmiduration ELSE PROCenduration   210  PRINT
“the normalised burst duration is  “ duration
                “ seconds”

220 END
230 :
240 DEF PROCD
250 D=10^(0.067*trail_height-5.6)
260 ENDPROC
261 :
270 DEF PROCtrail_height
280 trail_height = −17*LOG(frequency) + 124
290 PRINT
300 PRINT“average trail height “ trail_height “Km”
310 PRINT
320 ENDPROC
330 :
340 DEF PROCdiffusion_const
350 diffusion_const=(.0015*trail_height+.035+.0013*
    (trail_height-90)^2)*1E-3
360 ENDPROC
370 :
380 DEF PROCenduration
390 Rr=trail_height
400 PRINT“Rr= “Rr” Km“
410 Rt=SQR(6360^2+(6360+trail_height)^2-2*6360*
    (6360+trail_height)*COS(range/6360))
420 PRINT”Rt= “Rt” Km“
430 phi=(ASN(6360*SIN(range/6360)/Rt))/2
440 PRINT”phi= “phi” radians“
450 dur1=(8*PI^2*(diffusion_const)^2*Rt*1E6*Rr)*
    (COS(phi))^2
460 dur2=D*lambda*(Rt+Rr)*1E3*(1-((COS(beta))^2*
    (SIN(phi))^2))
470 duration=dur1/dur2
480 ENDPROC
490 :
500 DEF PROCmiduration
510 Rt=SQR((6360^2+(6360+trail_height)^2)-2*6360*
    (6360+trail_height)*COS(range/12720))
520 Rr=Rt
530 PRINT”Rt=Rr= “Rt
540 phi=ASN(6360*SIN(range/12720)/Rt)
550 PRINT”phi= “phi” radians“
551 duration=(1.248*lambda^2)/(32*PI^2*D*
    ((COS(phi))^2))
650 ENDPROC
660 DEF PROCtrail_radius
670 trail_radius=10^((.035*trail_height)-3.45)
680 ENDPROC
```

Program listing “DURJCW”

```
10 REM program for calculating burst duration for
```

```
    meteor burst systems
20 REM (c) J C Worsnop 1987
30 REM version 1 10/5/87
40 CLS:PRINT:PRINT"program for comparing burst
    duration in meteor burst systems"
50 PRINT"assuming both paths below Ft"
60 PRINT
70 INPUT"enter beta value "beta
80 PRINT
90 INPUT"enter system frequency in MHz "frequency
100 PRINT
110 INPUT"enter great circle range in Km " range
120 PRINT
130 INPUT"mid point or end point duration (M/E)",path$  140 PRINT
150 lambda=300/frequency
160 PROCtrail_height
170 PROCdiffusion_const
180 PROCtrail_radius
190 PROCD
200 IFpath$="M" THEN PROCmiduration ELSE PROCenduration   210 PRINT
"the normalised burst duration is " duration
    " seconds"
220 END
230 :
240 DEF PROCD
250 D=10^(0.067*trail_height-5.6)
260 ENDPROC
270 :
280 DEF PROCtrail_height
290 trail_height = -17*LOG(frequency) + 124
300 PRINT
310 PRINT"average trail height " trail_height "Km"
320 PRINT
330 ENDPROC
340 :
350 DEF PROCdiffusion_const
360 diffusion_const=(.0015*trail_height+.035+.0013*
    (trail_height-90)^2)*1E-3
370 ENDPROC
380 :
390 DEF PROCenduration
400 Rr=trail_height
410 PRINT"Rr= "Rr" Km"
420 Rt=SQR(6360^2+(6360+trail_height)^2-2*6360*
    (6360+trail_height)*COS(range/6360))
430 PRINT"Rt= "Rt" Km"
440 phi=(ASN(6360*SIN(range/6360)/Rt))/2
450 PRINT"phi= "phi" radians"
460 duration=(1.248*lambda^2)/(32*PI^2*D*
    ((COS(phi))^2))
470 ENDPROC
480 :
490 DEF PROCmiduration
500 Rt=SQR((6360^2+(6360+trail_height)^2)-2*6360*
    (6360+trail_height)*COS(range/12720))
```

```
510 Rr=Rt
520 PRINT"Rt=Rr= "Rt
530 phi=ASN(6360*SIN(range/12720)/Rt)
540 PRINT"phi= "phi" radians"
550 duration=(1.248*lambda^2)/(32*PI^2*D*
    ((COS(phi))^2))
560 ENDPROC
570 DEF PROCtrail_radius
580 trail_radius=10^((.035*trail_height)-3.45)
590 ENDPROC
```

```
10 REM program for plotting transition frequency
       against path length
20 REM (c) J C Worsnop 1987
30 REM version 2 1/3/87
40 REM main program
50 :
70 CLS:PRINT:PRINT"program for plotting transition
    frequency against path length"
80 PRINT
90 INPUT"mid point or end point (M/E) ", path$
100 PRINT
110 INPUT"enter system frequency in MHz "frequency
120 MODE1
130 PROCaxes
140 PROCscales
150 PROCtrail_height
160 PROCdiffusion_const
170 REM  PRINT:PRINT TAB(7)"RANGE";TAB(19) "Ftrans
      beta0" TAB(38)"Ftrans beta90" :PRINT
180 MOVE 50,150
190 FOR range = 0 TO 2200 STEP 100
200  IFpath$="M" THEN PROCmRt ELSE PROCeRt
210  PROClambda
220  PROCgraph(lambda0)
230  NEXT range
235 MOVE 50,150
240  FOR range = 0 TO 2200 STEP 100
250  IFpath$="M" THEN PROCmRt ELSE PROCeRt
260  PROClambda
270  PROCgraph(lambda90)
280  NEXT range
281 *GDUMP
290 END
300 :
320 DEF PROCtrail_height
330 trail_height = -17*LOG(frequency) + 124
340 ENDPROC
350 :
370 DEF PROCdiffusion_const
380 diffusion_const=(.0015*trail_height+.035+.0013*
     (trail_height-90)^2)*1E-3
390 ENDPROC
400 :
420 DEF PROClambda
430 lambda=((((256*PI^4)*(diffusion_const^2)*Rt*Rr*
     1E3)/(Rt+Rr))^(1/3))
440 lambda0=lambda*((COS(phi)^(4/3)))
450 lambda90=lambda*((COS(phi)^(2/3)))
460 ENDPROC
470 :
490 DEF PROCeRt
500 Rt=SQR(6360^2+(6360+trail_height)^2-2*6360*
     (6360+trail_height)*COS(range/ 6360))
```

```
505 Rr=trail_height
510 phi=(ASN(6360*SIN(range/6360)/Rt))/2
520 ENDPROC
530 :
550 DEF PROCmRt
560 Rt=SQR((6360^2+(6360+trail_height)^2)-2*6360*
      (6360+trail_height)*COS(range/12720))
565 Rr=Rt
570 phi=ASN(6360*SIN(range/12720)/Rt)
580 ENDPROC
590 :==================================
600 DEF PROCgraph(lambda)
610 GCOL 0,3
620 DRAW 50+range/2,150+1.536*(300/lambda)
630 ENDPROC
640 :==================================
650 DEF PROCaxes
660 GCOL 0,1
670 MOVE 50,150
680 FOR range=0 TO 2200 STEP 100
690   MOVE 50+(range/2),918
700   DRAW 50+(range/2),150
710 NEXT range
720 MOVE 50,150
730 FOR row=0 TO 768 STEP 76.8
740   MOVE 50,(row+150)
750   DRAW 1150,(row+150)
760 NEXT row
770 ENDPROC
780 :==============================
790 DEF PROCscales
800 GCOL 0,2
810 VDU5
820 value=0
830 FOR X=30 TO 1154 STEP 50
840 MOVE X,130
850 IF value=0 OR value=300 OR value=600 OR value=900
      OR  value=1200  OR  value=1500 OR  value=1800  OR
      value=2200 THEN PRINT;value   860  value=value+100   870   NEXT X
880  MOVE 100,80
890 PRINT "path length (Km) at"frequency" MHz"
900 yvalue=0
910 FOR yvalue=50 TO 500 STEP 50
920   MOVE 1190,160+(yvalue*1.536)
930   PRINT; yvalue
940  NEXT yvalue
950   MOVE 300,1000
960 PRINT path$;"   Transition frequency (MHz)"
970 VDU4
980 ENDPROC
```

Appendix (d)

Derivation of path equations

Meteor trails may be classified into two categories: *underdense* where the electron density is low enough for most of the incident energy to pass through unaltered, and *overdense* where the energy penetrates the trail but the electron density is sufficient to cause total reflection by the same mechanism as normal HF ionospheric layer reflection.

As the electron density depends on the mass and velocity of the meteoric particle, and the masses are distributed as described in chapter 2.1, underdense bursts make up the majority of usable bursts. Ref 22 describes a rule of thumb to determine whether a particular path relies on underdense or overdense bursts.

1. Path equations for underdense trails

The derivations, based upon the work of Sugar (20) will begin by considering the energy back-scattered by a long wavelength model of the meteor trail and progress to consider the forward scatter case and the short wavelength case.

1.1. Long wavelength case

1.1.1 Path loss

Initially assume the trail to be an infinitely long circular cylinder of electrons with negligible radius compared to the wavelength. Let r be the distance from the transmitter to the trail, and use the familiar radar equation to calculate the received signal power P_r at the source in terms of the effective echoing area A of the trail.

$$P_r = (P_t G_t G_r \lambda^2 A)/((4\pi)^3 r^4) \ldots\ldots\ldots (i)$$

This area can be estimated from the reflection coefficient of a cylindrical electron cloud with zero initial radius and expanding with a Gaussian radial electron distribution. As the trail expands by diffusion, the phase difference between energy from different parts of the trail increases and hence the received power decreases. The initial area will depend on the electron charge, the trail's radius in terms of the wavelength and the rate of decay of the area will depend on the rate of diffusion of the electrons. Ref 28 derives value of this area A as follows:

From (28) the reflection coefficient Γ of a cylindrical electron cloud can be expressed in the following terms:

$$\Gamma = r_e \pi q \exp(-16\pi^2 Dt/\lambda^2) \qquad \text{.....(ii)}$$

In terms of E_{sc}/E_{inc}, the ratio of scattered field strength at the receiver to the incident field strength at a single electron.

$$E_{sc}/E_{inc} = \frac{\Gamma\sqrt{\lambda}}{\sqrt{2r\pi}} \qquad \text{.....(iii)}$$

The effective echoing area A of such a cloud is

$$A = 4\pi r^2 (E_{sc}/E_{inc})^2 \qquad \text{.....(iv)}$$

Substituting for Γ from (ii) into (iii) and then for E_{sc}/E_{inc} in (iv) gives:

$$A = 2\pi r q^2 r_e^2 \lambda \exp(-32\pi^2 Dt/\lambda^2) \qquad \text{.....(v)}$$

D is the diffusion coefficient characterising the trail expansion with time.

By assuming that most of the energy is scattered back by the first Fresnel zone of the trail, and initially the trail consists of a line of electrons, we can intuitively explain the form of equation (v).

Fig Ad1 Fresnel zone of a meteor trail

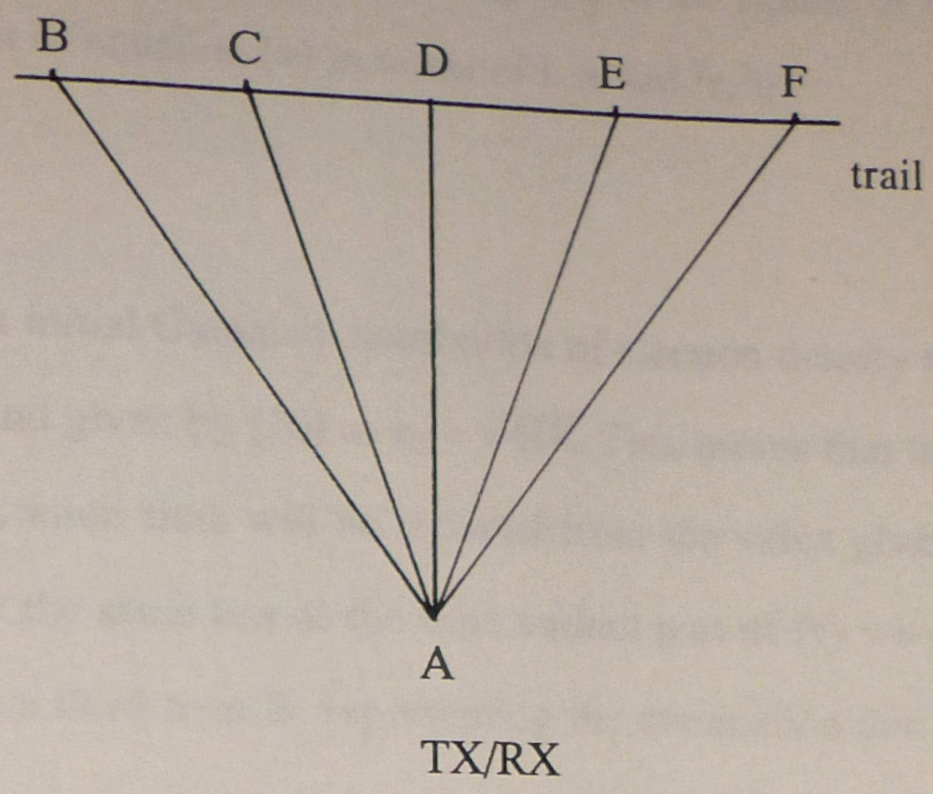

AD = r , AC = $r + \lambda/4$, CD = half of length of first Fresnel zone

Consider the energy scattered back from the trail and received at A. It will be made up from the phasor sum of the contributions from B C D etc. If length ACA > length ADA by half a wavelength, the contributions from C to E will reinforce the received signal. This region is the *first Fresnel zone* of the trail.

If ABA > ADA by one wavelength then the regions from B to C and E to F will add in anti-phase. This is the second Fresnel zone of the trail.

In Triangle ADC, $CD = L = \sqrt{(r+\lambda/4)^2 - r^2}$

$$= \sqrt{r^2 + r\lambda/2 + \lambda^2/16 - r^2}$$

$$= \sqrt{r\lambda/2} \quad \text{if } r \gg \lambda$$

We assume that the electrons scatter freely and independently, and that the received signal is the phasor sum of the individual contributions. The first term of (v) represents the maximum area, and reference to fig Ad1 shows that the length L of half the first Fresnel zone is approximately $\sqrt{r\lambda/2}$. As there are qL electrons in the zone and each

contributes to the received field in proportion to its radius the total field is proportional to the product $r_e qL$, and the effective scattering area to the square of this product. The time independent part of equation (v) in terms of L is $4\pi L^2 r_e^2 q^2$

Initial trail radius

If we now assume an initial Gaussian distribution of electron density then the effective trail radius is finite and given by (20) as $r_0 = \sqrt{4Dt}$. This means that the effective cross sectional area at formation time will be reduced from the value given by (v). As this reduction will follow the same law as the time variant part of (v) we can substitute for $Dt = r_0^2/4$ and define a third term B representing the attenuation due to the initial trail radius where

$$B = \exp(-8\pi^2 r_0^2 / \lambda^2) \quad \text{.....(vi)}$$

This attenuation factor B and the effective echoing area A multiply the expression for P_r in equation (i).

We now extend the analysis and consider the case where transmitter and receiver are not co-sited. Reflection is specular, and this condition determines that the trail must lie tangential to a prolate spheroidal surface with the ends of the link at the foci.

Two important changes now take place due to the oblique nature of the path.

(i) The length of the first Fresnel zone increases, thus containing more electrons and hence increasing the scattered signal.

(ii) The maximum possible path difference between the extreme edges of the trail decreases. This has the same effect as an increase in the signal wavelength and hence increases the maximum signal amplitude and decreases the rate of decay due to trail expansion, hence increasing the burst duration.

The length of the Fresnel zone for this case is:

$2\{\lambda R_t R_r/(R_t+R_r)(1-\cos^2\beta \sin^2\varnothing)\}^{0.5}$ ....(vii)

And the complete transmission equation becomes (20):

$P_r = K \exp(-8\pi^2 r_0^2 /\lambda^2 \sec^2\varnothing)\exp(-32\pi^2 Dt/\lambda^2 \sec^2\varnothing)$..(viii)

Where $K = \dfrac{P_t G_t G_r \lambda^3 q^2 r_e^2 \sin^2\alpha}{16\pi^2 R_t R_r (R_t + R_r)(1-\cos^2\beta\sin^2\varnothing)}$

α is the angle between the electric vector at the trail, and R_r, the line joining the centre of the Fresnel zone of the trail to the receiver location. The $\sin^2\alpha$ term accounts for the polarisation change on scattering. For horizontal polarisation and long links where transmitter and receiver are at different locations, $\sin^2\alpha$ is close to unity and this factor is usually ignored.

1.1.2 Trail duration

To obtain a figure for the duration of the trail it is usual to quote the time taken for the received power to fall to $1/e^2$ (-8.7dB) of its maximum value. Applying this criteria to the time dependent part of equation (viii):

duration = $(\lambda^2 \sec^2\varnothing)/(16\pi^2 D)$.....(ix)

1.2 Short wavelength case

1.2.1 Path loss

For the long wavelength case it has been assumed that the time to form the trail (ie the time for the meteoric particle to travel a distance equivalent to half the first Fresnel zone) is negligible, and the usable trail consists of the exponentially time decaying part of equation (vii). As this duration is proportional to the square of the wavelength, a point is reached with decreasing wavelength where the formation time becomes more significant than the duration defined by (ix). Below this transition wavelength a new

set of path equations must be used. It must be noted that this dividing line is not distinct, and may only be defined generally by equating the time for trail formation to the duration from equation (ix).

The time for trail formation is defined as the time taken for the meteor to traverse half of the first Fresnel zone of the trail. This is given by half of the zone length from equation (vii) divided by the meteor velocity v.

Equating this time to the duration in equation (ix) and rearranging, a transition wavelength can be defined for the forward scatter case as:

for transverse trails ($\beta=90^\circ$)

$$\lambda_t = \{(256\pi^4 D^2 R_t R_r)/v^2(R_t+R_r)\}^{1/3}\sec^{2/3}\varnothing$$

Or for in line trails ($\beta=0^\circ$)

$$\lambda_t = \{(256\pi^4 D^2 R_t R_r)/v^2(R_t+R_r)\}^{1/3}\sec^{4/3}\varnothing$$

In this case each part of the trail begins to diffuse as soon as it forms, therefore the trail has a smaller radius near the head. The trail may be considered as a paraboloid of revolution with the particle at the head. Sugar (20) suggests an expression for the scattering cross section of an effective length of the trail (ie that portion adding significantly to the received signal) is proportional to:

$v^2\lambda^4/D^2$ and a complete path loss equation as below

$$P_r = \frac{P_t G_t G_r \lambda^6 q^2 r_e^2 v^2 \sec^4\varnothing \sin^2\alpha}{4096\pi^6 R_t^2 R_r^2 D^2} \{\exp(-8\pi^2 r_0^2/\lambda^2\sec^2\varnothing)\} \left[1+\left(\frac{v^2 \sec\varnothing(1-\cos^2\beta\sin^2\varnothing)}{8\pi D R_t R_r \cos\varnothing/(R_t+R_r)}\right)^2 t^2\right]^{-1} \quad \ldots(x)$$

1.2.2 Trail duration

The burst duration is defined in (20) slightly differently to the long wavelength case. It is defined as the length of a rectangular pulse with the same peak amplitude and containing equal energy as the received pulse. It corresponds to the time taken for the pulse to fall to $1/(1+\pi^2/4)$ (-5.4dB) of its initial value. It is given as:

$$\text{duration} = \frac{8\pi^2 D R_t R_r}{\lambda v^2 \sec^2\varnothing (R_t+R_r)(1-\cos^2\beta\sin^2\varnothing)} \qquad \ldots\ldots(xi)$$

The duration function can be modified in equation (ix) (long wavelength case) to meet the same criterion by multiplying it by a factor of 0.624. This is used in the program MSDUR when comparing burst durations. Note that the actual duration measured on a practical system will depend on the system sensitivity. Any such system will have to define an amplitude or signal to noise ratio threshold above which a burst is counted as valid. The duration measured would normally be the time that the signal remains above that threshold. The consequence of this is that signals with different peak amplitudes, but with the same duration as defined in the theory above, could appear to have different durations when measured in such a system. In the applications described in this report the ratio of durations of signals from two similar systems is the important parameter, and hence the absolute durations are of less importance.

Appendix (e)

Calculation of duty cycle for meteor burst links

Duty cycle is defined as the percentage of time that the received signal is above a given threshold. In this appendix an expression for the long term duty cycle of a meteor burst link is evaluated based on the following assumptions:

I. isotropic distribution of meteor radiants.

II. underdense bursts

III. a flat earth

(I) and (II) can be justified by the fact that only the long term effects are being considered. Other radiant distributions affect the diurnal variations of duty cycle. Ref (34) shows that assumption (III) has little effect on the result.

To calculate the duty cycle, information is required about the probability of detection of suitable trails, their mean duration, and the relationship between received power and the ionisation density of the trails. The last two relationships were derived in appendix (d).

1. Probability density of detection of suitable trails.

This derivation follows the technique outlined by Eshleman and Manning (4),and extended by Nes (22). Using the following simplifying assumptions:

I. the trail only produces an echo if at least half of its first Fresnel zone is ionised.

II. all trails have the same length L

III. the plane containing the midpoints of these trails (the h plane) occurs at the same height h.

The probability density of detection p is defined as the fraction of those trails that pass through a differential area of the h plane, that are in the correct orientation to produce a reflection, ie tangential to an ellipsoid with the two path ends at the foci.

The trail must lie in the "m plane" perpendicular to the bisector OP of the scattering angle. By definition, the centre of the principal Fresnel zone at the scattering point is where the distance $R_t'+R_r'$ is a minimum. We may find the maximum value of deviation from this m plane condition (δ) which still allows half the Fresnel zone to be ionised, by finding the minimum value of equation (i) and substituting the condition z = +-(L/2) giving the approximate expression (ii).

Fig Ae1 Path geometry for reflection

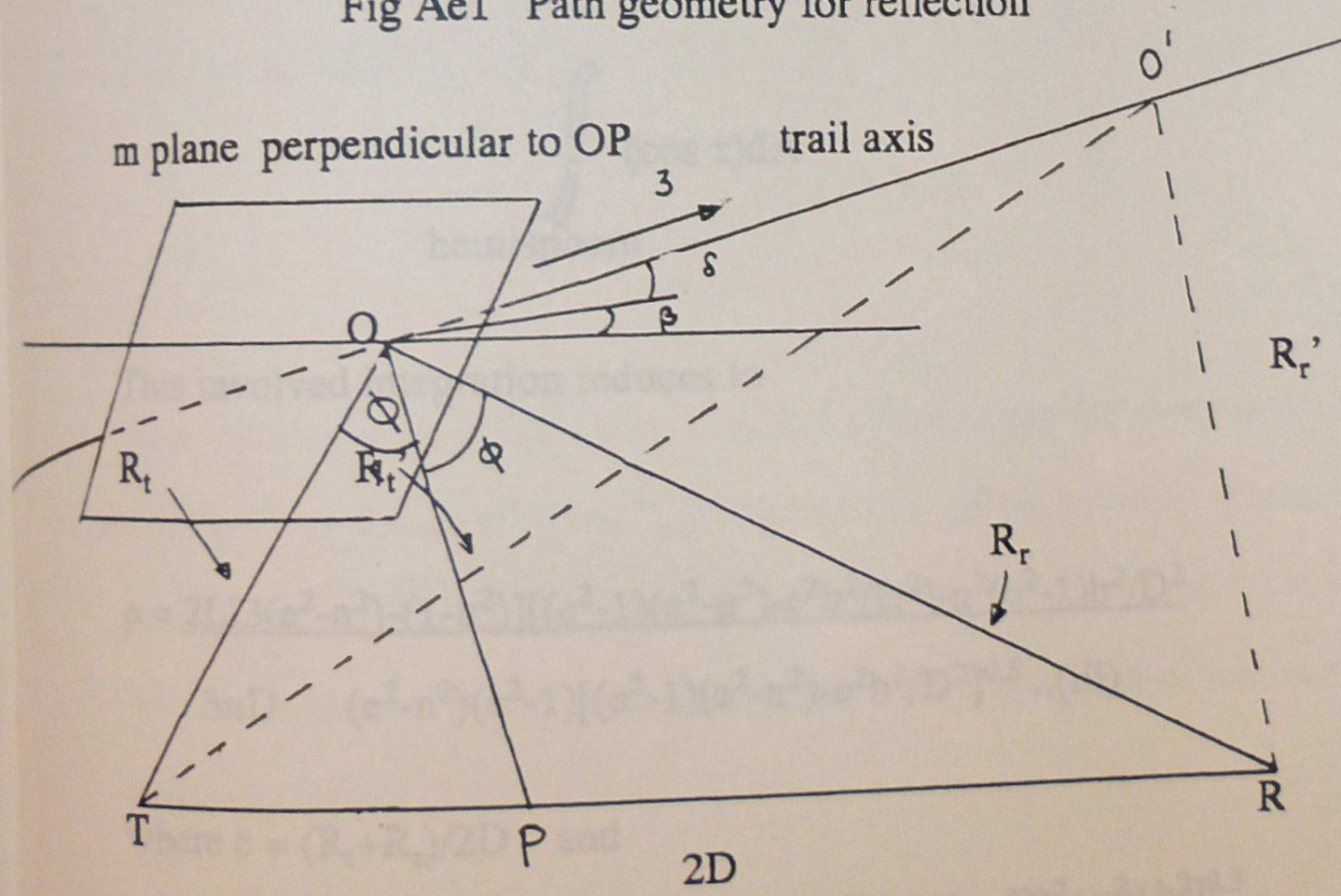

$$R_t'+R_r' = R_t+R_r+2z\cos\varnothing\sin\beta+z^2/2(1/R_t+1/R_r)(1-\sin^2\varnothing\cos^2\beta)$$

The above expression is minimised with $z = \pm L/2$ and $L \ll R_t$ and R_r

$$\text{if } \delta < \frac{L(R_t+R_r)}{4R_tR_r\cos\varnothing}(1-\sin^2\varnothing\cos^2\beta) \quad \text{.....(ii)}$$

All trails passing through a differential area of the h plane at O must be perpendicular to a unit hemisphere on the h plane centred at O. The intersection of the m plane (and its allowable deviation (δ)) with this hemisphere gives a narrow hemispherical band through which all correctly oriented trails must pass.

The total number of meteors passing through this band divided by the total number passing through the whole hemisphere gives the probability density of detection p. As the flux density of meteors varies as the cosine of the zenith angle (τ) of the radiant (assuming an isotropic distribution of radiants), p can be evaluated from :

$$p = \frac{\iint_{band} (\cos\tau)\,dA}{\iint_{hemisphere} (\cos\tau)\,dA}$$

This involved integration reduces to

$$p = \frac{2L[3(e^2-n^2)-(1-n^2)][(e^2-1)(e^2-n^2)-e^2h^2/D^2]-n^2(e^2-1)h^2/D^2}{3\pi D \quad (e^2-n^2)(e^2-1)[(e^2-1)(e^2-n^2)-e^2h^2/D^2]^{0.5}} \quad ..(iii)$$

where $e = (R_t+R_r)/2D$ and

$$R_t = [(x+D)^2+y^2+h^2]^{0.5} \quad ..(iv)$$

$$R_r = [(x-D)^2+y^2+h^2]^{0.5}$$

and $n = (R_t-R_r)/2D$

1.1 Probability-duration factor p"

Consideration of the probability density of detection associated with standard echo units ($p'' = p'\sec^2\varnothing$) as described in section 6 produces a simpler expression:

$$p'' = \frac{2L\,[(e^2-1)(e^2-n^2)-e^2h^2/D^2]^{0.5}}{\pi D\,(e^2-n^2)(e^2-1)^2} \quad \ldots(v)$$

Amplitude P_s of the standard echo is the peak value obtained by combining equations (i) and (ii) of appendix (d) ie

$$P_s = P_t(\lambda/4\pi r)^3\, 2\pi r_e^2 q^2 G_t G_r \quad \ldots\ldots(vi)$$

and the duration

$$t_s = \frac{\lambda^2}{16\pi^2 D} \quad \ldots\ldots\ldots\ldots(vii)$$

The rate of detection of these standard echoes may be evaluated by multiplying this "probability duration factor" p" by the rate of occurrence of trails per unit horizontal area of the sky and integrating the result over the area of the h plane illuminated by the system antennas. Multiplying this result by the duration of the standard echo gives the link duty cycle.

2. Rate of occurrence of trails

The rate of occurrence per unit horizontal area of the h plane of trails with electron densities exceeding some value q is given by Nes (22) as C_0/q

where $C_0 = 160\ m^{-3}\ s^{-1}$ the yearly average meteor intensity.

Hence the standard echo rate is

$$N = \iint_{h\ plane} (C_0/q)p''dA \quad \text{.....(viii)}$$

3. Duty cycle

The duty cycle is therefore $N_0 = Nt_s$ .....(ix)

Rearranging (vi) for q, (the threshold trail line density to give a received signal above the receiver threshold P_L), and substituting with (vii) in (ix) gives an expression for the yearly average duty cycle.

$$N_0 = [P_t(\lambda/4\pi r^2)^3/P_L]^{0.5} \sqrt{2\pi r_e} C_0 t_s \iint_{h\ plane} \sqrt{G_t G_r} p''\ dA \quad ..(x)$$

3.1 Method of solution for the integral in equation (x)

Equation (x) involves averaging the product $\sqrt{G_t G_r}\ p''$,over the relevant area of the h plane.

The first step in such a solution is to obtain expressions for the three quantities in terms of the h plane x and y co-ordinates as defined in Fig 6.5.

Equations (iv) and (v) already define p" fully, but we must perform co-ordinate conversions upon the gain functions of the antennas as defined in appendix (b) equations (ii) and (iii).

The integral was solved numerically, by dividing a 2000km by 1000km region of the h plane into grid points spaced by 20km, evaluating the product at each point, and averaging.

The final program to calculate the duty cycle is shown at the end of this section.

Its basis is as follows:

For each of 5000 points over the h plane

Evaluate the product SQRT(Gt*Gr)*p" at each point

Add to a running total

Divide this running total by 5000

Multiply this average value by area bounded

by maximum x and y values

The yearly average duty cycle is then calculated by multiplying the result of the above by the constants of equation (x).

To include the variation over the year, the model used by Nes was used.

$$\text{duty(date)} = (\text{average duty})*[1-0.3*\cos(2\pi*(\text{date})/365)]$$

Where date is the day number corresponding to the actual date.

The area of the h plane was finally chosen as y + – 500 Km and x + – 1000 Km to cover out beyond the p" = 0.1 contour of Fig 6.5.

Ranges beyond these values were tried but this had no significant effect upon the calculated duty cycle, as the antennas illuminated these areas with very low values of gain function, and the probability – duration factor was very low.

Also a finer grid of points was tried, but again, the effect on the calculated duty cycle was insignificant.

Program for calculation of duty cycle for paths in the region of 1000km.

```
program Dayduty11;
{Wroclaw-Barton path, mean duty cycle per day, new integral}
{version 1.3 5/9/89 modifications to az/el calculations}
{(c) J C Worsnop 1989}
{$N+}
const
        L=19;                   {trail length (25 scaled by root lambda)}
        D=587;                   {half path length}
        lambda=4.2451;          {system wavelength}
        eirp=120e3;

var
        intgrand,answer1,answer2,h,b                    : real;
        duty,t0,x,y,betat,Gt,alphar,betar               : real;
        Gr,e,Rt,Rr,n,p,p1,p2,num,den,diff               : real;
        count,hour,day,month,daynum,lyear,year,x1,y1    : integer;
        ant                                             : char;

function power(a,b :real) : real;   {calculates z=a^b}
                begin
                        power:=exp(b*ln(a));
                end;

        function atan(a,b:real):real;   {gets correct quadrant for angle in ARCTAN}
            begin
                    if b=0.0 then if a > 0.0 then atan:=pi/2
                                                    else atan:=-pi/2;
                    if a=0.0 then if b > 0.0 then atan:=0.0
                                                    else atan:=pi;
                    if(b<>0.0) and (a<>0.0) then
                    begin
                            if b>0.0 then if a>0.0 then
                            atan:=arctan(abs(a/b))
                            else atan:=-arctan(abs(a/b))
                            else if a>0.0 then
                            atan:=pi-arctan(abs(a/b))
                            else atan:=-pi+arctan(abs(a/b));
                    end;
            end;

procedure trail_height;
                begin
                        h:=124-17*(ln(300/lambda)/ln(10));
                                                    {trail height}
                        b:=(0.067*h)-5.6;
                        diff:=power(10,b);
                                                    {diffusion constant}
                end;

procedure daynumber;
                begin
                        If year/4=trunc(year/4) then lyear:=62
                        else lyear:=63;
```

```
                case month of
                    3,4,5,6,7,8,9,10,11,12:
                    daynum:=day+trunc(30.6*(month+1))-lyear;

                 daynum:=day+trunc(lyear*(month-1)/2);                1,2:
                end;
            end;

procedure TXantgain;    {transmitter antenna gain function}
            begin
                if x=D then x:=x-0.01;
                if x=(-D) then x:=x-0.01;
                betat:=atan(h,Sqrt(sqr(x+D)+sqr(y)));
                if x<-D then betat:=pi-betat;
                Gt:=exp(-25*sqr(betat));
            end;

procedure endRXantgain;        {RX ant gain function end}
            begin
                alphar:=atan(y,(D-x));
                betar :=atan(h,Sqrt(sqr(D-x)+sqr(y)));
                if x>D then betar:= pi-betar;
                Gr:=13.5*EXP(-(sqr(alphar)/3.5
                +(sqr(betar-(pi/2)))/4)*13.5);
                IF betar<PI/6
                    THEN Gr:=0.427;{End point back lobe}
                      if betar>(5*pi/6)
                      Then Gr:=0.427;
                      if betar<0.0524 then Gr:=0;
            end;

procedure midRXantgain;        {RX ant gain function mid}
            begin
                alphar:=atan(y,(D-x));
                betar :=atan(h,Sqrt(sqr(D-x)+sqr(y)));
                if x>D then betar:= pi-betar;
                Gr:=13.5*EXP(-(sqr(alphar)/3.5
                    +(sqr(betar))/4)*13.5);
                IF betar>PI/3
                    THEN Gr:=0.427;{mid point back lobe}
                    if betar<0.0524 then Gr:=0;
            end;
procedure pdf;    probability duration factor calculation}
            begin
                Rt:=sqrt(sqr(x+D)+sqr(y)+sqr(h));
                Rr:=sqrt(sqr(x-D)+sqr(y)+sqr(h));
                e :=(Rt+Rr)/(2*D);
                n :=(Rt-Rr)/(2*D);
                p1 :=(2*L)/(pi*D);
                den:=(sqr(e)-sqr(n))*sqr(sqr(e)-1);
                num:=(sqr(e)-1)*(sqr(e)-sqr(n))
                    -(sqr(e)*sqr(h))/(D*D);
                if num< 0 then num:=0;
                p2:=sqrt(num)/den;
                p :=p1*p2;
```

```
                end;

procedure integrand;
                begin
                        intgrand:=intgrand+p*sqrt(Gt*Gr);
                end;

                {***************main program***************}

begin
        writeln('mid point or end point  (m/e)');readln(ant);
        writeln('enter year');readln (year);
        writeln('enter month (1-12)');readln (month);
        writeln('enter day (1-31)');readln(day);
        trail_height;
        t0:=sqr(lambda)/(diff*16*sqr(pi));
        intgrand:=0;
        count:=0;
        writeln('Calculating Duty Cycle..... Please      wait');
        x1:=-990;
                repeat
                        y1:=-490;
                            repeat
                                    x:=x1;
                                    y:=y1;
                                    count :=count+1;
                                    TXantgain;
                                    case ant of
                                    'E','e': endRXantgain;
                                    'M','m':midRXantgain;
                                    end;
                                    pdf;
                                    integrand;
                                    y1:=y1+20;
                                until y1=510;
                            x1:=x1+20;
                        until x1=1010;
        answer1:=(intgrand/count);
        answer2:=answer1*2000e3*1000e3;
        duty:=answer2*t0*(sqrt(eirp*power((lambda
         /(4*pi*D*1e3)),3)/1e-14))*sqrt(2*pi)*160*2.8178e-15;
        daynumber;
        writeln('yearly average duty cycle is',duty*100,' %');
        duty:=duty*(1-0.3*cos(2*pi*daynum/(428-lyear)));
        writeln('duty cycle expected on ',day,'/' ,month,'/'
                                        ,year, ' is',duty*100,' %');
end.
```

Appendix (f)

Memory used by data logger program

```
&7F00
  :
  :
  : temporary  "Scratch pad" for 2 minutes of samples
  :
  :
&2140
  *
&213D 5 byte by 12 array
  :  12 MSB cumulative burst amplitudes
&2132
&2131
  :  12 LSB cumulative burst amplitudes
&2126
&2125
  :  12 MSB cumulative burst lengths
&211A
&2119
  :  12 LSB cumulative burst lengths
&210D
&210C
  :  12 burst totals,one for each 5 min period
&2100
&20FF
  :  BASIC program
&1900
  *
  * &0A31
  :  Assembler code for sampling routine
&0900
  *
  *

&0079 pointer used in 5 byte by 12 array
&0078 used for post indexed indirect adressing for scratch
      pad pointer
&0077 ____________________"____________________
&0076  MSB cumulative amplitude per 2 minute period
&0075  LSB cumulative amplitude per 2 minute period
&0074  temporary... running peak value of burst
&0073  number of bursts per 2 minute period
&0071  MSB sample count per  2  minute  period (cumulative
       duration)
&0070  LSB sample count per 2 minute period
&0000
```